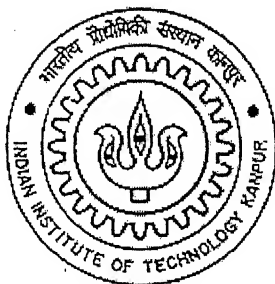


Steady State Analysis of Reactive Distillation Systems Using Homotopy Continuation

A Thesis Submitted

In Partial Fulfillment of the Requirements
for the Degree of
Master of Technology

By
Bhanu Pratap Singh



to the

**DEPARTMENT OF CHEMICAL ENGINEERING
INDIAN INSTITUTE OF TECHNOLOGY, KANPUR**

July, 2004

CERTIFICATE



It is certified that the work contained in the thesis entitled "**Steady State Analysis of Reactive Distillation Systems Using Homotopy Continuation**" by *Mr. Bhanu Pratap Singh* has been carried out under my supervision and that this work has not been submitted elsewhere for a degree.

A handwritten signature in black ink, appearing to read "Nitin Kaistha", with a horizontal line drawn underneath.

Dr. Nitin Kaistha

Assistant Professor

Department of Chemical Engineering

Indian Institute of Technology, Kanpur

July 2004

TN

CHE/2000/m

Sibbz

4 OCT 2004

गुरुचोत्तम काशीनाथ केलकर पुस्तकालय
भारतीय प्रौद्योगिकी संस्थान कानपुर
पचासि क्र० A...148879



A148879

Dedicated
to
My Father
(Late Shri Maharaj Singh)

ACKNOWLEDGMENT

I would like to express my deep gratitude towards my thesis supervisor Dr. Nitin Kaistha for his excellent guidance, support and constant encouragement throughout my thesis work.

I would like to thank my labmates, Ram Singh, Chetan, Pavan, Srikant, Vivek, my friends Akhilesh, Sukalyan and all for their great affection, care and timely criticism.

Finally, to my mother, my beloved sisters, goes my eternal gratitude for their constant love and support.

Bhanu Pratap Singh

ABSTRACT

Homotopy continuation, a powerful tool for identifying steady state multiplicities, is applied to reactive distillation systems to assess the impact of these multiplicities on column design, operability and control. The technique is applied in two distinct ways. In the first, continuation with respect to the catalyst weight is used to analyze multiplicities as reaction is introduced in simple distillation. An MTBE and a Methyl Acetate RD column are used as examples. For the MTBE column, upto five steady states in the kinetically controlled regime are detected. Of these, only three remain as the catalyst weight is increased and reaction equilibrium is approached on the trays. For the methyl acetate column, three steady states in both the kinetically controlled and reaction equilibrium regimes are obtained at fixed reflux rate and reboiler duty. If the column specification is changed to fixed reflux ratio and reboiler duty, only a single steady state solution is obtained for all catalyst weights. The result shows the substantial impact of column operating policy on the existence of multiple steady states.

In the second application of homotopy continuation to RD columns, continuation with respect to an input column specification is used to study its effect on output variables such as tray temperatures and compositions. The input-output relationships are systematically analyzed to synthesize robust column operating structures that ensure high product purity and reaction conversion in the face of major disturbances. The basic philosophy is to prefer control structures with nearly linear input-output relationships and avoid steady state multiplicities. Sensitivity analysis is used to obtain the sensitive tray location for the temperature / composition sensors used in a control structure. An MTBE RD column is used as an illustrative example.

CONTENTS

Abstract	v
List of FIGURES	viii
List of Tables	xi
Nomenclature	xii
1. Introduction	1
2. Literature review	10
2.1 Reactive Distillation Literature	10
2.2 Homotopy Continuation Literature	15
3. Homotopy Continuation Methods	19
3.1 Homotopy Continuation algorithms	20
3.1.1 Dynamic Reparameterization	22
3.1.2 Arc Length Continuation	25
3.2 Reactive Distillation Problem Formulation	27
3.2.1 Homotopy Continuation With Respect to Catalyst Weight	32
3.2.2 Homotopy Continuation About the Design Steady State	33
4. Homotopy Continuation With Respect to Catalyst Weight	35
4.1 Case Study I: Methyl Tertiary Butyl Ether (MTBE)	35
4.1.1 Column Configuration	37
4.1.2 Multiple Steady States by Continuation With Respect to Catalyst Weight	39
4.2 Case Study II: Methyl Acetate	50
4.2.1 Column Configuration	51
4.2.2 Multiple Steady States by Continuation With Respect to Catalyst Weight	53

5. Homotopy Continuation for Control Structure Synthesis	61
5.1 The MIBE Reactive Distillation Column	65
5.2 Effect of Column Inputs on Output Variables	67
5.3 Control Structure Synthesis	82
6. Conclusions and Future Work	96
6.1 Conclusions	96
6.2 Future Work	98
References	98

LIST OF FIGURES

1. FIGURE 1.1: A typical reactive distillation column	1
2. FIGURE 1.2: A pictorial comparison between conventional process and reactive distillation for methyl acetate production	4
3. FIGURE 1.3: Comparison of MTBE production by conventional and reactive distillation processes	5
4. FIGURE 1.4: Input and output multiplicities	7
5. FIGURE 3.1: A complicated solution diagram with turning points	21
6. FIGURE 3.2: Illustration of problems in branch tracking near turning points	22
7. FIGURE 3.3: Illustration of dynamic reparametrization for branch tracking around turning points	23
8. FIGURE 3.4: A pictorial view of reactive distillation column	28
9. FIGURE 3.5: A schematic representation of an equilibrium stage j	29
10. FIGURE 4.1: Reactive distillation column configuration for MTBE synthesis	38
11. FIGURE 4.2: Multiple steady states in MTBE for purity and conversion	42
12. FIGURE 4.3: MTBE formation rates for five steady states	44
13. FIGURE 4.4: Temperature profiles for five steady states for MTBE system	44
14. FIGURE 4.5: Composition profiles for five steady state solutions for all components	45
15. FIGURE 4.6: Reactive distillation column configuration for methyl acetate synthesis	52
16. FIGURE 4.7: Multiple steady states in methyl acetate system for fixed reflux rate and reboiler duty	54
17. FIGURE 4.8: Reaction rates for methyl acetate system	55
18. FIGURE 4.9: Temperature profiles rates for methyl acetate system	56

19. FIGURE 4.10: Composition profile for three steady states of methyl acetate system	57
20. FIGURE 4.11: Multiple steady states in methyl acetate system for fixed reflux ratio and reboiler duty	58
21. FIGURE 5.1: Control structures corresponding to two different specification sets	63
22. FIGURE 5.2: Multiple steady states in MTBE system for purity and conversion	66
23. FIGURE 5.3: Input output multiplicities at fixed reflux ratio and reflux rate with variation of reboiler duty	69
24. FIGURE 5.4: Responses of tray temperatures to changes in reboiler duty at fixed reflux ratio	70
25. FIGURE 5.5: Responses of tray composition to changes in reboiler duty at fixed reflux ratio	72
26. FIGURE 5.6: Temperature sensitivity with respect to reboiler duty	74
27. FIGURE 5.7: Tray temperatures for changes in MeOH feed flow	75
28. FIGURE 5.8: Tray compositions for changes in MeOH feed flow	76
29. FIGURE 5.9: Tray temperatures for changes in Butenes feed flow	78
30. FIGURE 5.10 Tray compositions for changes in Butenes feed flow	79
31. FIGURE 5.11: Sensitivity of the tray compositions with respect to fresh feed flow rates	81
32. FIGURE 5.12: Purity and conversion with the variation of fresh feed flow rates	83
33. FIGURE 5.13: Purity and conversion vs production rate change at fixed reflux ratio and reboiler duty with stoichiometric feeds	84
34. FIGURE 5.14: Purity and conversion with production rate change at fixed reflux ratio and tray 12 temperature with stoichiometric feeds	85
35. FIGURE 5.15: Purity and feed composition changes at fixed reflux ration and reboiler duty	86
36. FIGURE 5.16: Control structures with two control loops	88

37. FIGURE 5.17: Column Performance with Production Rate Changes Production rate Handle: MeOH	90
38. FIGURE 5.18: Column Performance with Production Rate Changes Production rate Handle: Butenes	91
39. FIGURE 5.19: Column Performance with Production Rate Changes Production rate Handle: MeOH	92
40. FIGURE 5.20: Alternative control structures	94

LIST OF TABLES

1. Table 3.1: Replacement functions of H_I and H_N	31
2. Table 3.2: Replacement equations for total condenser	31
3. Table 4.1: Wilson interaction parameters for MTBE system	36
4. Table 4.2: The distillate and bottoms composition and reaction conversion for five steady states of MTBE system	43
5. Table 4.3: Activity ratio, forward reaction rates, backward reaction rates and total reaction rates for five steady states of MTBE system	48
6. Table 4.4: Wilson interaction parameters for methyl acetate system	51
7. Table 4.5: The distillate and bottoms composition and reaction conversion for three steady states of methyl acetate system	54
8. Table 5.1: Niederlinski Index corresponding to butenes and MeOH feed flow	88

NOMENCLATURE

a	Activity
$a_{i,j}$	Wilson binary interaction parameter
B	Bottoms flow rate
C	Number of components in the system
D	Distillate rate
E	Equilibrium relationship equations
f	Feed component flow rate
F	Feed flow rate
\mathbf{h}	Vector homotopy function
h_L	Liquid enthalpy
h_V	Vapor enthalpy
H_1	Enthalpy balance for first stage
H_N	Enthalpy balance for last stage
H	Enthalpy balance equation
\mathbf{J}	Jacobian
k_f	Forward rate constant
K_{eq}	Equilibrium constant
K_r	Adsorption equilibrium constant
l	Liquid component flow rate
L/D	Reflux ratio
L	Total liquid flow rate
L	Catalyst weight factor

M	Material balance equation
M_c	Catalyst weight
N	Stage number
NRX	Number of reaction
P	Pressure
Q	Heat entering or leaving the tray
r	Rate of reaction
R	Universal gas constant
s	Dimensionless side-stream flow rate
S	Dimensionless side-stream flow rate
T	Temperature
U	Side stream liquid flow rate
v	vapor component flow rate
V	Vapor flow rate
V/B	Reboil ratio
W	Side stream vapor flow rate
x	Liquid mole fraction
\mathbf{x}	Vector function of iteration variables
\mathbf{x}_0	Known solution or initial guess vector
y	Vapor mole fraction
z	Feed composition

Greek Letters

γ	Activity coefficient
η	Tray efficiency
ν	Stoichiometric coefficient
λ	Homotopy parameter

Subscript

i	Component index
j	Stage index

Reactive distillation (RD) combines reaction and separation in a single column. It is a promising technology for process intensification with significant economic benefits over conventional “reactor followed by separator” processes. Besides the rectifying and stripping sections, reactive distillation columns comprise a reactive section in which reactants are converted into products. A typical RD column is shown in Figure 1.1.

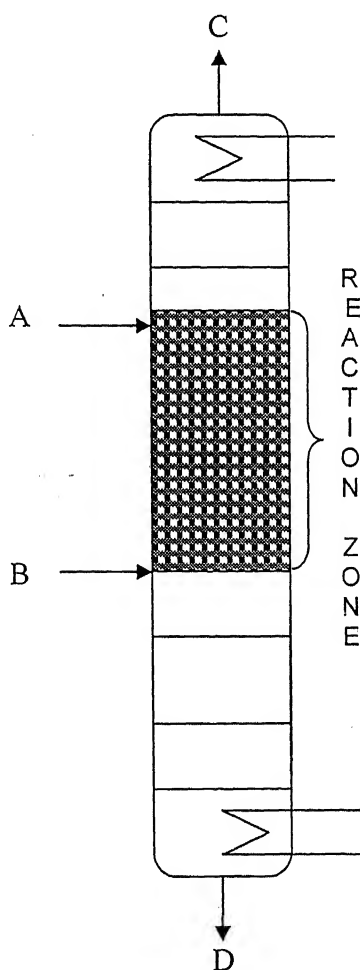


Figure 1.1: A typical reactive distillation column

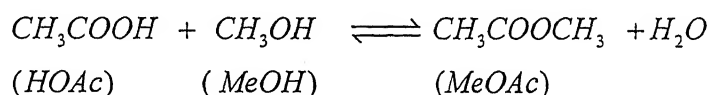
Commercial application of this process is mainly in esterification systems such as methyl acetate and etherification systems such as methyl tertiary butyl ether (MTBE), ethyl tertiary butyl ether (ETBE), and tertiary amyl methyl ether (TAME). Methyl acetate is a general solvent used for cellulose, lacquers, paints, resins, coatings, and perfumes and is also used as an intermediate in the manufacture of pharmaceuticals, artificial leather and synthetic flavoring. MTBE is valuable as gasoline additive for increasing the octane rating of the fuel. It is known as an "oxygenate" because it raises the oxygen content of gasoline and helps in its complete combustion reducing harmful CO emissions. MTBE is the key octane enhancing ingredient of unleaded gasoline. It has replaced the eco-unfriendly tetra ethyl lead (TEL), the octane enhancer in leaded fuels. ETBE and TAME are alternatives to MTBE for enhancing the fuel octane rating.

Reactive distillation when feasible has several advantages over conventional reactor-separator process:

1. Nearly complete conversion in equilibrium limited reactions due to the continuous removal of reaction products from the reactive zone. This is a consequence of the Le Chatelier's principle. Complete (increased) conversion eliminates (reduces) the costs associated with recycle.
2. Enhanced selectivity of the main reaction due to the removal of one (or more) reactants in the side reactions by volatilization.
3. Better heat utilization in the case of exothermic reactions where the heat of reaction is directly utilized for fractionation, reducing the reboiler duty.
4. Elimination of azeotropes due to reaction with other components. The azeotrope is literally "reacted away".

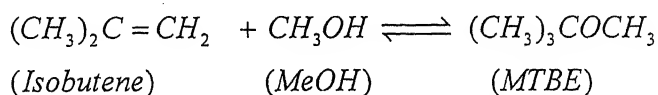
5. Process intensification with reaction and separation taking place in a single unit operation.

The methyl acetate reactive distillation process, first commercialized by the Eastman Chemical Company, is a classic success story in reactive distillation history. The improvement over the commercial process is so dramatic that the capital and operating costs reduce to one fifth of the conventional process. Figure 1.2 shows a schematic of the two processes. The main is as follows:



The traditional process consists of one reactor and a train of nine distillation columns. The separation of the reactor effluent into pure methyl acetate is complex due to the presence of azeotropes between methyl acetate and methanol, methyl acetate and water, and a near azeotrope between acetic acid and water. The RD process, in contrast, is a single column producing methyl acetate of greater than 95% purity with nearly 100% conversion. The column is thus a complete plant in itself.

Another commercially important example is MTBE production using RD technology. The production of MTBE is also traditionally carried out in a reactor followed by distillation column. MTBE is derived by the reaction of isobutene and methanol. The conventional and RD processes are shown in Figure 1.3. The main reaction in MTBE production is:



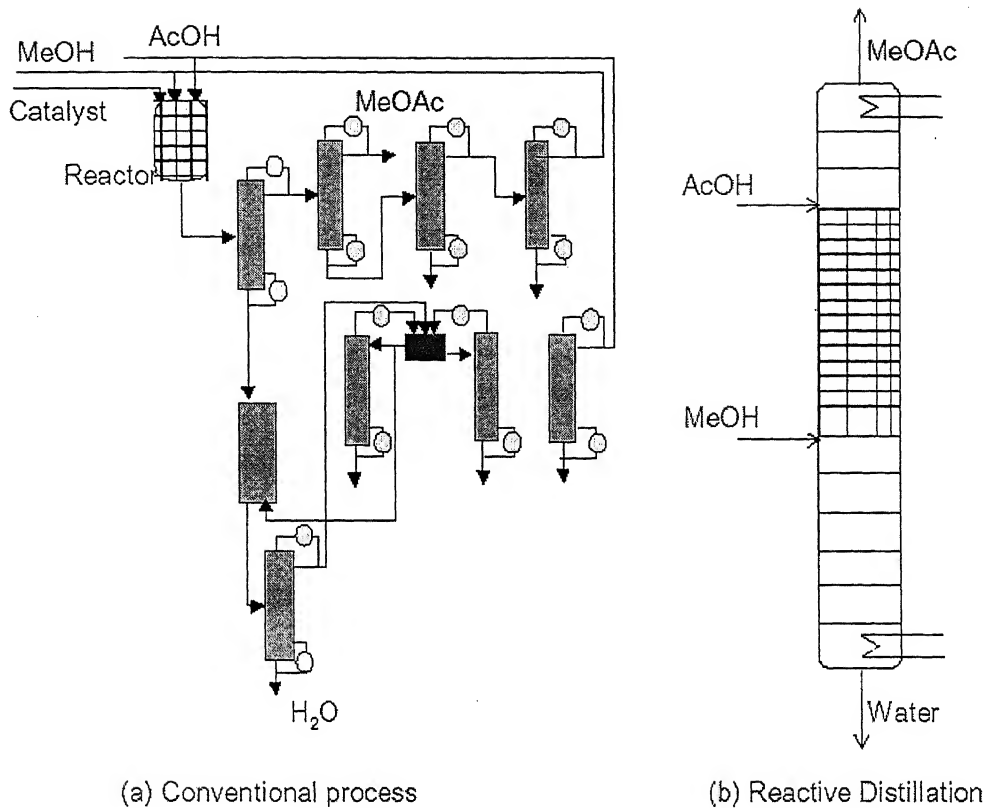
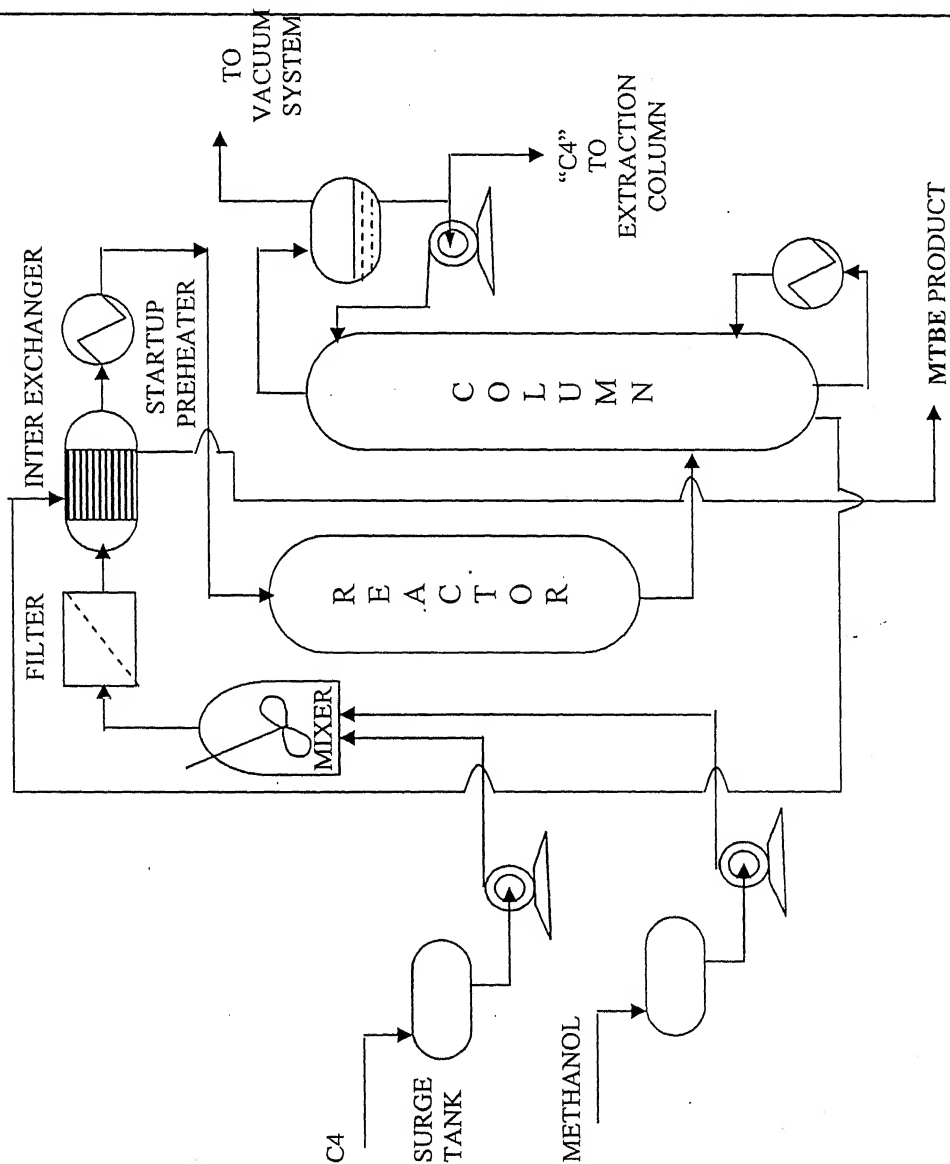


Figure 1.2: A pictorial comparison between the conventional process and reactive distillation for methyl acetate production. Adapted from Sirola (1995)

(a) Conventional Process



(b) Reactive Distillation

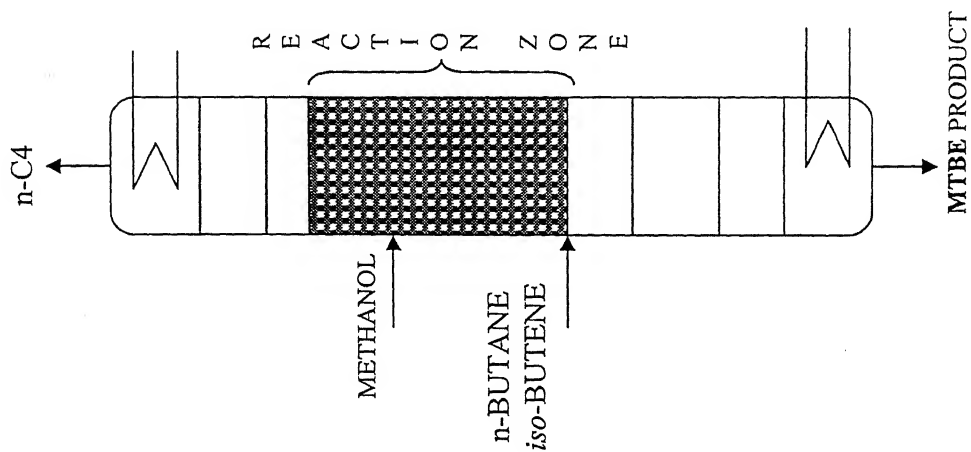


Figure.1.3: MTBE production by conventional and reactive distillation processes

It is emphasized that for RD to be a feasible production scheme, the relative volatility of the components should favor high reactant concentration in the reaction zone. Also the reaction rates at the mixture bubble point temperature should be large. RD is thus not an alternative for the production of each and every chemical. However, whenever feasible, the economic advantages of RD over conventional processes can be phenomenal.

The economic advantages of RD notwithstanding, the operation and control of RD columns is a complicated task that can be a hindrance in the successful implementation of the technology. The coupling of reaction and separation in a single unit makes the system highly nonlinear so that predicting column behavior in the presence of disturbances and changed operating conditions is non-trivial. Consequently, formulating the best operating strategy can be quite complex and non-intuitive and the strategy may change depending on the operating conditions. The issue is further complicated by the existence of multiple steady states that are to quite common in RD systems. A complete and thorough understanding of these multiplicities is a must for proposing robust control strategies for the proper regulation of the column in the face of disturbances.

We distinguish between two types of steady state multiplicities: input and output multiplicities. The former refers to different inputs (standard column specifications such as reboiler duty or reflux ratio) giving the same output (conversion or purity or distillate rate) while the latter refers to the same input giving different outputs. The idea of input and output multiplicity is illustrated in Figure 1.4(a) and 1.4(b) respectively.

In the literature on the simulation of RD columns, conventional algorithms such as Naphtali – Sandholm and Inside – Outside methods have been adopted for solving the governing MESH equations. These methods, depending on the initial guess can converge to any one of the multiple steady states, in case multiple steady states do exist. The methods are thus not geared towards detecting steady state multiplicities. A systematic approach for studying the steady state multiplicities is needed and this forms the main

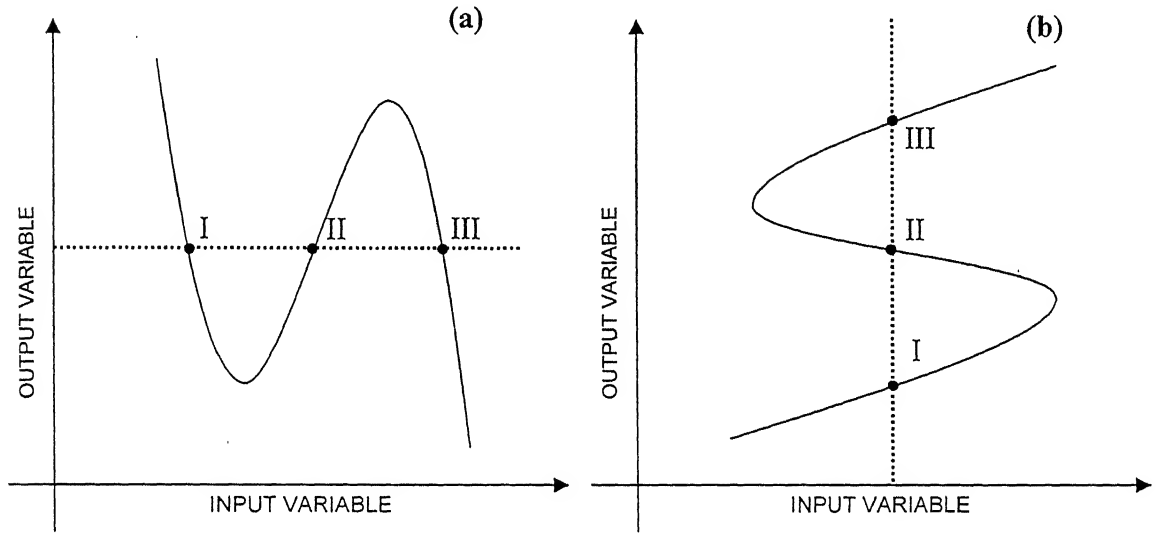


Figure 1.4: Input and output multiplicities

focus of this work. As shown in Figure 1.4, the steady state multiplicities are clearly revealed in the solution diagram. Traditional equation solvers give a point on the solution diagram (I, II or III) depending on the initial solution guess. Given a solution, the input (or output) can be varied about this solution to trace the complete solution path. This is referred to continuation with respect to a parameter. Thus continuation methods are a natural choice for obtaining the solution diagram and revealing multiplicities.

In order to start the continuation, one point on the solution branch is needed. This initial solution can be obtained in two ways as: a) the steady state solution to an ordinary distillation problem with no reaction and then introducing reaction as the continuation parameter and b) the steady state solution of the RD problem from conventional distillation solvers such as the Naphtali-Sandholm or inside-outside method and then varying an input (or output) about that steady state. In this work, RD columns of commercial interest viz Methyl Acetate and MTBE are studied for steady state multiplicities using approach (a). Approach (b) is applied for formulating the control strategy for a MTBE RD column.

Continuation using approach (a) described previously, is implemented using the catalyst weight as the continuation parameter. The ordinary distillation (no reaction) solution is obtained at zero catalyst weight and the desired reactive solution is approached by slowly increasing the catalyst weight. The homotopy path is thus traced from zero reaction extent to the design reaction extent. In the MTBE system, a reasonably large zone with five multiple steady states is obtained with the high conversion steady state corresponding to the design steady state. As the catalyst weight is further increased, two of these steady states disappear. Thus there are five steady states in the kinetically controlled RD regime in contrast to only three steady states in the reaction equilibrium controlled RD regime. For the methyl acetate column, three steady states in both the kinetically controlled and reaction equilibrium regimes are obtained at fixed reflux rate and reboiler duty. If specification set was changed to fixed reflux ratio and reboiler duty then no steady state multiplicities are seen. Using approach (b) as noted above with the high conversion steady state obtained using the NS method as the initial solution, input

and output multiplicities are clearly seen in MTBE system. Depending on the input variable (reboiler duty, feed flow rates) used for the continuation, there can be multiple solutions for the output variables. These results have important implications on formulating the control strategy for a RD column. Input variables that lead to nearly linear relationships with the output variables are preferred as potential manipulated variables. When output multiplicities cannot be avoided, inputs that have the design steady state far away from the region of multiplicities are preferred. The power of this simple rationale in the synthesis of RD column control structure screening is illustrated for the MTBE system.

The thesis is organized as follows. In Chapter 2, the literature related to multiple steady states in reactive distillation with emphasis on MTBE and methyl acetate is surveyed. A brief overview of the literature on homotopy continuation methods is also presented. Chapter 3 describes the homotopy continuation method in detail. In particular, the concept of dynamic reparametrization for tracing the solution diagram around turning points is discussed. The homotopy continuation method using approach (a) is applied to the methyl acetate and MTBE systems in Chapter 4. Homotopy continuation using approach (b) is applied to MTBE system for control structure synthesis in Chapter 5. The implications of the observed input / output multiplicities on control structure synthesis are discussed. Finally Chapter 6 presents the conclusions that can be drawn from this work and provides recommendations for future work.

Literature Review

This chapter briefly reviews the literature on reactive distillation and homotopy continuation. These distinct topics are reviewed in separate sections. Section 2.1 focuses on reactive distillation literature. In particular, emphasis is laid on reviewing published work on input output multiplicities and multiple steady states in reactive distillation systems. Section 2.2 provides a brief overview of the literature on homotopy continuation method. In particular, applications of the technique to RD columns are highlighted.

2.1 Reactive Distillation Literature

Reactive Distillation (RD) is an old process that combines reaction and separation in a single column. The first patent dates back to the early 1920s and was awarded to Backhaus for esterification systems (Backhaus (1921), (1922) and (1923 a, b)). The Eastman Kodak Company developed the first commercial RD process for the production of methyl acetate via the esterification of acetic acid and methanol with H_2SO_4 as the catalyst (Agreda and Partin (1984)). This process is a classic success of RD technology with reported capital and operating costs being a fifth of the traditional process (Agreda, (1990)). Given its potential, extensive research and development work in the past two decades have lead to commercial processes for MTBE, ETBE and TAME production (Degarmo (1992)).

RD can be advantageous in driving the conversion of equilibrium limited reactions to near completion due to the removal of products by vaporization, heat integration with the reaction heat being used for volatilization, side reaction suppression by the removal of side reaction precursors from the reaction phase and “reacting away” of azeotropes (Malone and Doherty (2000)). The realization of all these advantages requires favorable vapor liquid equilibrium and substantial reaction rates at the column operating temperatures as dictated by the tray mixture bubble point temperature. When realized, these advantages lead to process intensification with the complete plant being miniaturized into a single RD column, as in the case of methyl acetate production. Significant economic savings are therefore realized. Luyben (2004) has recently performed a quantitative comparative study on the economic benefits of RD over a conventional “reactor followed by separator” process. Ideal VLE is assumed in the study. The paper shows that when the relative volatilities of the components are favorable, the RD process is cheaper than the conventional process by a factor of 2-3 while the conventional process is the preferred option in case the relative volatilities are unfavorable.

The economic advantages provide a compelling reason for adopting RD as a technology. However, the operation and control of RD columns is a particularly challenging task. Compared to conventional processes, the control degree of freedom is reduced in RD processes so that the separation and reaction extent must be regulated using fewer available valves. Also, the coupling of reaction and separation leads to high non-linearity in the governing equations leading to multiple steady states and non-monotonic temperature profiles. The reader is referred to Taylor and Krishna (2000) for a

comprehensive review on the modeling of RD columns. A thorough understanding of RD column behavior through extensive modeling and simulation is a must for devising robust control strategies for the stable and economic operation of the RD columns in the face of disturbances. For this purpose systematically conducted simulations provide vital insight on the governing input-output relationships.

In this context, several researchers have, over the years, come across multiple steady states in RD column simulations. There are several reports on multiple steady states in RD literature. After the initial skepticism, multiple steady states have come to be accepted as routine phenomena in RD systems. Assuming the equilibrium stage model, Jacobs and Krishna (1993) reported a low conversion and a high conversion steady state in an MTBE column. Nijhuis et al (1993) have also reported multiple steady states in an MTBE column. Huan et al (1994) attempted to explain these multiplicities as due to the substantial increase in the activity of methanol in the presence of the inert n-butane leading to lower temperatures in the column with consequent lower reaction conversion. Chen et al (2002) used arc-length continuation to obtain upto three steady states for the MTBE system. They also reported three steady states for the TAME system in the kinetically controlled regime with only one steady state in the limit of reaction equilibrium on all the reactive stages. Higler et al (1999) reported multiple steady states in MTBE RD using the non-equilibrium stage model. Guttinger and Morari (1999a and 1999b) performed an ∞/∞ analysis, where the two infinities refer to total reflux and infinite number of stages, for predicting multiple steady states in RD columns. They use the MTBE system as an example case study in their work. Ciric and Miao (1994) explored steady state multiplicities in an RD column producing ethylene glycol from

ethylene oxide and water. They observed two sets of multiplicities, a three branch multiplicity that occurs at large reactive stage holdup and a complex switchbacking multiplicity that occurs at small reactive stage hold up.

All the above articles on multiple steady states are based on simulations only. Reports detailing much needed experimental evidence have also been published in the open literature. Rapmund et al (1998) have experimentally validated the existence of multiple steady states in the production of TAME. Mohl et al (1999) have experimentally validated the existence of multiple steady states in both the MTBE and TAME systems.

As mentioned earlier, the existence of multiple steady states and input-output multiplicities make the task of RD column regulation using appropriate control strategies, a challenging one. In recent years, many articles have appeared in the literature on the operation and control of RD columns. Prominent among these is the pioneering work of Luyben (1999, 2000, 2002, 2002 (a) and 2002 (b)) who have published a series of articles on the control of RD columns. Their work offers much insight on the key issues that govern the synthesis of control structures for RD columns. Control of an RD column with ideal VLE is studied in Al Arfaj and Luyben (2002). The authors show that controlling a tray temperature in the stripping section and a composition in the reactive section provides good control for production rate changes. The control of the industrially important methyl acetate column with highly non-linear VLE is studied in Al Arfaj and Luyben (1990). A control structure that maintains a tray temperature in the reactive section and the stripping section using the acetic acid feed and methanol feed respectively, with fixed reflux ratio and the reboiler heat input as the production rate handle provides the best performance of all the control structures studied. It is worth

mentioning that this is the control system implemented by Eastman for operating their column. The results show that composition measurement based control structures that work well for the ideal column do not work for the methyl acetate column. This is attributed to the high nonlinearity between the input output relationships for the composition based control structures. The non-linearity is much less severe if temperature is used as an inferential measurement so that good control is obtained. Al Arfaj and Luyben have also studied the control of an olefin-metathesis column (Al Arfaj and Luyben (1999)), an ethylene glycol column (Al Arfaj and Luyben (2000)) and the design and control of a RD based TAME process (Al Arfaj and Luyben (2002)).

Other authors have also studied the operation and control of RD columns. These include N Vora and Doutidis (2000) who study the non-linear control of an ethyl acetate column. Sneesby and 'O Tade (1999) study the control of an ethylene glycol column. Pattern based control of an ETBE column is studied by Y.-C. Tian et al (2003). Most of the work is however esoteric and un-necessarily mathematical and does not provide much intuitive insight on the operation and control of RD columns. A notable exception is the work of Wang, Wong and Lee (2003) on the control of an MTBE column. They show that good control is obtained when the reflux ratio and the feed ratio is kept fixed and a tray temperature in the stripping section is maintained using reboiler heat duty. A tray composition must be controlled to maintain the stoichiometric feed balance by manipulating the isobutylene feed in a cascade arrangement. The fresh methanol feed thus acts as the production rate handle.

The key to devising good control structures for RD columns is to choose the manipulated (input) and controlled variables (output) carefully so that the input-output

pairings avoid input or output multiplicities. This idea is well illustrated in the paper by Wong, Wang and Lee. Given that these input-output relationships can be quite complex for RD columns with turning points causing multiplicities (see Figure 1.4), homotopy continuation about the design operating conditions is used to obtain these relationships. This is done to avoid convergence problems near the turning points. A brief review of homotopy continuation as applied to ChE systems (RD in particular) is provided in the next section. It is noted that in this work, we also use homotopy continuation with respect to catalyst hold up in a reactive stage to analyze for multiple steady states in RD systems.

2.2 Homotopy Continuation Literature

Steady state modeling problems in chemical engineering involve the solution of nonlinear algebraic equations. This is true for isolated unit operations such as reactors and distillation columns as well as for complete plants with material and energy recycle. In case of highly non-linear equations, convergence using traditional methods such as the Newton Raphson method may be difficult. More importantly, in case of multiple steady states, the locally convergent Newton Raphson method would converge to the nearest solution depending on the initial guess provided and miss the other solutions. In such situations, homotopy continuation methods are a possible alternative for obtaining all the steady state solutions to the governing equations.

The basic idea behind homotopy continuation is to start from a known steady state solution and then slowly vary a parameter about this steady state and trace the complete solution diagram (Pushpavanam (2000); and Kubicek and Marek (1977)). In cases where multiple solutions exist, turning points that are bifurcations of the simplest type, may be

encountered so that the solution branch turns back around the turning point. This is illustrated in Figure 1.4. The existence of multiple steady states for a given value of the continuation parameter is thus clearly revealed in the solution diagram.

Homotopy continuation may also be used to solve a difficult problem $g(x) = 0$ by first starting with an easy problem with known solution $f(x) = 0$. A mixed homotopy function $h(x)$ is then defined by mixing $f(x)$ and $g(x)$ using a mixing parameter t . The homotopy function is then solved by continuing along the mixing parameter t from the limit where $h(x) = f(x)$ for which the solution is known, to the limit where $h(x) = g(x)$. In some sense, the simple function $f(x)$ is bent or twisted slowly to the complex function $g(x)$ using continuation along the parameter t . An example for the homotopy function is $h(x) = t.g(x) + (1-t).f(x)$. Thus t is varied from 0 to 1 with $h(x)$ at $t = 1$ corresponding to the desired solution of $g(x) = 0$.

JD Seader at the University of Utah and WD Seider at Penn State have pioneered the application of homotopy continuation to chemical engineering problems. A good review of the method is available in Wayburn and Seader (1987) and the interested reader is referred to the same. Lin et al apply homotopy continuation for computing multiple solutions to systems of interlinked separation columns. Kovach and Seider, (1987) apply homotopy continuation methods to azeotropic distillation columns. The algorithm of Allgower and Georg (1981) is applied to obtain two steady states for an industrial azeotropic distillation column over a very narrow range of reflux ratios. In addition; the authors detect five steady states for the classic ethanol-water-benzene system for the dehydration of ethanol. Jalali and Seader (1999) have used homotopy continuation for robust multi-phase and multi-reaction equilibrium calculations. Another interesting

application of the method is for calculating all the azeotropes in a general multicomponent vapor-liquid mixture (Malone and Doherty (1998)). The algorithm is used in the commercial process simulator Aspen Plus.

Homotopy continuation methods have been extensively used in the literature for the simulation of reactive distillation systems. Chang and Seader (1987) use homotopy continuation for solving the highly non-linear governing MESH equations for the steady state simulation of an ethyl acetate RD column for different sets of specifications. Sneesby et al (1998) apply homotopy continuation to obtain multiplicities in ETBE and MTBE RD columns. A high conversion and a low conversion steady state are found in the solution diagram for the ETBE system. In the MTBE system, the authors have reported a narrow operating zone with five steady states at constant reboiler duty. Chen et al perform a bifurcation study using homotopy continuation with the Damkohler number as the continuation parameter, to obtain zones with three steady states in TAME and MTBE systems. Ciric and Miao (1994), apply homotopy continuation for the detection of multiple steady states in an ethylene glycol RD column using catalyst weight as the continuation parameter.

In addition to its widespread use for the detection of multiple steady states in RD systems, homotopy continuation has also been used for understanding the complex input output relations in RD systems. Al Arfaj and Luyben (2002) use homotopy continuation to detect input and output multiplicities in a methyl acetate RD column. Plots between the distillate rate and the reboiler duty at constant reflux rate or reflux ratio show the operating zones of output multiplicity. These plots clearly show that operating at constant reflux ratio is preferable over constant reflux as the zone of output multiplicity is very

narrow in case of the former. In a similar vein, Wang et al (2003) study steady state input output relations for an MTBE column to propose effective control strategies.

This completes a brief review of the literature on reactive distillation and homotopy continuation. Homotopy continuation will be extensively used in the our work for control structure screening and a systematic study of multiple steady states in commercially important RD systems for methyl acetate and MTBE production. Accordingly, the next chapter describes the mechanics of homotopy continuation as applied in our work to RD systems.

Homotopy Continuation Methods

The primary motivation behind this thesis is the systematic steady state analysis of RD columns for obtaining simple and robust control strategies. In this context, homotopy continuation is extensively used as a tool for understanding the steady state behaviour of RD columns. Continuation is applied to RD columns in two distinct ways. In the first case, continuation with respect to catalyst weight (or reactive tray hold-up) is used to study the presence of multiple steady states. The catalyst weight per tray is an important design variable that must be chosen so that steady state multiplicities are minimized. In the second case, continuation about a design steady state is used for studying the relationships between potential manipulated (input) and controlled (output) variables to verify the presence (or absence) of input or output multiplicities. A systematic study would reveal potential input output pairings that avoid multiplicities so that good control structures that ensure robust regulation of the column in the presence of disturbances are obtained.

Given the central role of homotopy continuation as a steady state analysis tool, this chapter describes the theory of popular homotopy continuation algorithms and its formulation for RD columns as applied in this work. The principal challenge in using homotopy continuation for obtaining the complete solution diagram is the strategy for continuation around turning points. Two popular methods in the literature are dynamic reparameterization and arc-length continuation. These are discussed in Section 3.1.

Section 3.2 formulates the homotopy continuation problem for RD columns for the two cases as discussed in the previous paragraph: (a) continuation with respect to the catalyst weight and (b) continuation with respect to operating conditions about a design steady state.

3.1 Homotopy Continuation Algorithms

Let us say we are interested in finding the variation in the steady state solution of a system of equations

$$\mathbf{h}(\mathbf{x}, \lambda) = 0 \quad \dots\dots\dots (3.1)$$

with respect to the parameter λ . Assuming that \mathbf{x}_0 is a known solution at $\lambda = \lambda_0$ so that $\mathbf{h}(\mathbf{x}_0, \lambda_0) = 0$, the parameter can be changed incrementally to $\lambda + \Delta\lambda$, and the corresponding solution $\mathbf{x}_0 + \Delta\mathbf{x}$ obtained using iterative equation solving algorithms such as the Newton Raphson method. The iterative algorithm will converge easily as the new solution $\mathbf{x}_0 + \Delta\mathbf{x}$ is close to \mathbf{x}_0 so that \mathbf{x}_0 is a good initial guess to start the iterations. Once the exact new solution is found, the procedure can be repeated to trace the complete solution branch that plots the variation of \mathbf{x} with respect to λ starting from \mathbf{x}_0 and λ_0 . This is the basic idea behind continuation methods.

In case the function $\mathbf{h}(\mathbf{x}, \lambda)$ is simple and there is a one to one correspondence between \mathbf{x} and λ , the above method can be applied with no problems. Complications however arise when there are multiple solutions \mathbf{x} that satisfy $\mathbf{h}(\mathbf{x}, \lambda) = 0$ for a particular value of the parameter λ . The case where all these solutions lie on the same solution branch indicates the presence of turning points with respect to λ . This is illustrated in Figure 3.1 where there are two turning points with three steady states between $\lambda = a$ and λ

= c. These three steady states are shown for $\lambda = b$ in the figure. The two turning points are also labeled.

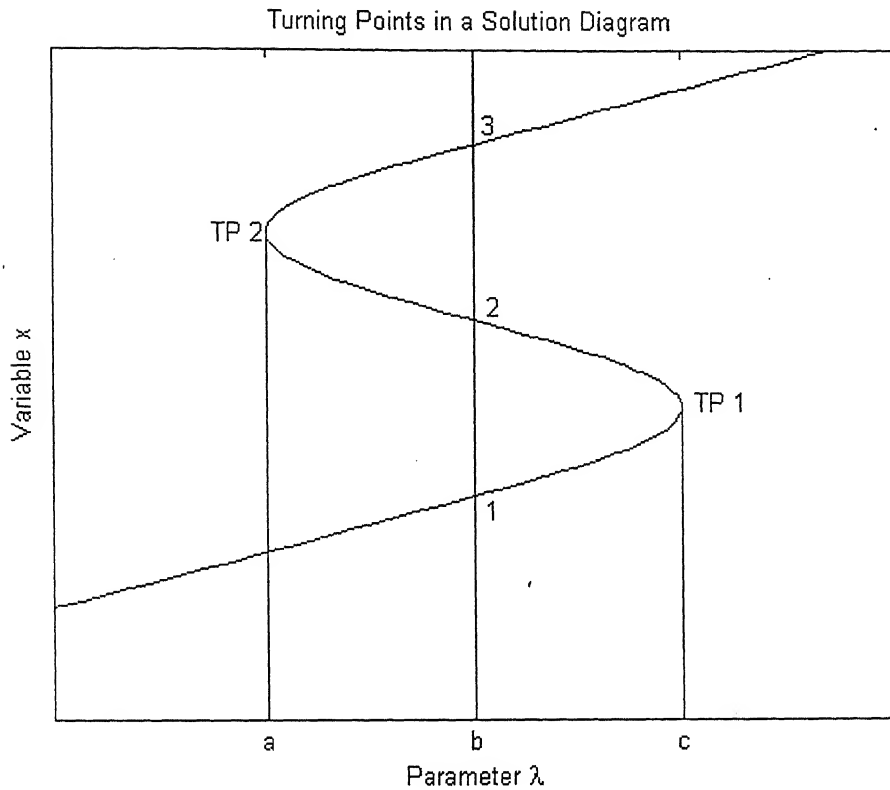


Figure 3.1: A complicated solution diagram with turning points

Tracing the solution diagram around the turning points is complicated as when the parameter value is increased beyond the turning point, the previous converged solution is no longer a good starting guess for the Newton Raphson (or other) equation solver. Even if convergence is obtained, the middle portion of the solution diagram will be completely missed. This is illustrated in Figure 3.2. Two popular methods, namely, dynamic reparameterization and arc-length continuation are employed in the literature to trace the

solution branch in a reliable manner around a turning point. These are discussed in the following sub-sections.

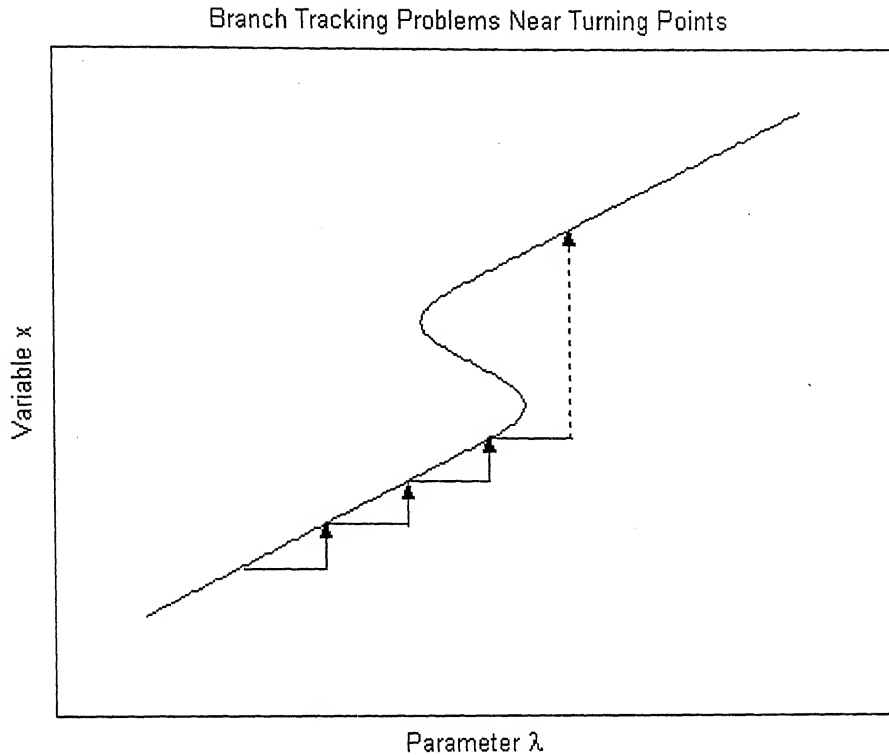


Figure 3.2: Illustration of problems in branch tracking near turning points

3.1.1 Dynamic Reparameterization

Dynamic reparameterization is in some sense, a “trick” method that utilizes the fact that a turning point with respect to λ is generally not one with respect to at least one of the variables x_j in \mathbf{x} . Thus rather than choosing a value of λ and then solving for \mathbf{x} , we choose a value of x_j and then solve for λ and the remaining \mathbf{x} variables. In other words, λ is replaced with x_j as the continuation parameter around turning points. The concept is

illustrated in Figure 3.3 for a scalar x variable. Note that at a turning point $dx/d\lambda = \infty$. Choosing the variable x_j with the smallest rate of change $dx_j/d\lambda$ as the new continuation variable is generally a good way for solution branch tracking.

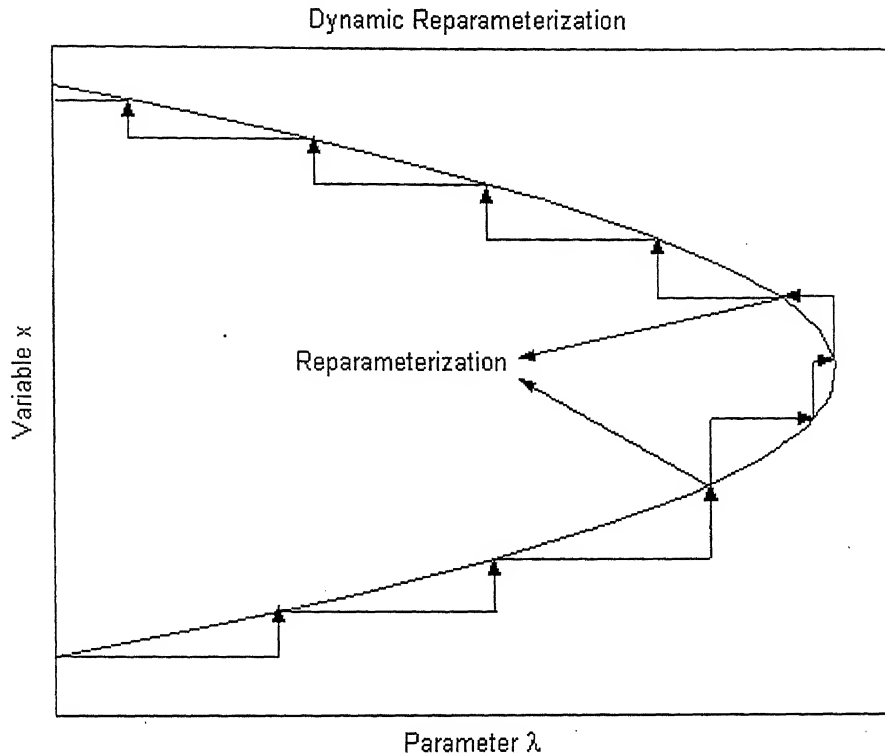


Figure 3.3: Illustration of dynamic reparameterization for branch tracking around turning points

Mathematically, let $\mathbf{x}_{j,\lambda+}$ denote \mathbf{x} with its j^{th} element replaced by λ i.e

$$\mathbf{x}_{j,\lambda+} = [x_1 \ x_2 \dots x_{j-1} \ \lambda \ x_{j+1} \dots x_n]^T$$

Then if x_j is used as the continuation parameter around a turning point, a value of x_j close to the previous point is chosen and the new value for $\mathbf{x}_{j,\lambda+}$ is found via Newton Raphson iterations. The Newton Raphson update formula is

$$\mathbf{x}_{j,\lambda+}^{k+1} = \mathbf{x}_{j,\lambda+}^k + t.[\mathbf{J}_{j,\lambda+}]^{-1} \cdot \mathbf{h}(\mathbf{x}_{j,\lambda+}) \dots\dots\dots (3.2a)$$

where t is the step-correction between 0 and 1 and $\mathbf{J}_{j-, \lambda+}$ is the Jacobian of \mathbf{h} with respect to $\mathbf{x}_{j-, \lambda+}$ and is obtained as

$$\mathbf{J}_{j-, \lambda+} = \begin{bmatrix} \partial h_1 / \partial x_1 & \cdots & \partial h_1 / \partial x_{j-1} & \partial h_1 / \partial \lambda & \partial h_1 / \partial x_{j+1} & \cdots & \partial h_1 / \partial x_n \\ \vdots & \ddots & \vdots & \vdots & \vdots & \ddots & \vdots \\ \partial h_j / \partial x_1 & \cdots & \partial h_j / \partial x_{j-1} & \partial h_j / \partial \lambda & \partial h_j / \partial x_{j+1} & \cdots & \partial h_j / \partial x_n \\ \vdots & \ddots & \vdots & \vdots & \vdots & \ddots & \vdots \\ \partial h_n / \partial x_1 & \cdots & \partial h_n / \partial x_{j-1} & \partial h_n / \partial \lambda & \partial h_n / \partial x_{j+1} & \cdots & \partial h_n / \partial x_n \end{bmatrix}$$

Once the turning point is crossed, the standard method of choosing a value of λ and then solving for \mathbf{x} is used. The Newton Raphson iteration formula in this case is

$$\mathbf{x}^{k+1} = \mathbf{x}^k + t \cdot [\mathbf{J}]^{-1} \cdot \mathbf{h}(\mathbf{x}^k, \lambda^k) \quad \dots\dots\dots (3.2b)$$

Here the Jacobian \mathbf{J} is defined as

$$\mathbf{J} = \begin{bmatrix} \partial h_1 / \partial x_1 & \cdots & \partial h_1 / \partial x_j & \cdots & \partial h_1 / \partial x_n \\ \vdots & \ddots & \vdots & \ddots & \vdots \\ \partial h_j / \partial x_1 & \cdots & \partial h_j / \partial x_j & \cdots & \partial h_j / \partial x_n \\ \vdots & \ddots & \vdots & \ddots & \vdots \\ \partial h_n / \partial x_1 & \cdots & \partial h_n / \partial x_j & \cdots & \partial h_n / \partial x_n \end{bmatrix}$$

Note that the Jacobian $\mathbf{J}_{j-, \lambda+}$ is the same as \mathbf{J} except that the j^{th} column in \mathbf{J} is replaced by $d\mathbf{h}/d\lambda$. Limits on the slope $dx/d\lambda$ may be used to trigger reparametrization as the solution branch is tracked. Thus if $dx/d\lambda > \text{tolerance1}$, x_j is used as the continuation and once the turning point is crossed and $dx/d\lambda < \text{tolerance2}$, we continue with respect to λ as the continuation parameter. Note that sign of the slope $dx/d\lambda$ determines if a positive or negative incremental change is made to λ . A similar argument also holds for other continuation variables.

It is quite clear from the discussion that the idea of dynamic reparameterization is very simple and easily programmable. We have therefore used it in this work on steady

state reactive distillation modeling. For the sake of completeness, a brief overview of the other popular method, arc-length continuation, is provided in the next sub-section.

3.1.2 Arc Length Continuation

In this case, the arc-length s is used to parameterize the solution branch. For the homotopy function $\mathbf{h}(\mathbf{x}, \lambda)$, no change in the function value occurs if we move exactly on the solution branch. In other words

$$\mathbf{dh} = \mathbf{h}_x \cdot d\mathbf{x} + \mathbf{h}_\lambda \cdot d\lambda = 0 \quad \dots\dots\dots (3.3)$$

along the solution branch with $\mathbf{h}_x = \partial \mathbf{h} / \partial \mathbf{x}$ and $\mathbf{h}_\lambda = \partial \mathbf{h} / \partial \lambda$. Dividing by the differential arc-length ds and putting the equation in matrix form, we get

$$\begin{bmatrix} \mathbf{h}_x & \mathbf{h}_\lambda \end{bmatrix} \begin{bmatrix} \dot{\mathbf{x}} \\ \dot{\lambda} \end{bmatrix} = 0 \quad \dots\dots\dots (3.4a)$$

where

$$\dot{\mathbf{x}} = d\mathbf{x}/ds$$

and

$$\dot{\lambda} = d\lambda/ds$$

For an n -element \mathbf{x} vector, there are $n+1$ total variables ($\dot{\mathbf{x}}$ and $\dot{\lambda}$) in equation 3.4a and only n relations. An additional relation is defined by the definition of arc-length from Pythagoras theorem as

$$\dot{\mathbf{x}}^2 + \dot{\lambda}^2 = 1 \quad \dots\dots\dots (3.4b)$$

Equations 3.4a and b form a square set of $n+1$ equations for $n+1$ variables. However, the arc-length definition (3.4b) is non-linear so that iterative methods may be necessary for solving the equations. The difficulty is however mitigated if we choose an arbitrary value

for $\dot{\lambda}$, solve for $[\dot{\mathbf{x}} \ \dot{\lambda}]^T$ and then normalize $[\dot{\mathbf{x}} \ \dot{\lambda}]^T$ to unit length to satisfy the arc-length definition constraint. For a chosen value of $\dot{\lambda} = 1$, from equation 3.4a, we get

$$\begin{bmatrix} \mathbf{h}_{\mathbf{x}} & h_{\lambda} \\ \mathbf{0} & 1 \end{bmatrix} \begin{bmatrix} \dot{\mathbf{x}} \\ \dot{\lambda} \end{bmatrix} = \begin{bmatrix} \mathbf{0} \\ 1 \end{bmatrix} \quad \dots\dots\dots (3.5a)$$

and obtain

$$\begin{bmatrix} \dot{\mathbf{x}} \\ \dot{\lambda} \end{bmatrix}_u = \begin{bmatrix} \mathbf{h}_{\mathbf{x}} & h_{\lambda} \\ \mathbf{0} & 1 \end{bmatrix}^{-1} \begin{bmatrix} \mathbf{0} \\ 1 \end{bmatrix} \quad \dots\dots\dots (3.5b)$$

The vector $[\dot{\mathbf{x}} \ \dot{\lambda}]_u^T$ gives the direction of the rate of change of \mathbf{x} and λ with respect to the arc length as we proceed along the solution branch. The subscript u is used to emphasize that the vector is unscaled. For standardization, this direction vector is normalized to a unit vector. The tangent direction unit vector at a point on the solution branch is then obtained as

$$[\dot{\mathbf{x}} \ \dot{\lambda}]^T = [\dot{\mathbf{x}} \ \dot{\lambda}]_u^T / \| [\dot{\mathbf{x}} \ \dot{\lambda}]_u^T \| \quad \dots\dots\dots (3.5c)$$

This tangential direction is also referred to as the Euler Predictor. If we proceed along this Euler Predictor direction with small enough arc-lengths, the complete solution branch can be tracked. In other words, if a small step Δs is taken along the Euler predictor direction, a new point on the solution branch is obtained as

$$\begin{bmatrix} \mathbf{x} \\ \lambda \end{bmatrix}_{\text{next}} = \begin{bmatrix} \mathbf{x} \\ \lambda \end{bmatrix}_{\text{current}} + \begin{bmatrix} \dot{\mathbf{x}} \\ \dot{\lambda} \end{bmatrix} \Delta s$$

In order to avoid accumulation of errors as the branch is tracked, the Newton Raphson method is used with $[\dot{\mathbf{x}} \ \dot{\lambda}]_{\text{next}}^T$ as the initial guess for the iteration variables to ensure accurate tracking of the branch. In the above formulation, turning points are still a

problem as near a turning point, \dot{x} obtained from equation 3.5 becomes very large as $d\lambda/ds = 0$. As in dynamic reparameterization, a different slope \dot{x}_j should be set to 1 instead of $\dot{\lambda}$ in equation 3.5(b) to calculate the tangential direction. Such reparametrization would ensure that the branch tracking progresses smoothly.

This completes a brief overview of popular homotopy continuation algorithms in the literature. The interested reader is referred to Seader (1987) for an excellent review of the method. The next section formulates function $h(x, \lambda)$ for reactive distillation problem as used in this work.

3.2 Reactive Distillation Problem Formulation

Reactive distillation involves simultaneous reaction and separation in a single column. Figure 3.4 shows a schematic of a general column with top down tray numbering. In order to develop a steady state model for the column, it is assumed that the vapor and liquid streams leaving a tray are at equilibrium. The equilibrium tray model is thus used to model the trays and the partial reboiler. A partial condenser is assumed so that it can also be treated as an equilibrium tray.

Figure 3.5 shows a tray with all the material and energy flows. In the nomenclature, the subscript i is used to denote the components while subscript j is used to denote the tray number. The capital letters F , V and L denote feed, vapor and liquid material streams respectively. Corresponding small letters are used to denote component flows. The letter Q is used to denote energy streams.

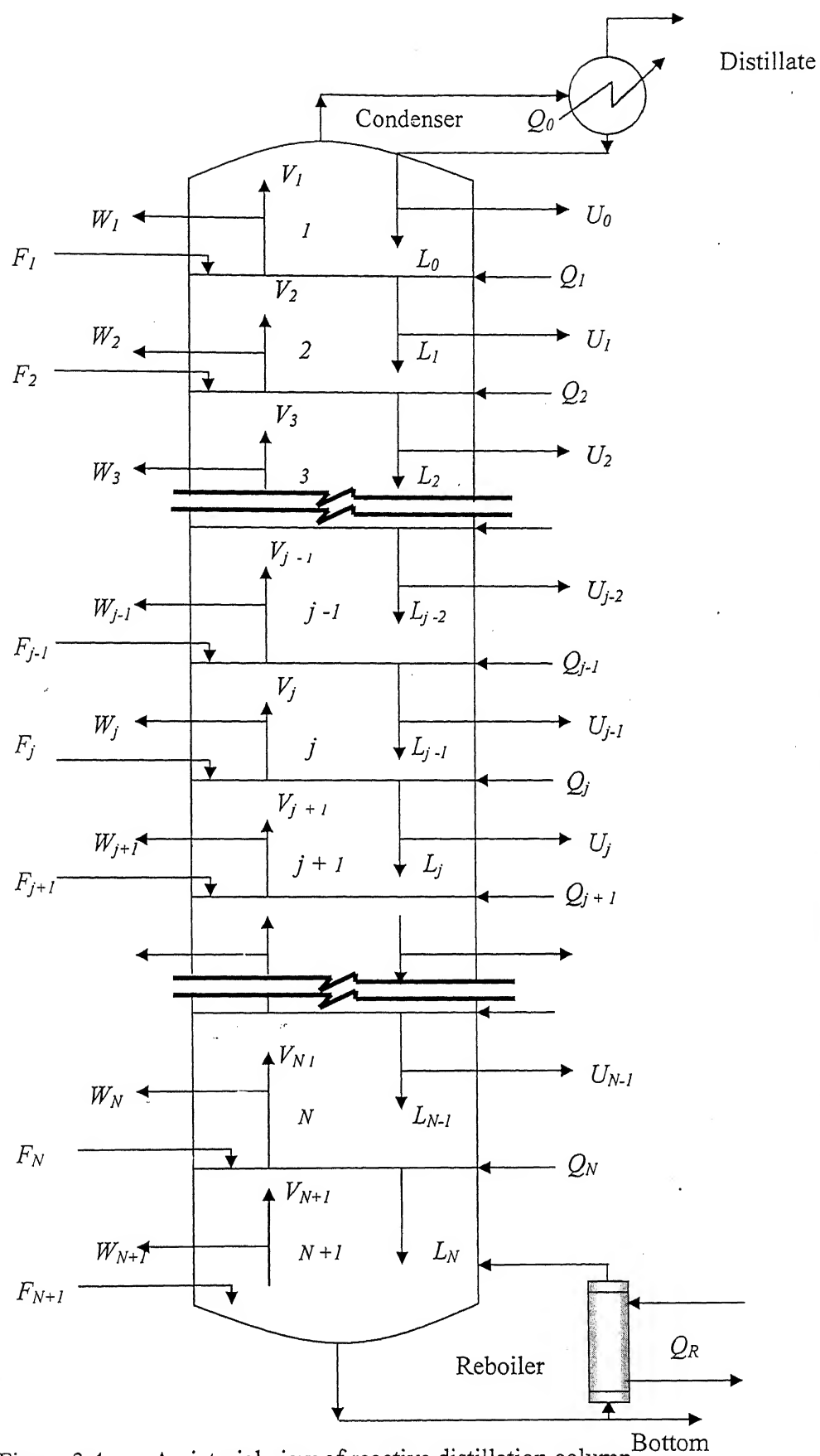


Figure 3.4 A pictorial view of reactive distillation column

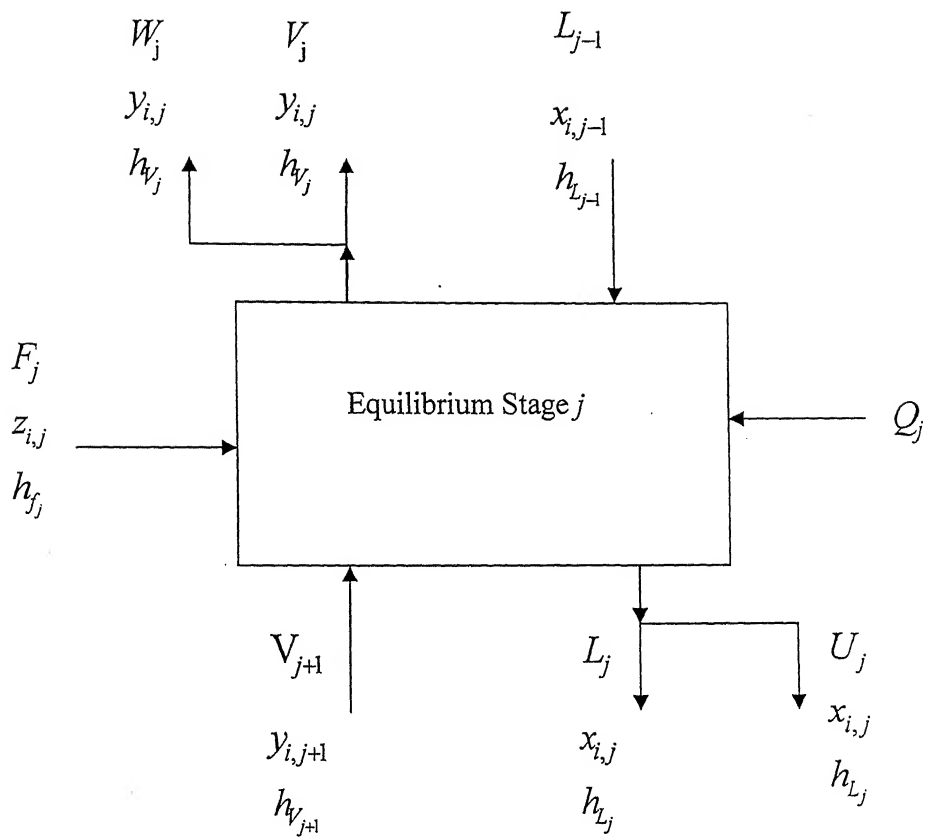


FIGURE 3.5: A schematic representation of an equilibrium stage j

Of the various possible steady state model formulations, the Naphtali-Sandholm formulation has been used in this work. The reader is referred to Singh, (2004) for an excellent treatise on the Naphtali-Sandholm method for reactive distillation systems. In brief, at steady state the mole balances, equilibrium relations and heat balance must be satisfied for all the trays, reboiler and partial condenser. For an N -tray, C -component system with NRX number of reactions, if all the feed material streams, heat streams, stage pressures and side stream splits are specified, a square system of equations results with $(N+2) \cdot (2C+1)$ equations and an equal number of variables. The governing MEH equations are

$$M_{i,j} = l_{i,j}(1 + s_j) + v_{i,j}(1 + S_j) - l_{i,j-1} - v_{i,j+1} - f_{i,j} - \sum_{n=1}^{NRX} v_{i,n} r_{j,n} = 0 \quad \dots (3.6)$$

Equilibrium Relations

$$E_{i,j} = \frac{\eta_j K_{i,j} l_{i,j} \sum_{k=1}^c v_{k,j}}{\sum_{k=1}^c l_{k,j}} - v_{i,j} + \frac{(1 - \eta_j) v_{i,j+1} \sum_{k=1}^c v_{k,j}}{\sum_{k=1}^c v_{k,j+1}} = 0 \quad \dots (3.7)$$

Heat Balance

$$H_j = h_{L,j}(1 + s_j) \sum_{i=1}^c l_{i,j} + h_{V,j}(1 + S_j) \sum_{i=1}^c v_{i,j} - h_{L,j+1} \sum_{i=1}^c l_{i,j+1} - h_{V,j+1} \sum_{i=1}^c v_{i,j+1} - h_{F,j} \sum_{i=1}^c f_{i,j} - Q_j = 0 \quad \dots (3.8)$$

In the above relations $i = 1$ to C and $j = 1$ to $N+2$ so that there are a total of $(N+2)(2C+1)$ MEH equations. The above formulation assumes that the condenser and reboiler duties are specified since these are tray heat specifications for tray 1 (condenser) and tray $N+1$ (reboiler) respectively. In other words, the column degree of freedom is 2. Specifying the condenser duty and the reboiler duty is not a good idea as the two are related through an overall energy balance around the column. Thus if values that cannot satisfy the energy balance are input, the algorithm would refuse to converge. Alternative specifications that make more sense and converge easily are certainly possible. This is done by replacing the enthalpy balances for the condenser and reboiler respectively by the appropriate specification equations. Table 3.1 lists the replacement equations for some common specifications. The replacement equations for a total condenser are also noted in Table 3.2.

Table 3.1: The replacement functions for H_I and H_N

S.No.	Specification	Replacement for H_I	Replacement for H_N
1	Distillate or Bottom rate	$\sum_{i=1}^C v_{i,1} - D = 0$	$\sum_{i=1}^C l_{i,N} - B = 0$
2	Reflux or reboil ratio	$\sum_{i=1}^C l_{i,1} - (L/D) \sum_{i=1}^C v_{i,1} = 0$	$\sum_{i=1}^C v_{i,N} - (V/B) \sum_{i=1}^C l_{i,N} = 0$
3	Condenser or reboiler temperature	$T_1 - T_d = 0$	$T_N - T_B = 0$
4	Component mole fraction in product	$\sum_{i=1}^C v_{i,1} - (\sum_{i=1}^C v_{i,1}) y_{iD} = 0$	$\sum_{i=1}^C l_{i,N} - (\sum_{i=1}^C l_{i,N}) x_{iB} = 0$
5	Component flow rate in distillate or bottom	$v_{i,1} - d_i = 0$	$l_{i,N} - b_i = 0$
6	Reflux rate or Boilup rate	$\sum_{i=1}^C l_{i,1} - L_1 = 0$	$\sum_{i=1}^C l_{i,N} - L_N = 0$

Table 3.2: Replacement equations for total condenser

Equation	Partial	Total
Equilibrium equations	$E_{i,j} = \frac{\eta_j K_{i,j} l_{i,j} \sum_{k=1}^C v_{k,j}}{\sum_{k=1}^C l_{k,j}} - v_{i,j} +$ $\frac{(1 - \eta_j) v_{i,j+1} \sum_{k=1}^C v_{k,j}}{\sum_{k=1}^C v_{k,j+1}} = 0$ <p>for $i = 1 : C$</p>	$E_{i,1} = \sum_{p=1}^C (K_{i,p} l_{i,p} \frac{\sum_{k=1}^C v_{k,1}}{\sum_{k=1}^C l_{k,1}} - v_{i,p})$ <p>for first component</p> $E_{i,1} = l_{i,1} \frac{\sum_{k=1}^C v_{k,1}}{\sum_{k=1}^C l_{k,1}} - v_{i,1} = 0$ <p>for $i = 2 : C$</p>

In the Naphtali Sandholm method, the component vapor and liquid flows leaving a tray and the tray temperatures are used as iteration variables. The governing MEH equations are linearized and the Newton Raphson method is used to converge to a bonafide steady state. The tridiagonal algorithm is used to arrive at reasonable initial guesses for the iteration variables.

3.2.1 Homotopy Continuation With Respect to Catalyst Weight

The mole balances in the governing equations contain a generation term due to reaction. In the limiting case when this term is set to 0, the problem reduces to ordinary distillation with no reaction. A solution to the problem is easily found using the Naphtali-Sandholm method. This is akin to setting the catalyst weight (or hold-up for homogenous reactions) to 0 so that no reaction occurs. The catalyst weight can now be slowly increased to reach the steady state solution at the design catalyst weight. In order to implement the continuation, a catalyst weight factor L is used in the M equations such that at $L=0$, the reaction term vanishes and at $L=1$, the reaction term corresponds to the design catalyst weight. More formally, the M equation is modified as

$$M_{i,j} = l_{i,j}(1 + s_j) + v_{i,j}(1 + S_j) - l_{i,j-1} - v_{i,j+1} - f_{i,j} - L \sum_{n=1}^{NRX} v_{i,n} r_{j,n} = 0 \quad \dots (3.9)$$

Continuation with respect L generates the solution diagram of interest that clearly shows the existence of steady state multiplicities. The Naphtali-Sandholm algorithm for a given value of L is used to obtain the converged solution. Around turning points, dynamic

reparameterization is used and the appropriate column of the Jacobian matrix is replaced by dh/dL .

$$\text{Note that } \frac{dh}{dL} = - \sum_{n=1}^{NRX} v_{i,n} r_{j,n} \dots\dots\dots (3.10)$$

3.2.2 Homotopy Continuation About the Design Steady State

Reactive distillation columns are designed for high purity products with high reaction conversion. Given that multiple steady states are routine in RD systems, appropriate control strategies must be implemented to ensure that the product purity and reaction conversion is maintained for all throughputs and expected feed composition changes. This requires a systematic study of the different input-output relationships in the column.

For this purpose, continuation about the design steady state with respect to one of the specification variables such as reflux ratio, reboiler duty, tray temperature or tray composition is used to study the input-output relationships around the design steady state. In real-time operation appropriate control loops are used to maintain the column at these specifications. The specifications that result in simple input-output relationships with no multiplicities while maintaining product purity and reaction conversion are the ones that should be implemented. The corresponding control structure would be most robust in regulating the column for different production rates and disturbances such as feed composition change. Homotopy continuation techniques are necessary as the input-output relationships can be highly non-linear with output / input multiplicities. Output multiplicities occur when there are more than one values for the output variables such as

reaction conversion, product purity and tray temperature / composition profiles for a particular specification such as the reboiler duty, reflux rate and reflux ratio. Input multiplicities occur when there are multiple input specifications that give the same value for an output variable.

It is noted that continuation about a design steady state is easier to implement than the catalyst weight homotopy continuation described earlier. This is because a standard RD simulator can be used to obtain the solution diagram as one of the specification variables is changed. It is also highlighted that the various choices of specifications in the Naphtali-Sandholm method would ensure accurate branch tracking around turning points using dynamic reparameterization.

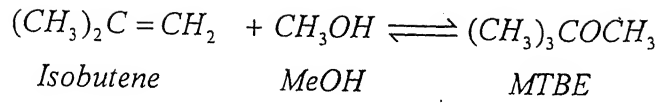
This completes a brief overview of the homotopy continuation method and its formulation for reactive distillation as applied in this work. The next two chapters describe, respectively, the application of catalyst weight continuation to methyl acetate and MTBE RD systems and control structure screening for an MTBE column using continuation with respect to a column specification about the design steady state.

Homotopy Continuation with respect to Catalyst Weight

In this chapter, homotopy continuation with respect to catalyst weight is applied to two RD systems of commercial interest, namely, MTBE and methyl acetate. In the MTBE system, for a specified reflux ratio and bottoms flow rate, upto five steady states are detected in the solution diagram on two distinct branches. Two of these steady states disappear in the limit of reaction equilibrium on reactive stages at high catalyst weight. For the methyl acetate system, at fixed reflux rate and reboiler duty, three distinct steady states are seen in the solution diagram on two separate branches. In case the column specification is changed to fixed reflux ratio and reboiler duty, the solution diagram shows only a single steady state for all catalyst weights. Since each specification set corresponds to a particular column control strategy, these results show that the number of steady states can be affected by the control structure used and the catalyst weight per tray. The same must be chosen appropriately to minimize the steady state multiplicities for robust column operation and control.

4.1 Case Study I: Methyl Tertiary Butyl Ether (MTBE)

MTBE is an important industrial chemical used as a key octane enhancing ingredient in unleaded gasoline. Isobutene reacts with methanol to produce the desired product, MTBE, in the presence of an inert component, n-butane. The reaction is as follows



An activity- based rate model expression is used to describe the kinetics of MTBE synthesis catalyzed by an ion exchange resin. The kinetic expression from Seader and Henley (1998) is used after replacing the component mole fractions with component activities. The modified rate expression for the forward reaction is

$$r_{forward} = 3.67 \times 10^{12} \exp(-92440 / RT) a_{IB} / a_{MeOH}$$

The corresponding backward rate law is

$$r_{backward} = 2.67 \times 10^{17} \exp(-134,454 / RT) a_{MTBE} / a_{MeOH}^2$$

where,

$$a_i = \gamma_i x_i$$

The units of r are in moles per second per equivalent of acid groups. The catalyst is a strong ion exchange resin with 4.9 equivalents of acid groups per kilogram of catalyst. T is in kelvins and x_i is the liquid mole fraction. The liquid-phase activity coefficients γ_i are modeled using the Wilson equation. The Wilson binary interaction parameters are taken from Doherty (2002) and are tabulated in Table 4.1.

Table 4.1: Wilson interaction parameters for MTBE system

Wilson Parameters		IB	MeOH	MTBE	NB
$a_{i,j}$	IB	0.0	-0.7420	0.2413	0.0729
	MeOH	0.7420	0.0	0.9833	0.8149
	MTBE	-0.2413	-0.9833	0.0	-0.1684
	NB	-0.0729	-0.8149	0.1684	0.0
$b_{i,j}$	IB	0.0	-85.5447	30.2477	0.0
	MeOH	-1296.719	0.0	-746.3971	-1149.280
	MTBE	-136.6574	204.5029	0.0	0.0
	NB	0.0	-192.4019	0.0	0.0

4.1.1 Column Configuration:

The reactive distillation column shown in Figure 4.1 is used as the basis for this study. A similar column has been studied by Wang et al. (2003). The column consists of 15 trays, a total condenser, and a partial reboiler. There are three zones in the column, a rectification zone (tray 1 and 2), a stripping zone (trays 11-15) and a reactive zone (trays 3- 10). Mixed-butenes vapor at 350 K comprising 36% isobutylene and 64% inert n-butane by mole is fed to the column on tray 10. Pure methanol liquid at 320 K is fed on tray 9. The flow rates of methanol and mixed-butenes are nearly stoichiometric at 712.8 and 1969.2 kmol/hr, respectively. The reflux ratio and bottoms flow rate are specified as 7 and 640.8 kmol/hr, respectively. Pressure throughout the column is assumed to be 11 atmospheres. High purity MTBE leaves in the bottoms stream while the unreacted isobutene and methanol and the n-butane inert are removed in the distillate stream.

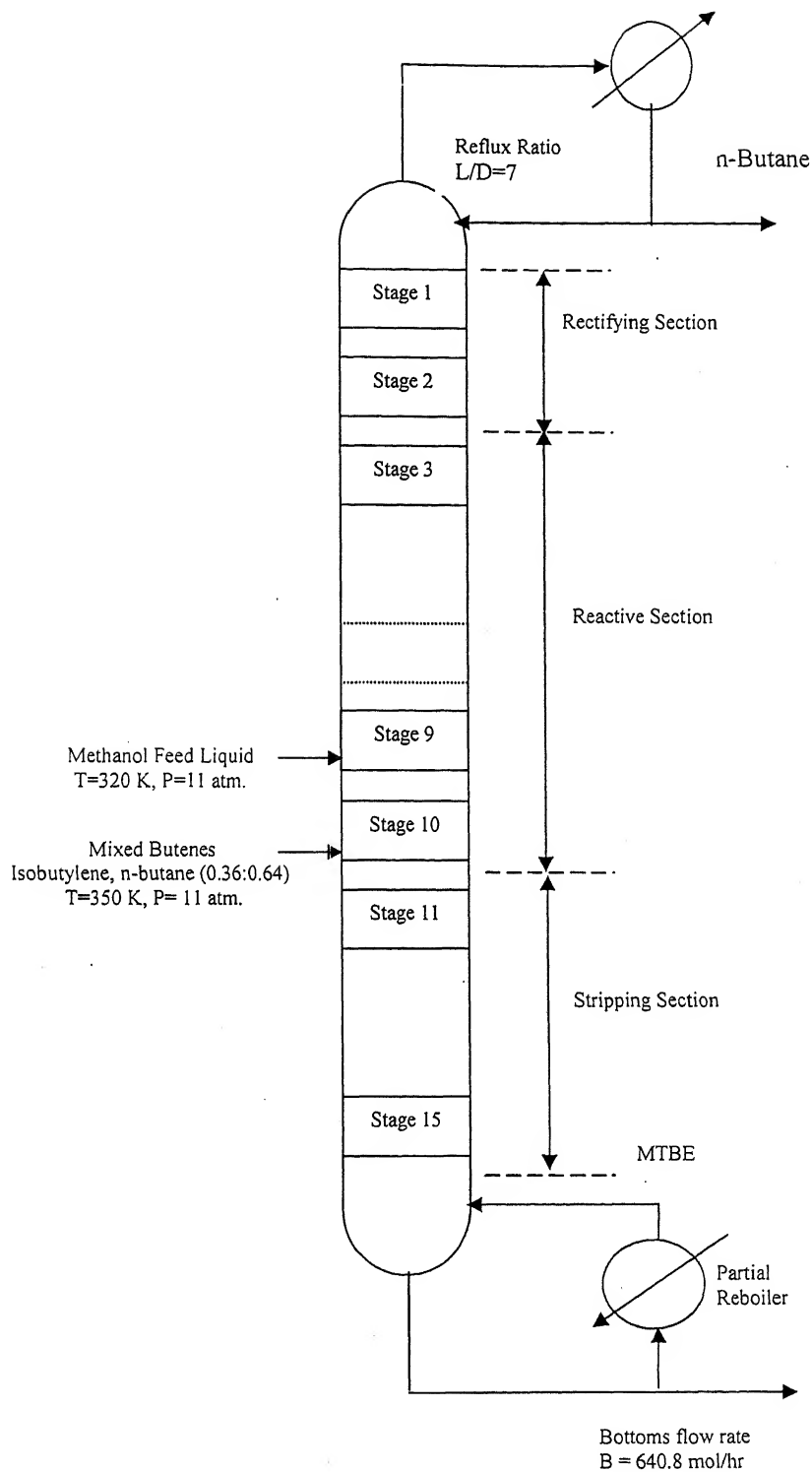


Figure 4.1: Reactive distillation column configuration for MTBE synthesis

4.1.2 Multiple Steady States by Continuation with Respect to Catalyst Weight:

Homotopy Continuation with respect to catalyst weight is used to obtain the complete solution diagram. The reflux ratio and bottoms flow rate are assumed fixed as in Figure 4.1. In order to easily see the steady state multiplicities, the conversion and bottoms MTBE purity are plotted against L , the catalyst weight factor in Figure 4.2. Two distinct branches are seen in the solution diagram for both purity and the conversion. Branch 1 is obtained by starting from the non-reactive solution and then introducing reaction by slowly increasing L . A starting point on branch 2 is obtained by solving the governing steady state RD equations using the traditional Naphtali-Sandholm method for the design catalyst weight ($L=1$). Continuation with respect to L about this steady state solution traces the second branch.

Branch 1 has a single turning point at $L = 0.705$ while Branch 2 has two turning points at $L = 1.068$ and $L = 0.293$ respectively. These turning points divide the complete solution diagram into four distinct regions with different number of steady states. As the catalyst weight factor is increased, the number of solutions increase or decrease by 2 when a turning point is crossed. In the first region corresponding to low catalyst weights ($L < 0.293$) only one steady state solution exists on Branch 2. On crossing the turning point corresponding to $L = 0.293$ on Branch 2, the number of steady states increases to three are seen in the second region for which $0.293 < L < 0.705$. All these solutions lie on Branch 2. As the catalyst weight is further increased, two additional steady states corresponding to Branch 1 are encountered so that there a total of five steady states in the third region for which $0.705 < L < 1.068$. Moving beyond the $L = 1.068$ turning point on Branch 2, two of

the steady state solutions on Branch 2 disappear so that only three steady state solutions remain in the fourth region with $L > 1.068$. Two of these solutions lie on Branch 1 while the remaining one lies on Branch 2. The number of steady state solutions thus increases from one at low catalyst weights to three at intermediate catalyst weights. Five steady states are seen for a narrow range of catalyst weights in the kinetically controlled regime which reduces back to three at high catalyst weights when reaction equilibrium is approached on the reactive stages.

The design catalyst weight ($L=1$), lies in region three so that there are a total of five steady states. The five steady states are labeled in Figure 4.2. Steady states I and II, lie on solution Branch 1 while the remaining steady states, III, IV and V, lie on Branch 2. The distillate and bottoms composition and reaction conversion for these five steady states are tabulated in Table 4.2. Of all these steady states, the high conversion steady state (Steady State V) with a conversion of 90.28% and product purity of 99.92%, is the most important as process economics dictates that conversion be as high as possible to enhance product purity and minimize the recycle of unreacted reactants.

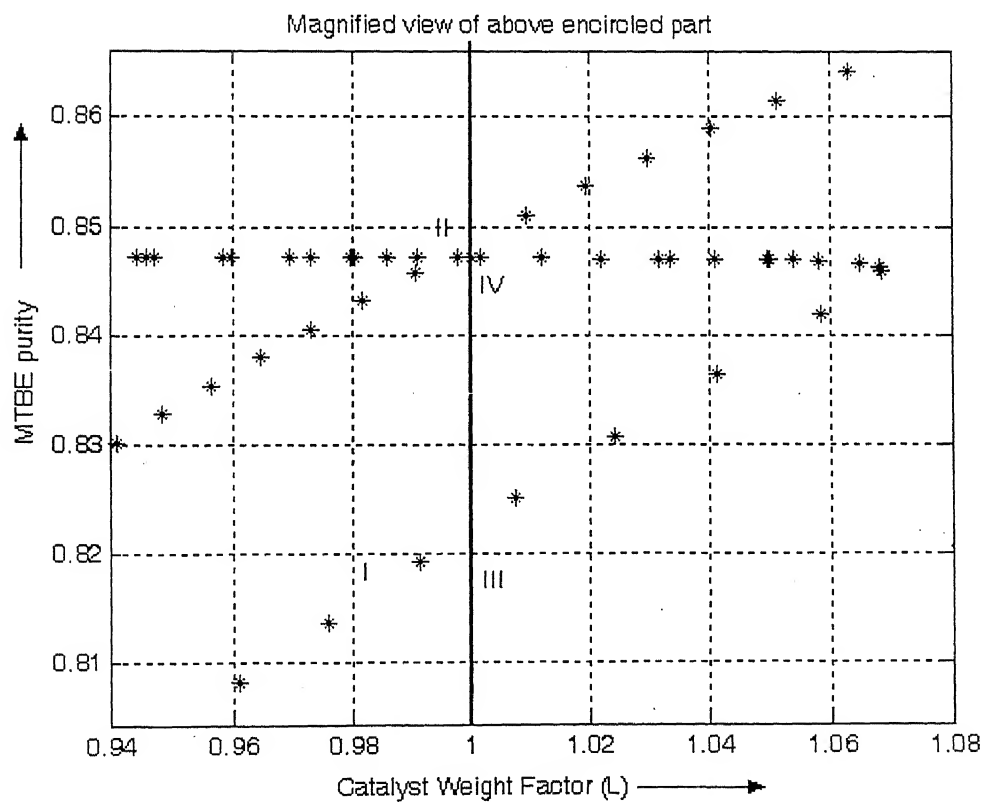
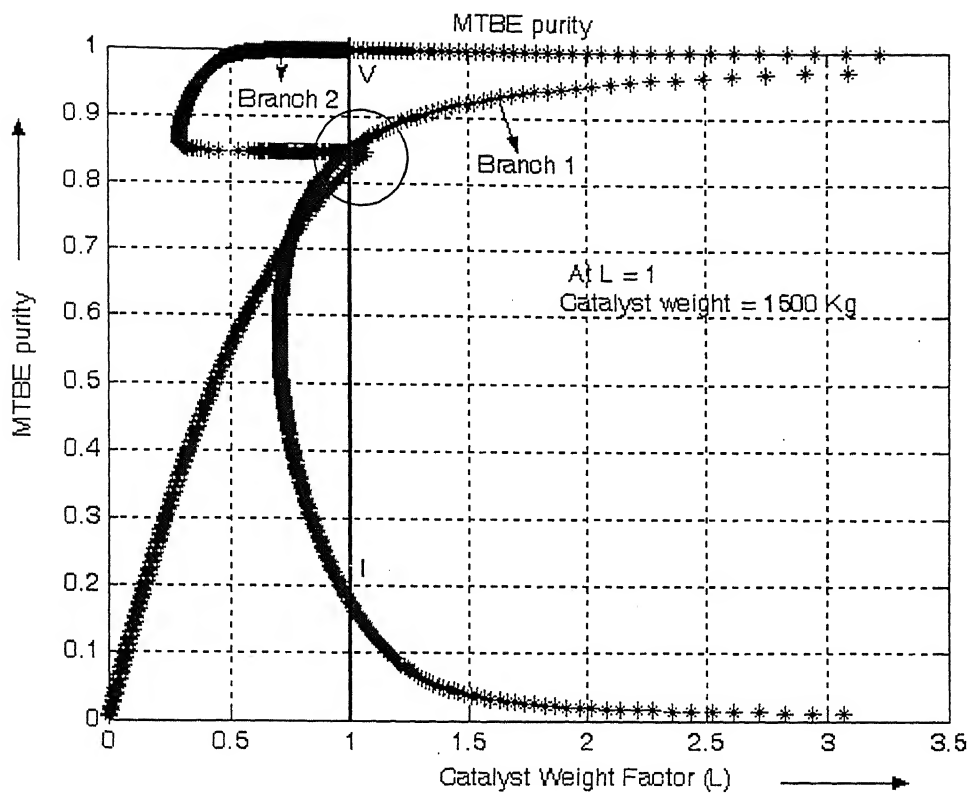


Figure 4.2: Multiple steady states in MTBE for purity

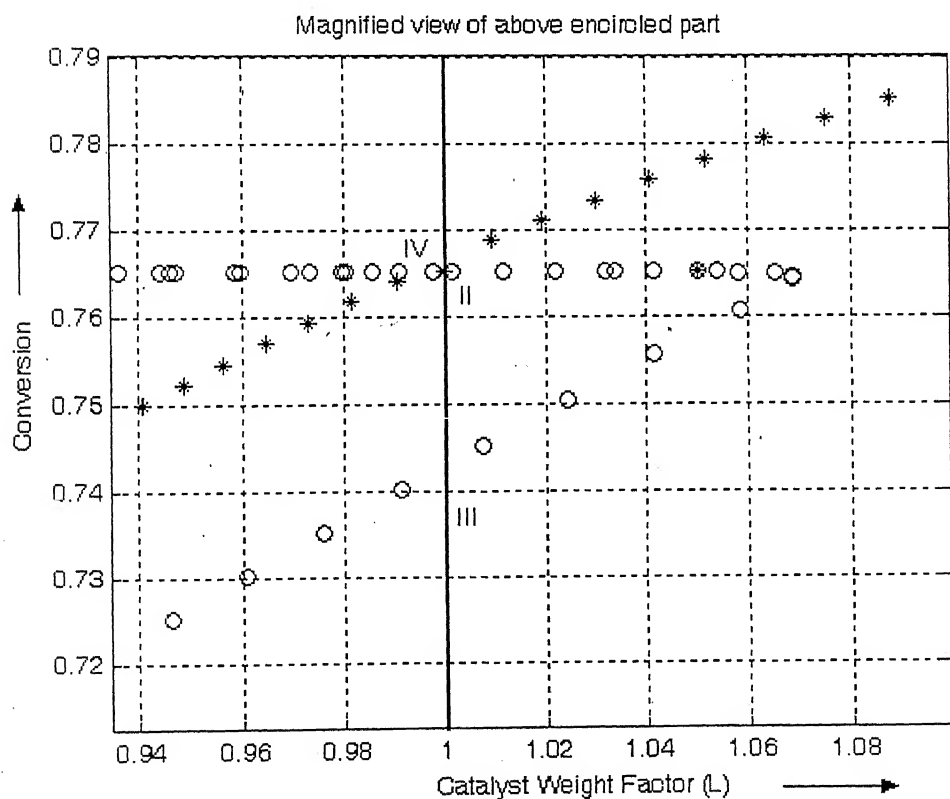
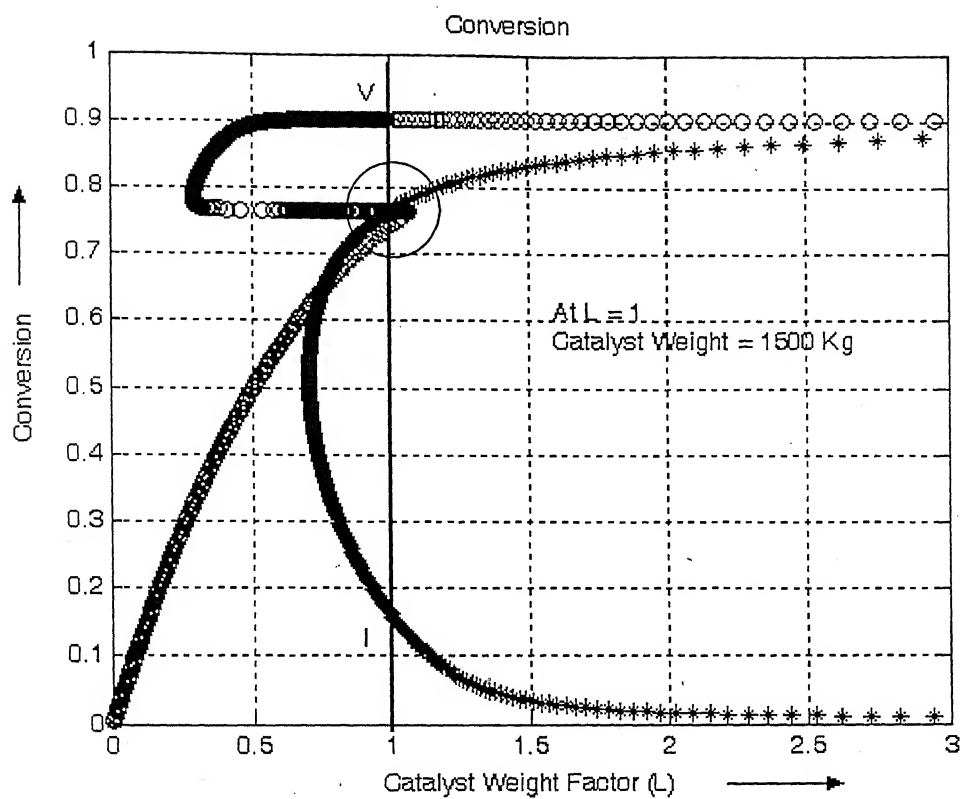


Figure 4.2: Multiple steady states in MTBE for conversion

Table 4.2: The distillate and the bottoms composition and reaction conversion for five steady states MTBE system

SS	Distillate Composition				Bottoms Composition				Conversion
	IB	MeOH	MTBE	NB	IB	MeOH	MTBE	NB	
I	0.2791	0.0110	0.0015	0.7084	0.0000	0.8243	0.1757	0.0000	15.95 %
II	0.0970	0.0156	0.0006	0.8868	0.0000	0.1515	0.8485	0.0000	76.67 %
III	0.1008	0.1138	0.0001	0.7853	0.0062	0.0257	0.8193	0.1488	74.02 %
IV	0.0921	0.1141	0.0001	0.7937	0.0054	0.0001	0.8471	0.1474	76.53 %
V	0.0428	0.172	0.0003	0.9397	0.0000	0.0001	0.9992	0.0007	90.28 %

In order to better understand these steady states, Figure 4.3 plots the product formation rate on the reactive trays for the five steady states. The temperature and components composition profiles are also shown in the Figure 4.4 and Figure 4.5 respectively. Since the kinetic expression is quite complex with the methanol activity being in the denominator, it is hard to interpret the reasons for the very different product formation rates for the five steady states.

For the low conversion steady state (SS I), a substantial temperature increase of more than 30 K occurs on the reactive trays (4-11). Since the activation energy of the backward reaction is larger than that for the forward reaction, the backward rate constant increases about 50 times while the forward rate constant only increases by about 15 times. Also, since for the backward reaction, the reaction order with respect to methanol is -2, the a_3/a_2^2 term remains more than 1 as we move to tray 11. Thus even though substantial forward reaction occurs on reactive stages 4 to 7, the net production is nearly zero as the backward reaction is favored on trays 8 to 10 due to larger backward reaction rate. The increase in temperature for SS 2 is less severe so that the backward reaction on trays 8-11 is relatively lesser than the forward reaction on trays 4-8. An intermediate conversion of 76.7% is therefore obtained.

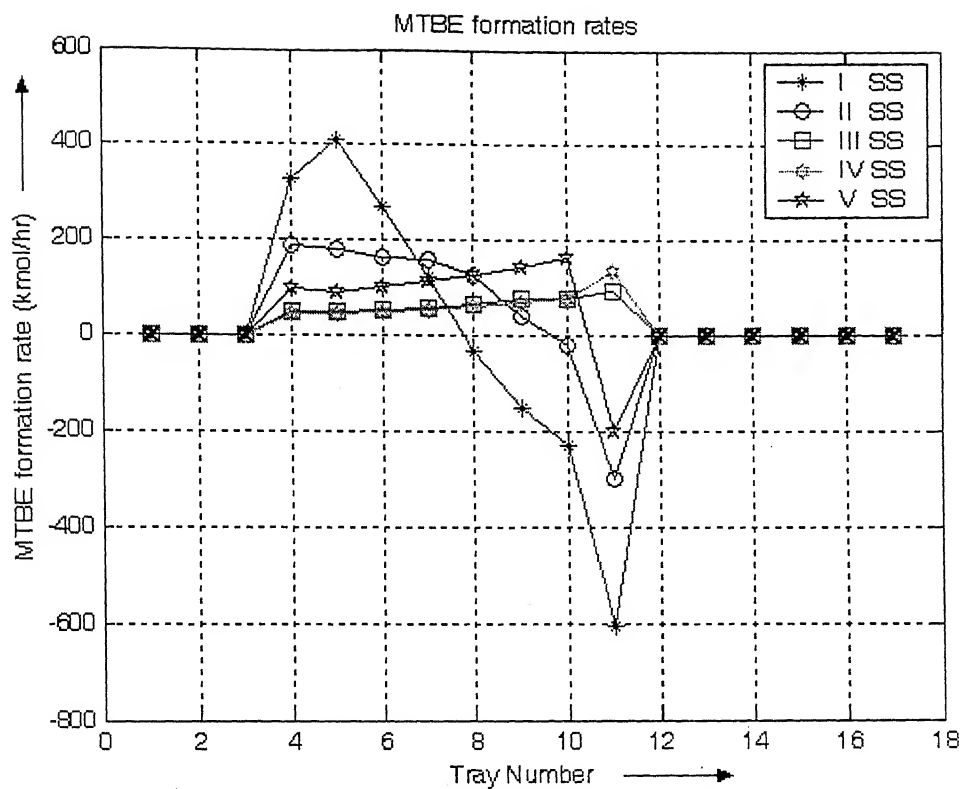


Figure 4.3: MTBE formation rates for five steady states

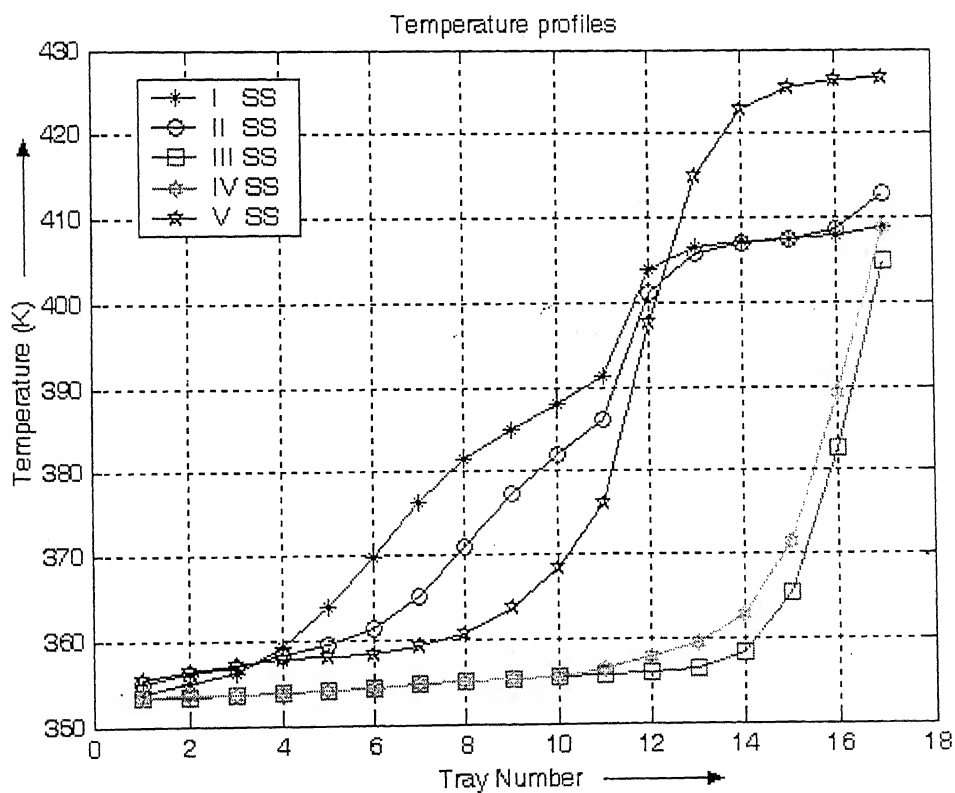


Figure 4.4: Temperature profiles for five steady states for MTBE system

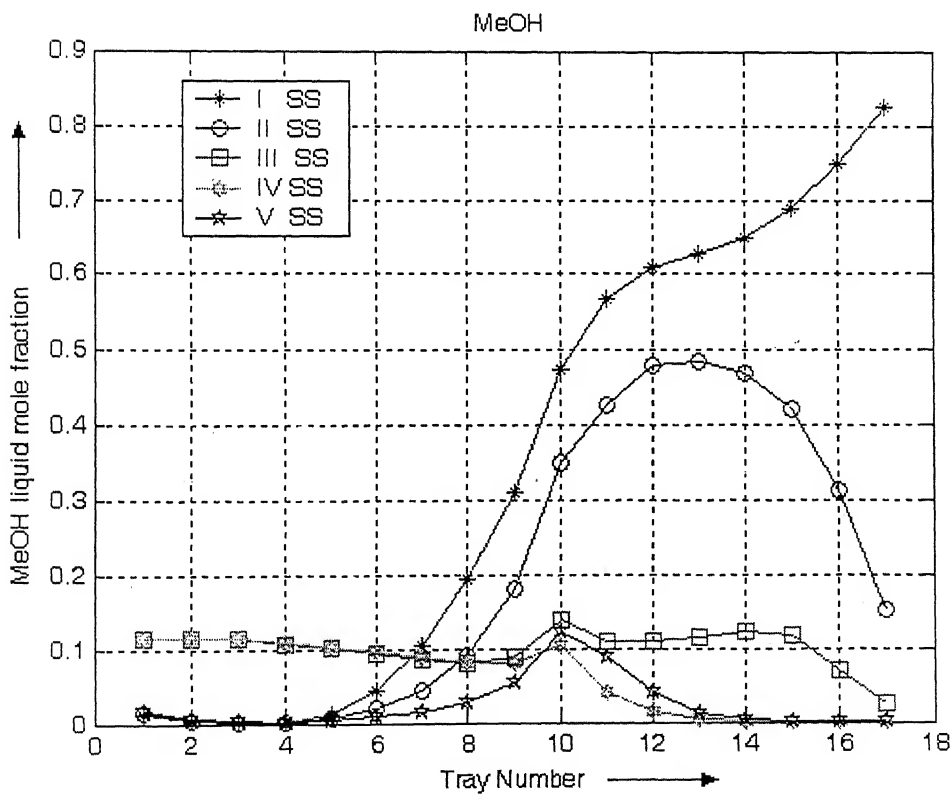
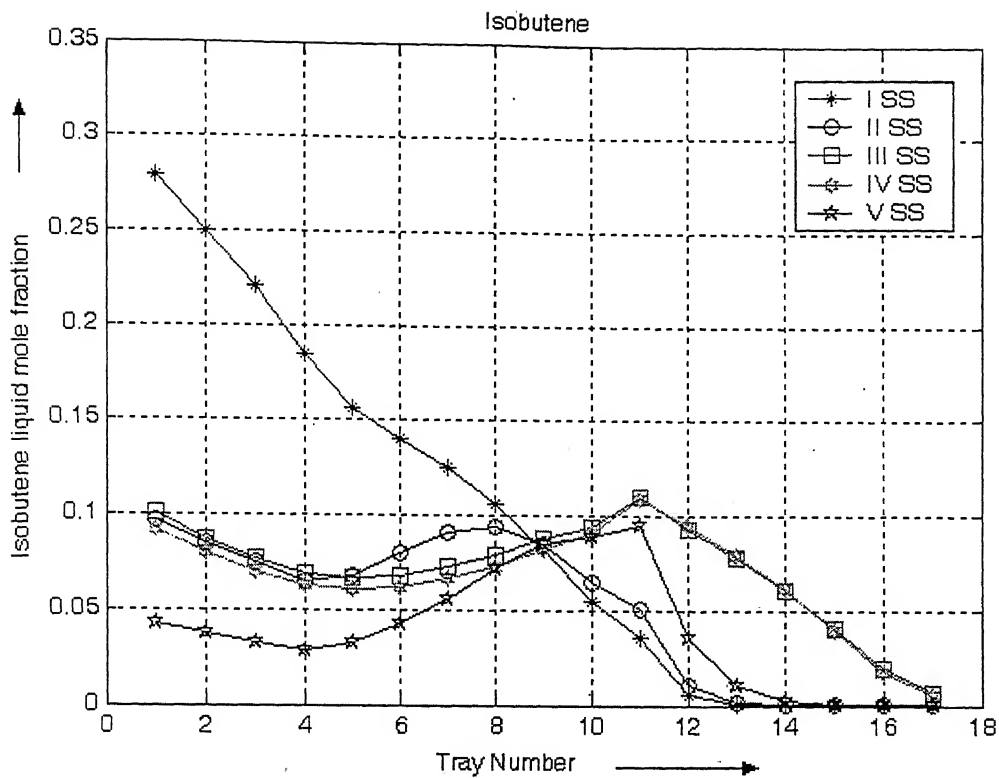


Figure 4.5: Compositions profiles for five steady states for MTBE system

Contd...

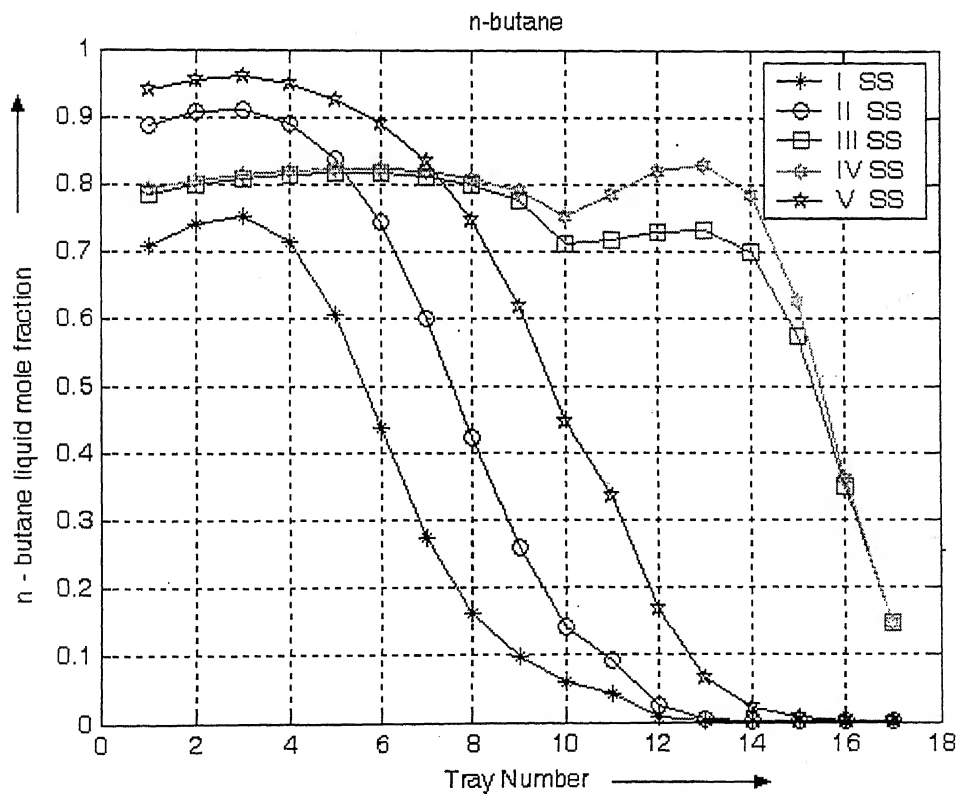
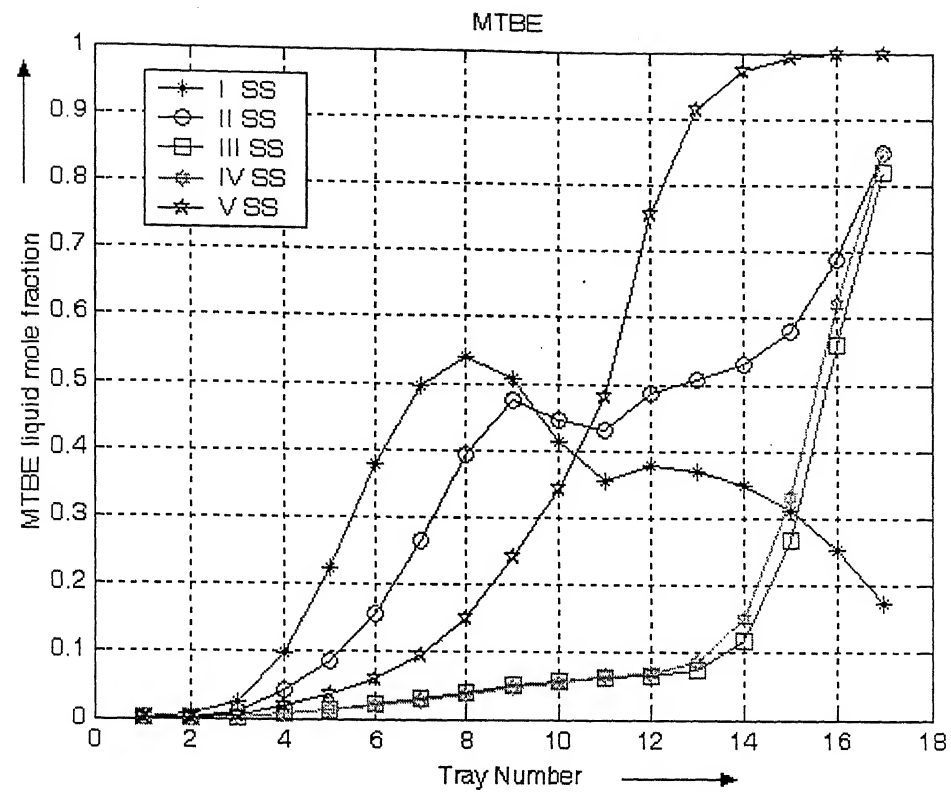


Figure 4.5: Compositions profiles for five steady states for MTBE system

The next two steady states, SS III and IV are very similar to each other in that a negligible change in temperature occurs on the reactive trays 4-11. The product formation profile is therefore flat. A net formation of MTBE occurs on all the reactive stages. Since the tray temperatures are lower compared to all other steady states, the product formation rates are also lower giving again an intermediate conversion of 74% and 76.5%, respectively. For the high conversion steady state, SS V, higher product generation occurs for stages 4 to 10 with net consumption occurring on stage 11. The consumption on tray 11 is due to the substantial temperature rise across the reactive stages. Also, the low methanol mole fraction on tray 11 causes a_3/a_2^2 to be nearly 4 leading to a net backward reaction on tray 11. The overall effect of higher product generation on all the reactive trays except tray 11 is a net conversion of about 90%. The Activity ratios, forward and backward reaction rate are tabulated in Table 4.3.

For the MTBE system, several researchers have reported multiple steady states. Jacobs and Krishna (1993) found a high and a low conversion steady state. Chen et al. (2002) use catalyst weight homotopy continuation to report another steady state with intermediate conversion. Of the total three steady states, two lie on one solution branch and the last one on another solution branch. Sneesby et al (1998) trace the solution diagram by varying the reflux ratio at constant reboiler duty. They report a narrow zone of operating conditions with five steady states. Our results therefore are in qualitative agreement with these different literature reports.

Table 4.3. Activity ratio, forward reaction rate, back ward reaction rate and total reaction rates for five steady states of MTBE system

Table 4.3a		$k_f, \text{ kmol hr}^{-1} (\text{kg catalyst})^{-1}$					a_1/a_2					$r_f \times 10^{-3}, \text{ kmol hr}^{-1}$				
S.S.		I	II	III	IV	V	I	II	III	IV	V	I	II	III	IV	V
Tray No.																
4		0.486	0.446	0.304	0.305	0.426	5.846	1.533	0.109	0.099	0.625	4.260	1.026	0.050	0.045	0.398
5		0.716	0.491	0.311	0.312	0.436	1.238	0.567	0.107	0.097	0.366	1.330	0.417	0.050	0.046	0.240
6		1.188	0.576	0.319	0.319	0.451	0.557	0.368	0.112	0.102	0.293	0.984	0.318	0.053	0.049	0.198
7		1.989	0.792	0.327	0.327	0.481	0.377	0.303	0.122	0.112	0.266	1.126	0.360	0.060	0.055	0.192
8		2.949	1.284	0.337	0.336	0.550	0.288	0.261	0.138	0.127	0.252	1.274	0.502	0.070	0.064	0.208
9		3.845	2.104	0.346	0.345	0.711	0.221	0.219	0.152	0.144	0.236	1.277	0.690	0.079	0.074	0.252
10		4.788	3.063	0.349	0.348	1.042	0.161	0.171	0.155	0.154	0.212	1.155	0.785	0.081	0.080	0.331
11		6.151	4.176	0.353	0.378	1.926	0.115	0.143	0.188	0.254	0.306	1.060	0.897	0.100	0.144	0.883

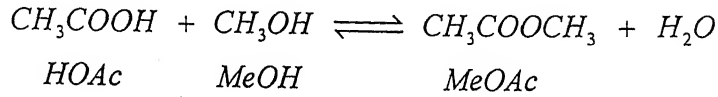
Table 4.3b		$k_b, \text{ kmol hr}^{-1} (\text{kg catalyst})^{-1}$					a_3/a_2					$r_b \times 10^{-3}, \text{ kmol hr}^{-1}$				
S.S.		I	II	III	IV	V	I	II	III	IV	V	I	II	III	IV	V
Tray No.																
4		0.027	0.024	0.049	0.014	0.022	96.55	23.31	0.014	0.133	8.917	3.933	0.839	0.000	0.000	0.300
5		0.048	0.028	0.051	0.014	0.023	12.83	5.697	0.028	0.026	4.281	0.920	0.235	0.001	0.001	0.149
6		0.099	0.035	0.053	0.014	0.024	4.828	2.977	0.044	0.041	2.653	0.714	0.155	0.001	0.001	0.100
7		0.211	0.055	0.055	0.015	0.027	3.171	2.431	0.067	0.061	1.962	1.005	0.202	0.002	0.001	0.079
8		0.375	0.112	0.057	0.016	0.033	2.325	2.229	0.095	0.089	1.659	1.306	0.303	0.002	0.002	0.081
9		0.551	0.229	0.060	0.017	0.047	1.729	1.883	0.120	0.117	1.532	1.429	0.648	0.003	0.003	0.109
10		0.758	0.396	0.060	0.017	0.082	1.216	1.355	0.109	0.119	1.337	1.383	0.805	0.003	0.003	0.165
11		1.092	0.621	0.062	0.019	0.201	1.018	1.284	0.141	0.316	3.590	1.667	1.197	0.004	0.009	1.085

Table 4.3c		4	5	6	7	8	9	10	11	Total Rate, kmol hr
Tray No.										
S.S.										
I	327.	410.4	270.3	121.4	31.9	-51.4	-227.2	-607.4	111.5	
II	187.	181.7	163.0	158.4	129.0	42.7	-19.3	-300.1	542.6	
III	49.5	49.40	52.43	58.56	67.28	76.05	78.61	96.22	528.13	
IV	45.2	44.96	47.70	53.34	61.76	71.43	77.34	134.8	536.53	
V	99.2	90.69	101.1	113.6	126.9	143.5	165.7	-202.02	638.68	

The results show that the interaction of reaction and separation can lead to enough non-linearity in the system so that steady state multiplicities occur. Note that when the reaction conversion is small, only a single steady state exists. In contrast, at higher conversions, three or five steady states exist. This shows that the reaction term in the governing equations is a major source of non-linearity. In practice, it is desirable to operate the column at high conversions such that the number of steady states in an open loop column is as low as possible. The task of regulating a column using appropriate control loops to maintain the product purity and conversion in the face of disturbances is easiest in case there are no steady state multiplicities and becomes progressively difficult as the open loop multiplicities increase. In the context of the MTBE column studied, it would therefore be desirable to provide a large amount of catalyst since there are only three steady states in contrast to five steady states at intermediate catalyst weights. Designing a column for still lower catalyst weights is not acceptable as the conversion and product purity become unacceptable. This is another example where operability and control considerations necessitate over-design.

4.2 Case Study II: Methyl Acetate

Methyl acetate is produced by the esterification of acetic acid with methanol in the presence of sulphuric acid or an acidic ion exchange resin.



An activity based reaction rate model for heterogeneous catalysis, developed by Song et al (1998), is used in this work. The rate expression is

$$R_{MeOAc} = \frac{M_{cat} k_1 \left(a_{HOAc} a_{MeOH} - \frac{a_{MeOAc} a_{H_2O}}{K_{eq}} \right)}{\left(1 + K_{HOAc} a_{HOAc} + K_{MeOH} a_{MeOH} + K_{MeOAc} a_{MeOAc} + K_{H_2O} a_{H_2O} \right)^2}$$

where a denotes the component activities and M_{cat} is the catalyst weight on a tray.

The reaction rate constant, k_1 and equilibrium constant, K_{eq} , are modeled as

$$k_1 = 6.942 \times 10^{10} \exp\left(\frac{-6287.7}{T}\right)$$

$$K_{eq} = 2.32 \exp\left(\frac{782.98}{T}\right)$$

Constant values for the adsorption equilibrium constants are used with

$$K_{HOAc} = 3.18, K_{MeOH} = 0.82, K_{MeOAc} = 0.82, \text{ and } K_{H_2O} = 10.5$$

$$a_i = \gamma_i x_i$$

In the above expressions, the reaction rate constant is in mole/ g cat / h, the catalyst weight is in grams and the temperature is in K. The net reaction on a tray is thus in kmol/hr.

The unwanted dehydration of methanol to dimethyl ether (DME) and water is ignored in this study, as is the case with most literature reports. Accurate prediction of the VLE is very important for simulation and design of the column. The VLE is affected by the dimerization of acetic acid in the vapor phase. This is modeled using Marek's method (Marek (1955)). Since the liquid phase is highly non-ideal, the Wilson equation is used to model the liquid phase activity coefficients. The Wilson parameters for the components are tabulated in Table 4.4.

Table 4.4: Wilson interaction parameters for methyl acetate system

Wilson Parameters		HOAc	MeOH	Water	MeOAc
$a_{i,j}$	HOAc	0.0	-0.2583	-1.1582	0.3275
	MeOH	0.2583	0.0	-0.8999	0.5859
	Water	1.1582	0.8999	0.0	1.4858
	MeOAc	-0.3275	-0.5859	-1.4858	0.0
$b_{i,j}$	HOAc	0.0	-1275.9	-119.5	-565.2
	MeOH	275.6	0.0	-54	-409.3
	Water	-331.2	-236.3	0.0	-965.4
	MeOAc	350.4	-15.7	-325.0	0.0

4.1.1 Column Configuration:

The reactive distillation column shown in Figure 4.6 is used as the basis for this study. A similar column has been studied by Al-Arfaz and Luyben (2002). The column consists of 35 trays, a total condenser, and a partial reboiler. There are three zones in the column, a rectification zone (trays 1-7), a stripping zone (trays 26-35) and a reactive zone (trays 8-25). Methyl acetate and water is formed between trays 8 and 25. Pure acetic acid is fed to the column on stage 8 and pure methanol is fed on tray 25. Both feeds are saturated liquids and in exact stoichiometric proportion. The fresh feed rate is 300 kmol/hr. The pressure throughout the column is taken as 1.25

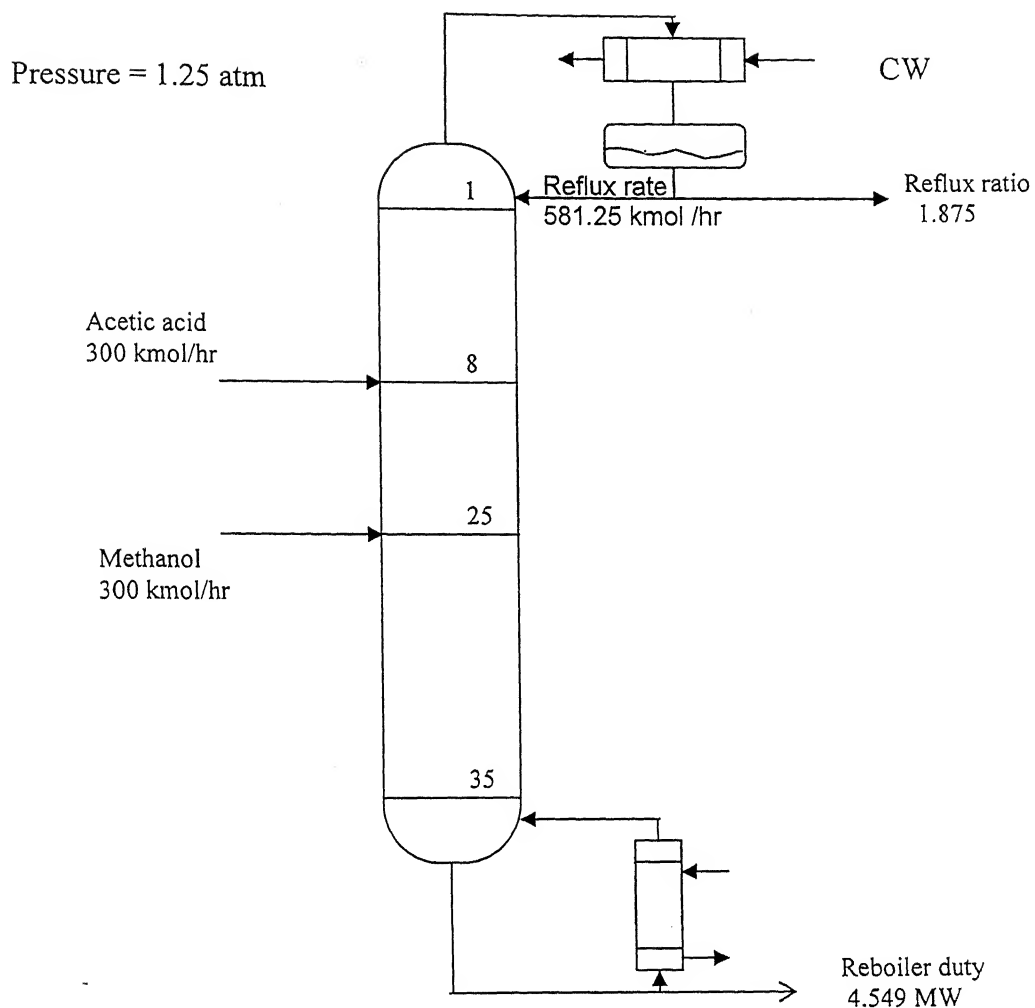


Figure 4.6: Reactive distillation column configuration for Methyl acetate synthesis

atmospheres. At the design catalyst weight of 1000 kg / reactive tray, high purity methyl acetate leaves the column in the distillate while nearly pure water leaves in the bottoms.

4.2.2 Multiple Steady States by Continuation with respect to Catalyst Weight:

Homotopy continuation with respect to catalyst weight is used to study the steady state multiplicities in this RD system. A reflux rate specification of 581.25 kmol/hr and a reboiler duty specification of 4.549 MW is used. Figure 4.7 plots the conversion versus the catalyst weight homotopy factor L . Two distinct branches are seen. These are labeled in the figure. Branch 1 is obtained by starting from the ordinary distillation solution at $L = 0$ and then introducing reaction by slowly increasing L . Branch 2 is traced by continuation about the reactive solution ($L = 1$) obtained using the conventional Naphtali-Sandholm simulator. In Branch 1, there are no turning points while Branch 2 has one turning point at $L = 0.15$. The turning point divides the solution diagram into two regions, I and II, with one and three steady states respectively. For the design catalyst weight at $L=1$, there are a total of three steady states viz a high conversion, an intermediate conversion and a low conversion steady state. The distillate and bottoms compositions and the reaction conversion for these steady states are tabulated in Table 4.5. As in the MTBE case, it is the high conversion steady state that is of practical importance.

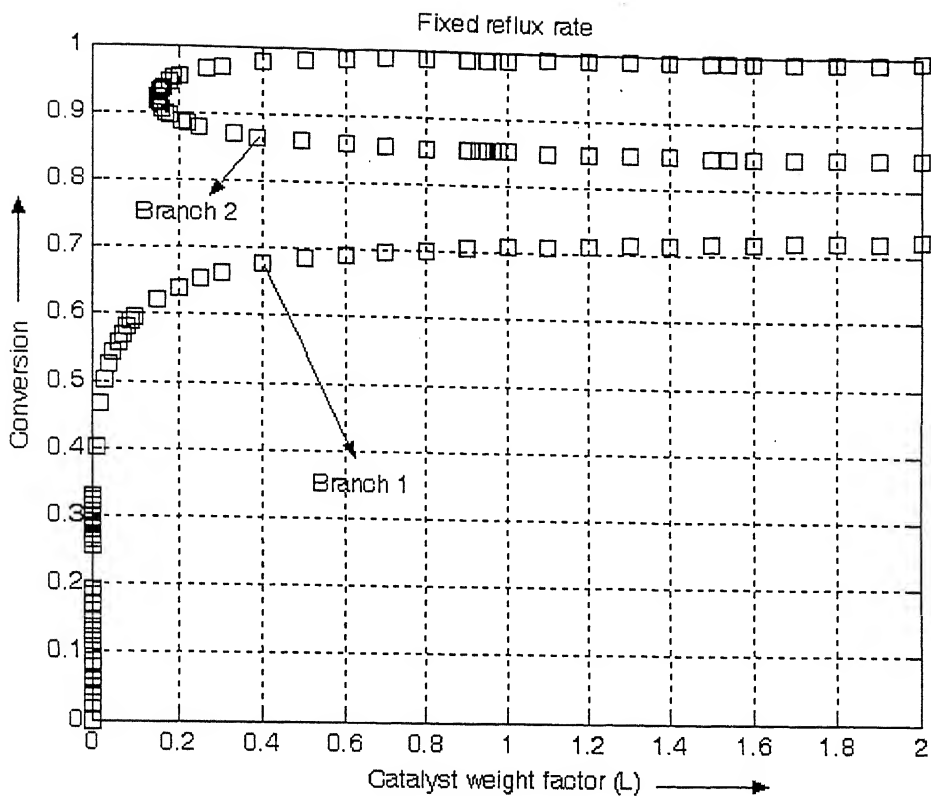


Figure 4.7: Multiple steady states in methyl acetate system for fixed reflux rate and reboiler duty

Table 4.5: The distillate and bottoms composition and reaction conversion for three steady states

SS	Distillate Composition				Bottoms Composition				Conversion
	HOAc	MeOH	Water	MeOAc	HOAc	MeOH	Water	MeOAc	
High Conversion.	0.0000	0.0080	0.0271	0.9648	0.0120	0.0036	0.9844	0.0000	98.83 %
Intermediate Conversion	0.0000	0.0053	0.0176	0.9771	0.1319	0.1278	0.7402	0.0000	85.10 %
Low Conversion	0.0000	0.0041	0.0001	0.9829	0.2271	0.2249	0.5427	0.0054	70.08 %

In order to better understand the steady state multiplicities, Figure 4.8 plots the net rate of product formation on the trays for the three steady states.

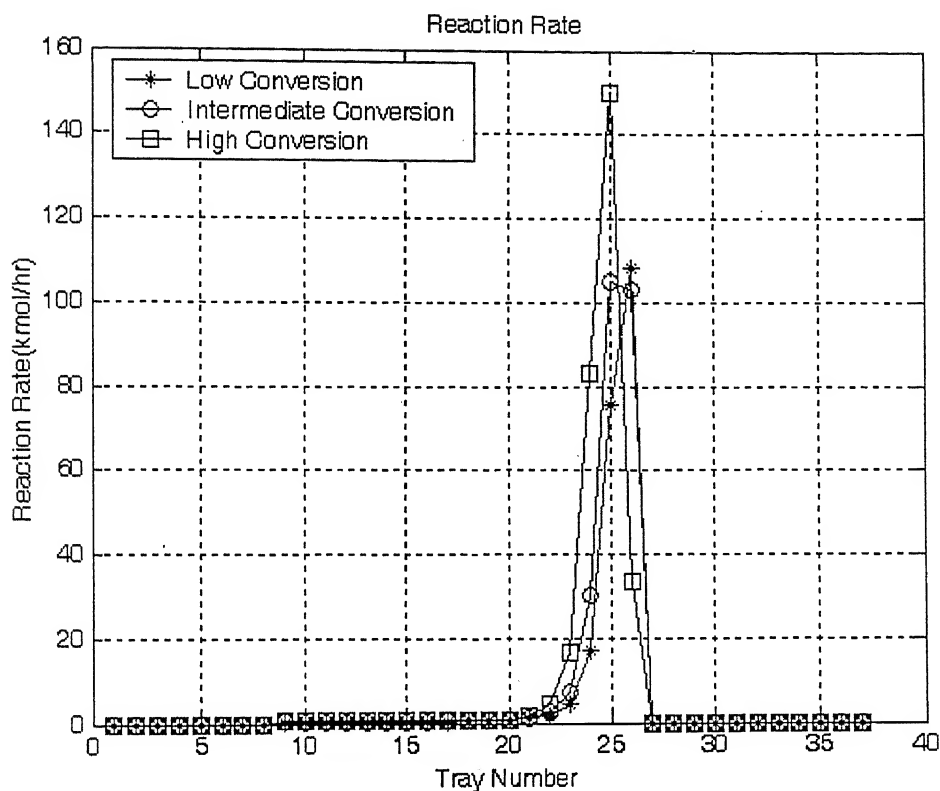


Figure 4.8: Reaction rates for methyl acetate system

The corresponding temperature profiles are also plotted in the Figure 4.9. Unlike the MTBE system, the temperature rise across the reactive section is only 10 K, which is not substantial.

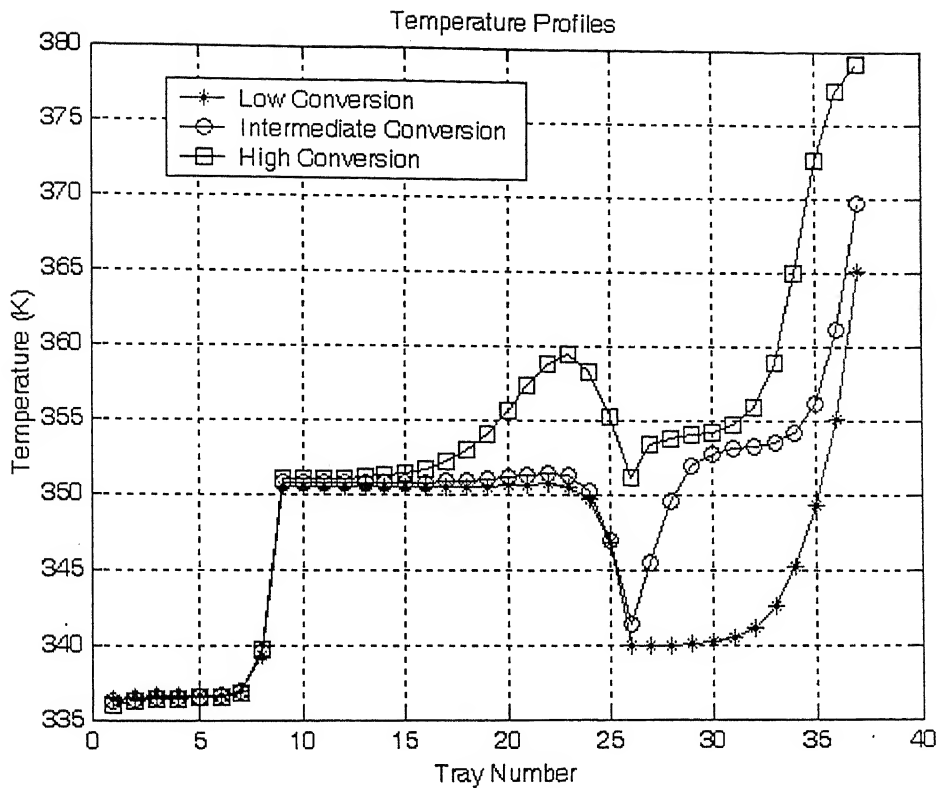


Figure 4.9: Temperature profiles and reaction rates for methyl acetate system

The differences in the overall conversion are therefore largely determined by the composition profiles across the reactive section are shown in Figure 4.10. For the high conversion steady state, the mol fraction of acetic acid, a reactant, is substantially higher on trays 16 to 24 while the mol fraction of methyl acetate, a product, is substantially lower than the other two steady states. This leads to higher product formation rates resulting in nearly complete conversion. For the intermediate and low conversion steady states, the temperature profiles for are very similar so that the rate and equilibrium constants are the same.

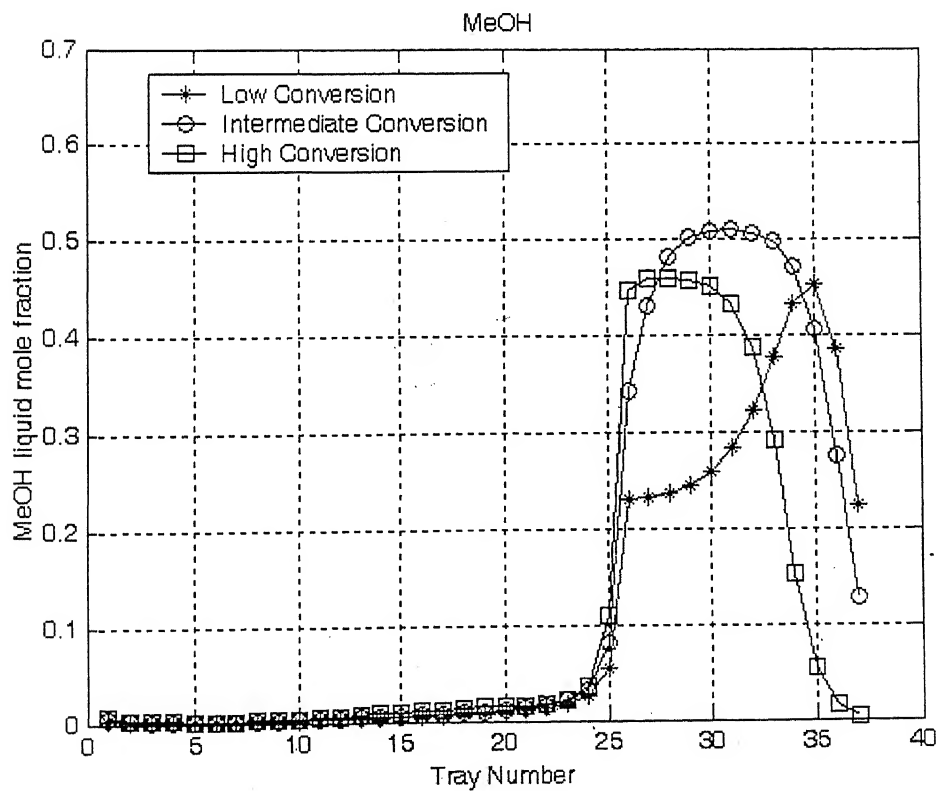
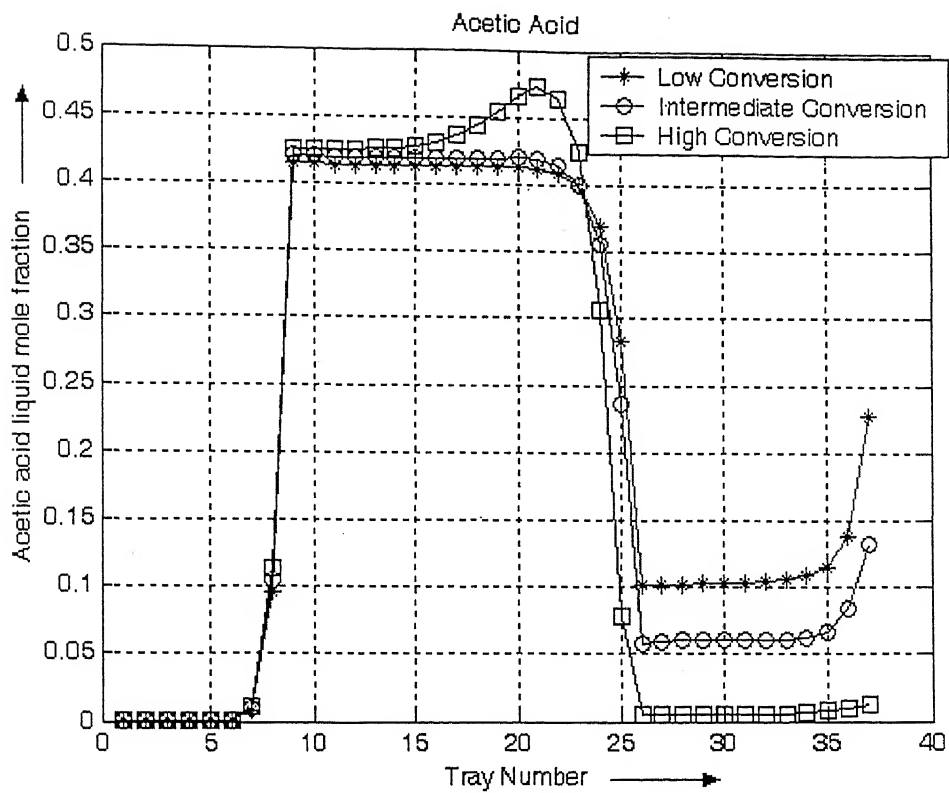


Figure 4.10: Composition profile for three steady states of methyl acetate system

Contd...

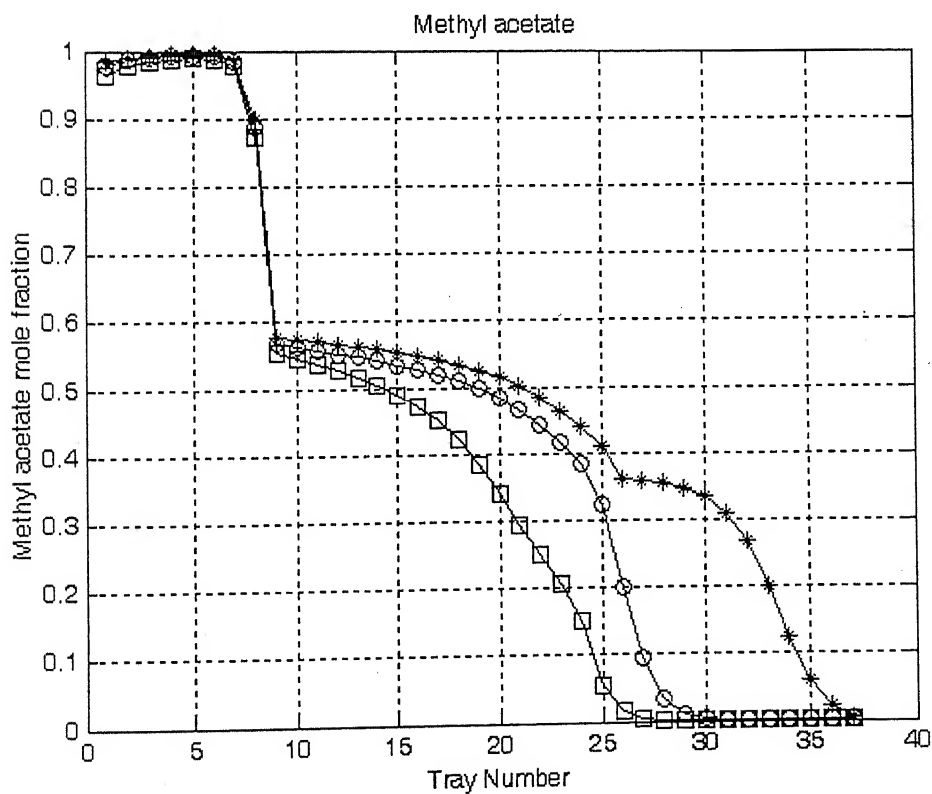
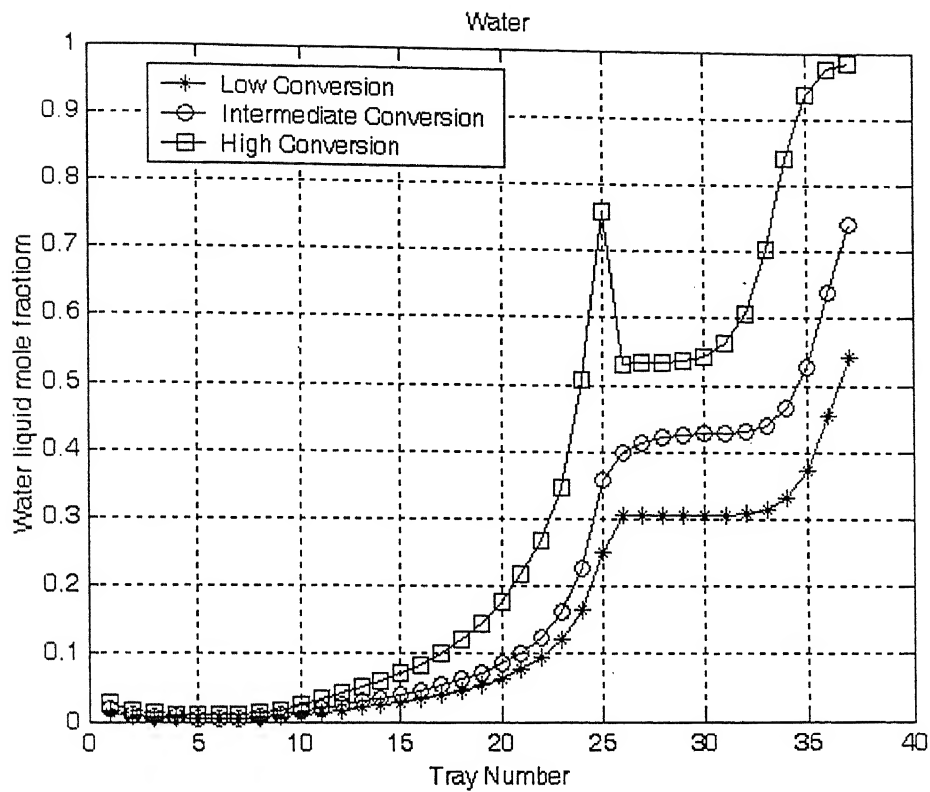


Figure 4.10: Composition profile for three steady states of methyl acetate system

An examination of the net formation rate profile indicates that the net generation rates are nearly the same for all the reactive trays except trays 24 and 25. The reason is that for the intermediate conversion steady state, the unreacted methanol composition is significantly higher than for the low conversion steady state. This causes a larger forward reaction leading to nearly 85% conversion.

As an aside, in order to study the effect of the column specification variables on steady state multiplicities, the specification set was changed to fixed reflux ratio of 1.875 and reboiler duty of 4.549 MW. These specification values are equal to the corresponding high conversion steady state values obtained previously. The solution diagram corresponding to this specification set is shown in Figure 4.11.

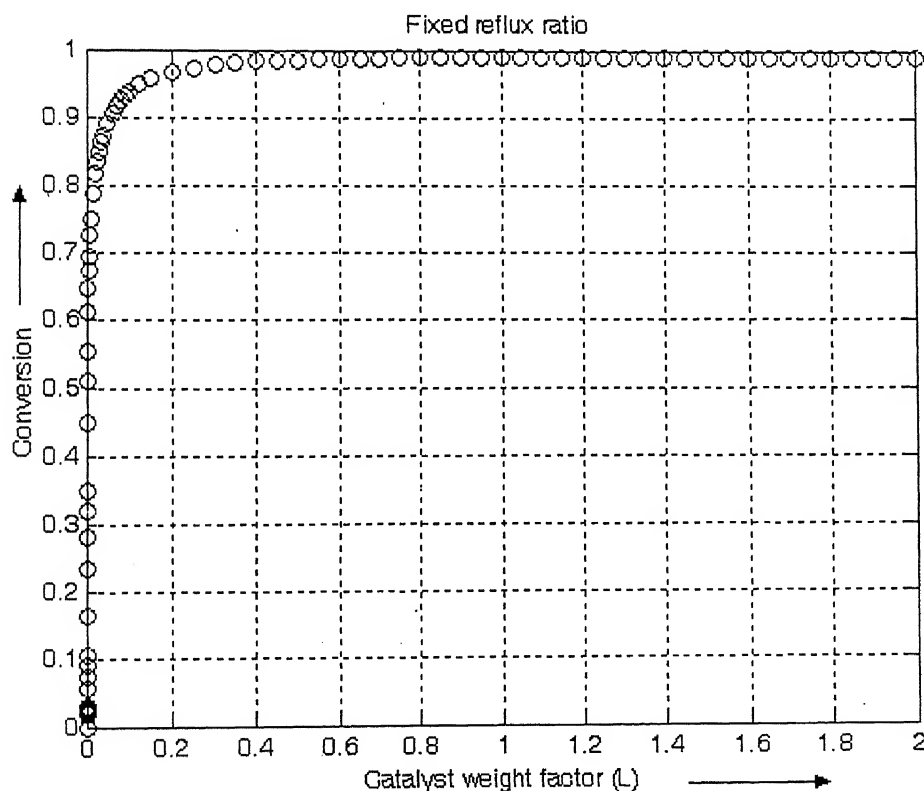


Figure 4.11: Multiple steady states in methyl acetate system for fixed reflux ratio and reboiler duty

No steady state multiplicities are seen. It may be that another branch does actually exist but has not been traced because a starting point on that branch has not been obtained. We have used the Naphtali Sandholm RD simulator with several initial guesses for the iteration variables. It however always converges onto the branch shown in Figure 4.11. The results thus show that the column specification used can impact the number and also the regions of steady state multiplicities. Given that each column specification set corresponds to a particular column operating policy, for example, a fixed reflux rate or a fixed reflux ratio, the results show that the column operating policy determines the number of steady state multiplicities. This has important implications on the dynamic operation and control of an RD column. This aspect will be demonstrated in detail in the next Chapter using the MTBE column as an example.

It is noted that in both the MTBE and methyl acetate case studies, in case multiple steady states occur, the reactive solution obtained using the NS method lies on a branch that is not connected to the branch that starts from the ordinary distillation solution. Thus homotopy continuation from a non-reactive solution provides additional steady state solutions that otherwise would be missed using conventional algorithms such as the NS method and the Inside-outside method. The synergy between the computationally intensive homotopy continuation method and the traditional NS method in detecting multiple steady states in an RD column is thus obvious.

Homotopy Continuation for Control Structure Synthesis:

An MTBE Case Study

An RD column must be operated so that the product purity and reaction conversion are maintained close to their design values for major disturbances entering the column. A robust control system needs to put in place that can regulate the column for anticipated production rate changes and changes in the feedstock composition, the principal disturbances into a column. In the design of such a control system, the selection of the control structure is the most crucial decision.

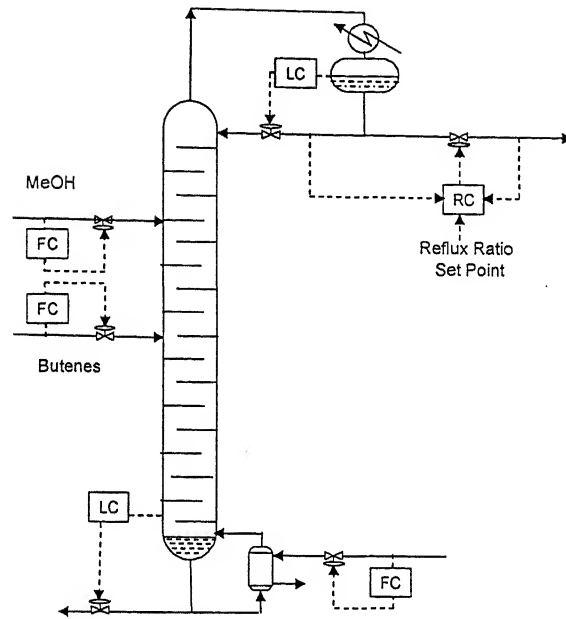
A control structure refers to the number of control loops and the specific input-output pairing used in the loops. Potential input variables are the reflux rate, reflux ratio, reboiler duty, reboil ratio, distillate rate and bottoms rate. Potential output variables are easily measurable variables such as tray / stream temperatures and compositions. There are thus several possible input (manipulated) variables and output (controlled) variables even in a simple RD column. The various permutations and combinations lead to a large number of possible control structures from which a small set of “good” control structures must be chosen. Evidently, the key to successful column operation is this screening of control structures to zero in on the most appropriate controlled variables and effective handles to manipulate them so that by maintaining the controlled variables at their set-points, the purity and conversion of the column remain near the design specifications for the primary disturbances. Indeed, for a good control structure, other control system design decisions such as the choice between sophisticated versus simple control

algorithms becomes obvious. For a good control structure, simple PI control should provide the adequate column regulation. On the other hand, no amount of sophistication in the control algorithm can compensate for an inherently poor control structure.

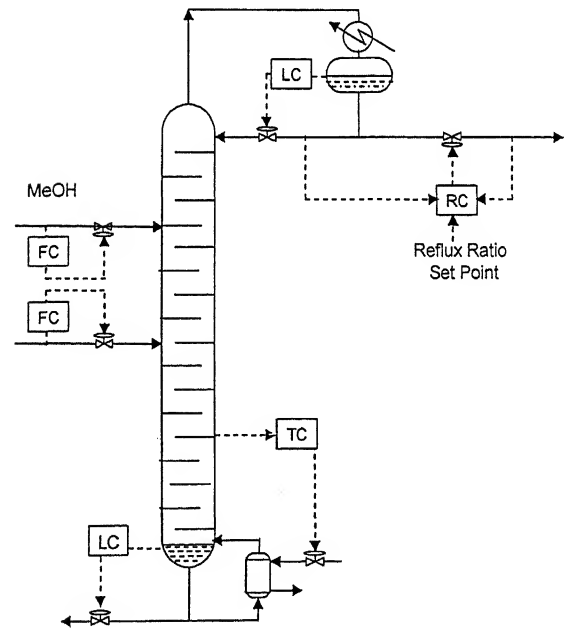
A good control structure is one that rejects disturbances effectively. In order to do so, controlled variables that are sensitive to the occurrence of the primary disturbances should be chosen so that timely control action can be initiated to regulate the column. Also, the manipulated variables used for control should affect the controlled variables in a substantial and easily predictable way. Such a choice assures enough "stick" for column regulation even for large disturbances. At steady state, linear or nearly linear input-output relationships are certainly desirable so that the process gain does not change appreciably and simple control algorithms suffice. In case multiple control loops are used, the input output pairings should not cause stability problems due to interaction between the loops. Last but not least, since sensor measurements are never exact, the column performance metrics such as reaction conversion and product purity should not be very sensitive to the set-point chosen for the controlled variables. In other words, the column performance should be robust to typical measurement errors or errors in the set-point inputs.

Systematic steady state analyses can be conducted to reveal the control structure/s that provides effective column regulation for the primary disturbances in a column. These analyses include sensitivity studies for obtaining output variables that are sensitive to disturbances as well as manipulated variables. Sensitivity is an inherent property of a variable. Thus, a variable sensitive to disturbance will also be sensitive to manipulated variable. Note that each column specification set corresponds to a particular control structure.

Figure 5.1 shows the control structures corresponding to two different specification sets



CS1: Control structure for fixed reflux ratio and reboiler duty as specifications



CS2: Control structure for fixed reflux ratio and tray temperature as specifications

Figure 5.1: Control structures corresponding to two different specification sets

In reactive distillation systems, the coupling of reaction and separation in the same column leads to a highly non-linear system. The steady state input-output relationships are complex and multiplicities are known to occur. We distinguish between two types of multiplicities: output multiplicity and input multiplicity. The former refers to multiple output values for the same input specification while the latter refers to multiple input specifications giving the same output. This was illustrated in Figure 1.4. From a control perspective, input variables are potential manipulated variables such as the reboiler duty or reflux ratio while output variables are potential controlled variables such as tray temperatures / compositions etc. The choice of the control structure substantially affects the number of steady state multiplicities and the size of the operating space in which these multiplicities occur. In other words, the complexity of the input-output relationships depends on the control structure. The control structure chosen must avoid output multiplicities to ensure that the column does not drift from say a high conversion steady state to a low conversion steady state even though there is no apparent change in the inputs to the column. Input multiplicity must be avoided as the sign of the gain between the input and output variable changes depending on the column operating condition. Such changes in the sign of the gain can easily lead to dynamic instability problems. Also, if the output variable is used in a control loop, the range of feasible set-point specifications becomes limited so that measurement biases can drive the control system to seek an infeasible steady state.

Systematic steady state analyses can be conducted to formulate good control structures that would regulate the column in the presence of disturbances. Two distinct approaches are possible to control structure design. In the first, all reasonable candidate

control structures are first enumerated and then accepted or rejected depending on their ability to maintain the column close to the design purity and conversion for the primary disturbances. Structures with linear input-output relationships and no steady state multiplicities are preferred. Alternatively, in the second approach, the effect of varying the input handles about their base case values, on the column outputs is first studied to identify potential input-output pairings. Pairings that are sensitive avoid multiplicities and give nearly linear input output relationships are short listed. Next, control loops are systematically added and the column steady state response to the primary disturbances evaluated until we arrive at the simplest control structure that provides adequate regulation in the presence of disturbances.

This chapter demonstrates the application of the latter approach to the synthesis of a “good” control structure for a double feed MTBE RD column. The preferred control structure operates at fixed reflux ratio and uses a temperature inferential control loop for maintaining the product purity by manipulating the reboiler duty. A reactive tray composition is controlled for balancing the fresh feed into the column as per the reaction stoichiometry by manipulating a fresh feed rate. The isobutene fresh feed or the methanol fresh feed can be used as the manipulated variable in the composition loop. The tray location for composition measurement must be carefully chosen to avoid stability problems due to loop interactions.

5.1 The MTBE Reactive Distillation Column

The double feed column described earlier in Chapter 4 is used for the control structure synthesis case study. A schematic of the column and the base case operating

conditions are shown in Figure 4.1. A similar column has been studied by Wang et al (2003) for control strategy of reactive distillation for MTBE synthesis. Reaction kinetics used by same as follows:

$$r = M_c k_r \left[\frac{a_{IB}}{a_{MeOH}} - \frac{a_{MTBE}}{K_a a_{MeOH}^2} \right]$$

$$k_r = 3.67 \times 10^{12} e^{-11110/T} \text{ mol/(equiv)}$$

$$K_a = \exp(-16.33 + 6820/T) \text{ and } a_i = \gamma_i x_i$$

Where K_a represents the reaction equilibrium constant and T is temperature in K.

Corresponding to this reaction kinetics homotopy continuation with respect to catalyst weight is applied shown in Figure 5.2.

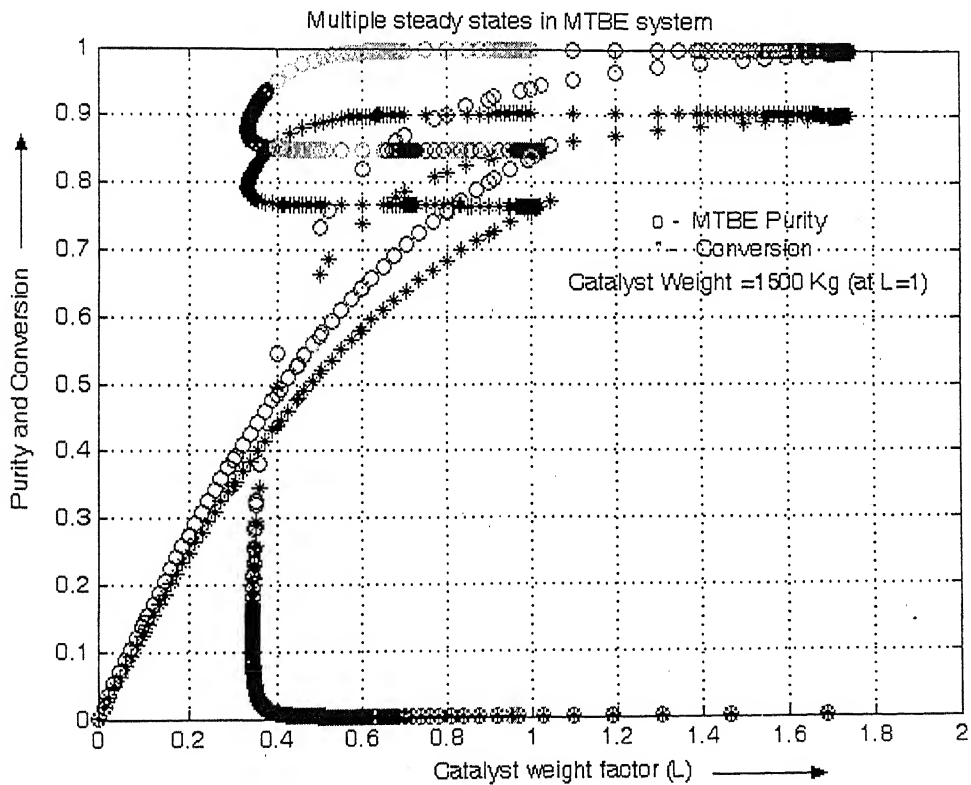


Figure 5.2: Multiple steady states in MTBE system for purity and conversion

This solution diagram also shows five steady states for a unique catalyst weight. This diagram is different from earlier one which also shows five steady state solutions. The difference is attributes to the different kinetic parameters as described in earlier chapter 4. The catalyst weight must be chosen appropriately to minimize the steady state multiplicities for robust column operation and control. Therefore, 1800 kg catalyst ($L = 1.2$) is chosen at which only three steady states are present with high conversion purity.

The column operates at a high reflux ratio of 7 with a base case conversion of 90% with >99% pure MTBE leaving from the bottoms. A control system that maintains the product purity and reaction conversion near the design values is desired. It should provide smooth transitions for production rate changes and compensate for any changes in the butene feed composition. In order to synthesize such a control structure the effect of the various potential manipulated variables on the column tray temperatures and compositions is studied.

5.2 Effect of Column Inputs on Output Variables

The potential input variables or valves that can be manipulated to regulate the column are the two fresh feeds, the two product streams, the reflux rate and the reboiler duty. It is also possible to maintain the flow ratios of two streams such as the reflux ratio or the reboil ratio. Manipulating the reflux rate or ratio for column regulation is not a good idea since the hold up (or catalyst weight) on each reactive stage in an RD column is large so that the column response can be extremely sluggish. In contrast, manipulating the reboiler heat duty causes an immediate change in the vapor rate throughout the column. These dynamic considerations indicate that fixed reflux rate or reflux ratio

operating policies are preferable and the reboiler duty and feed flows can be used for regulating the separation and the reaction in the column.

Now in order to decide between the fixed reflux rate vs fixed reflux ratio policy, Figure 5.3 plots the steady state purity and conversion as the reboiler duty is varied with the feed conditions at their base case values for the two operating policies. Output multiplicity is evident for both the fixed reflux rate and the fixed reflux ratio policies. It is however noted that in the latter case, the base case point is away from the zone of output multiplicity while output multiplicity occurs in the former even for the base case. The column can thus drift from a high conversion steady state to a low conversion steady state even as the reboiler duty and the feed conditions remain the same for a fixed reflux rate. The same cannot happen in case the reflux ratio is kept fixed. Clearly, for this column the fixed reflux ratio is preferable over the fixed reflux rate policy.

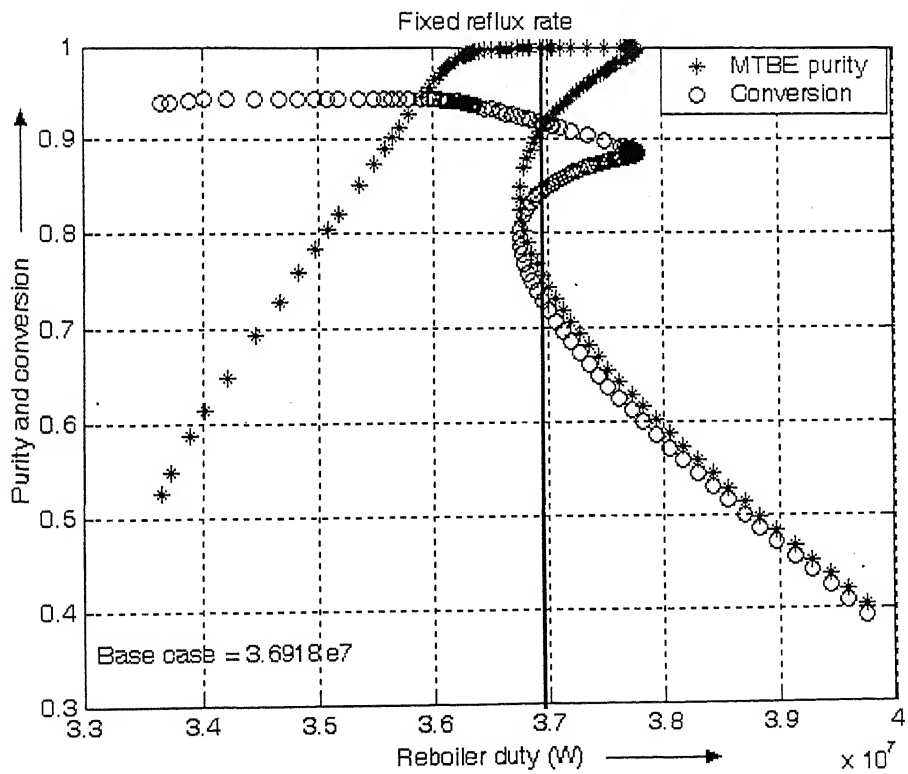
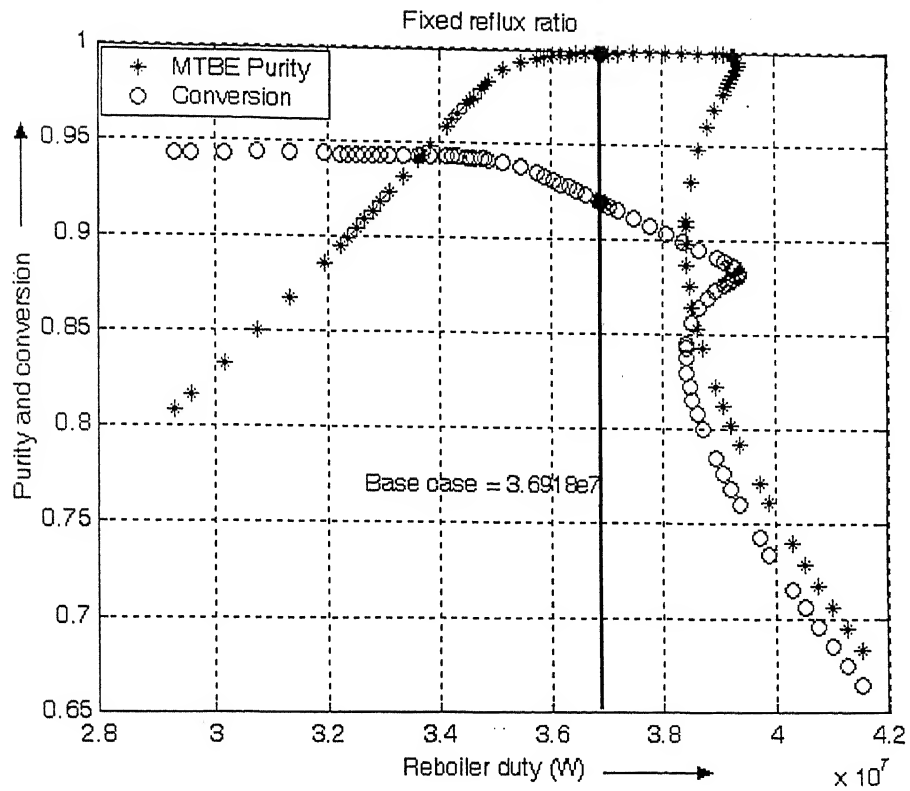


Figure 5.3: Input output multiplicities at fixed reflux ratio and reflux rate with variation of reboiler duty

Having decided on maintaining a fixed reflux ratio, the response of the tray temperatures and compositions to changes in one of the remaining input variables is studied. Figures 5.4 and 5.5 plot the steady state tray temperature and composition responses to changes in the reboiler duty about the base case respectively.

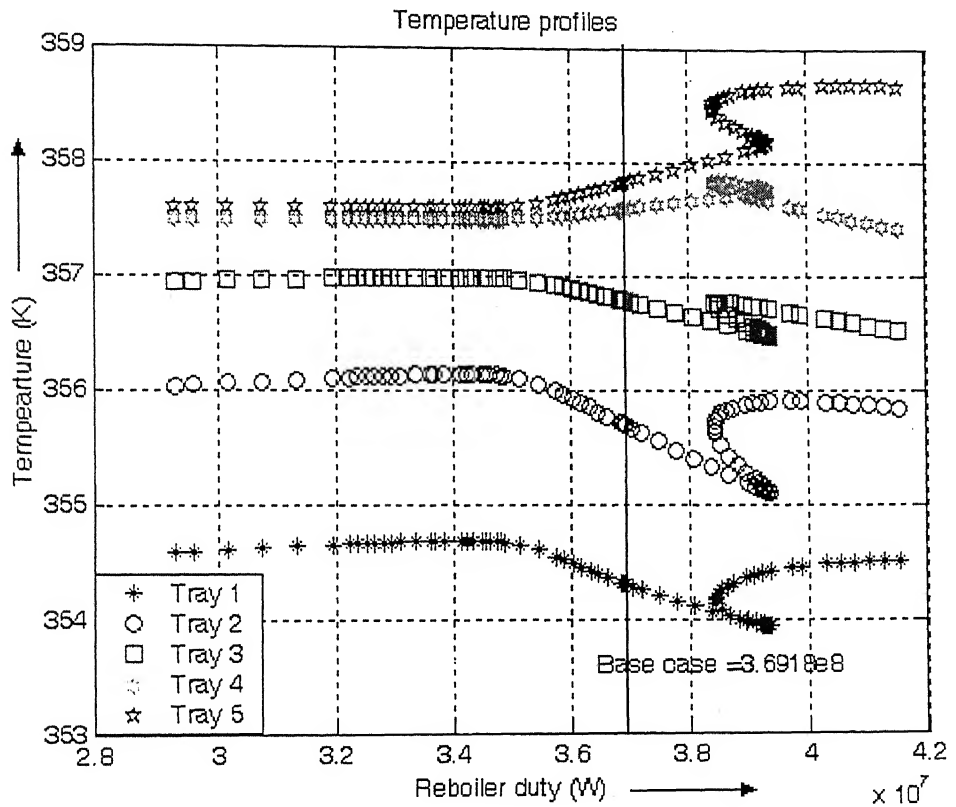


Figure 5.4: Responses of tray temperatures to changes in reboiler duty at fixed reflux ratio

Contd...

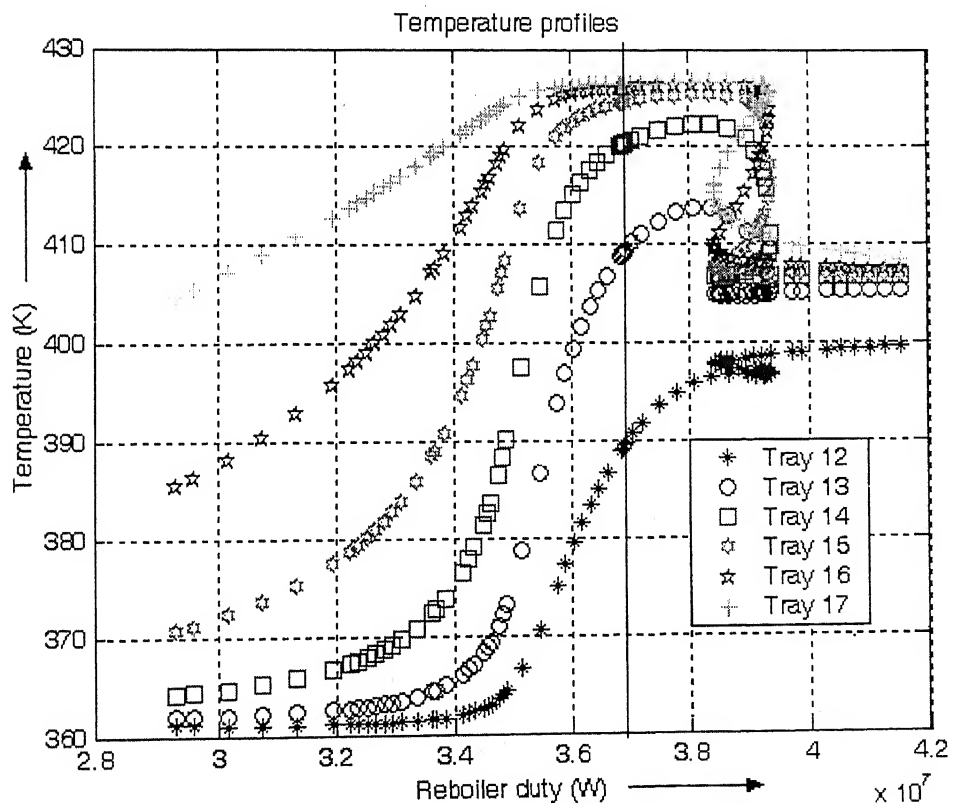
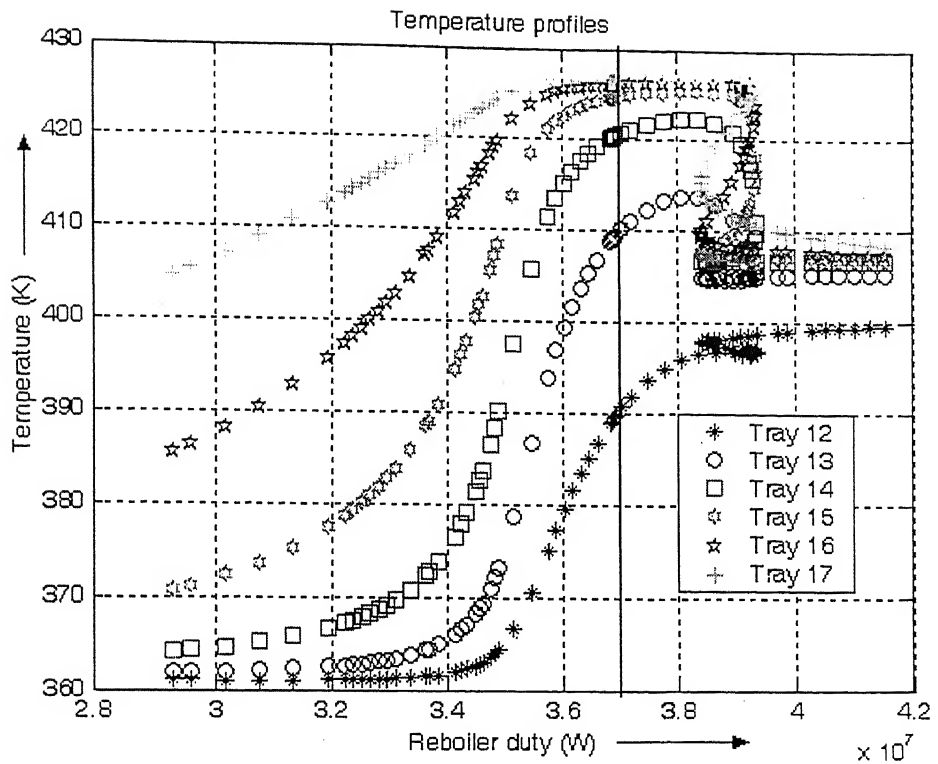


Figure 5.4: Responses of tray temperatures to changes in reboiler duty at fixed reflux ratio

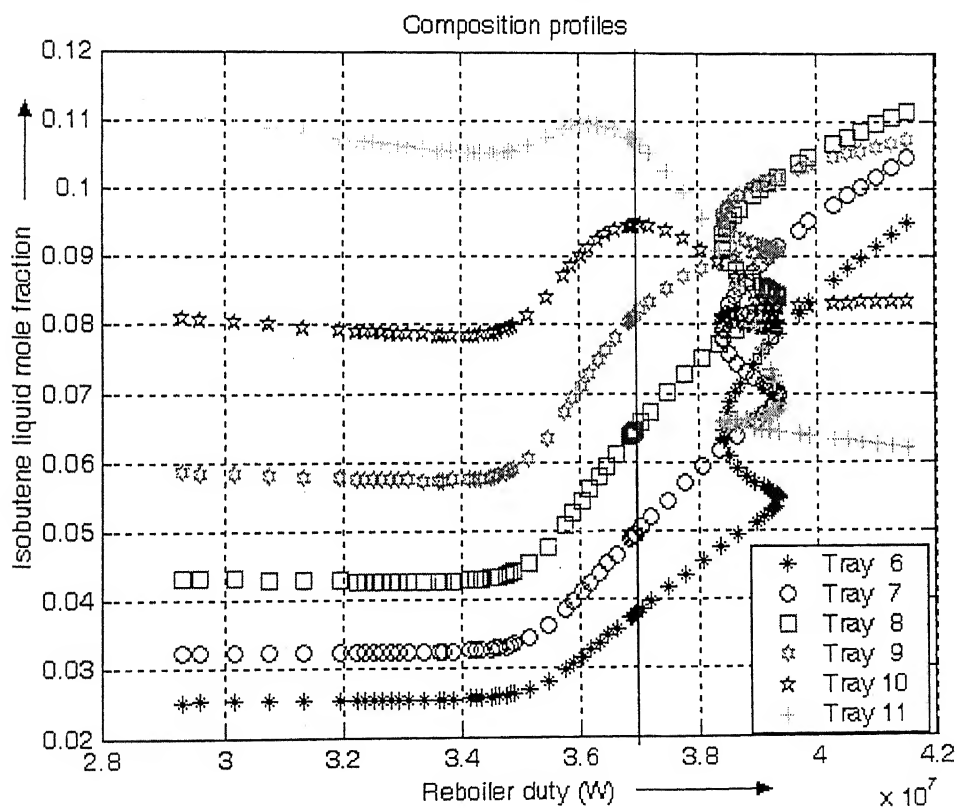
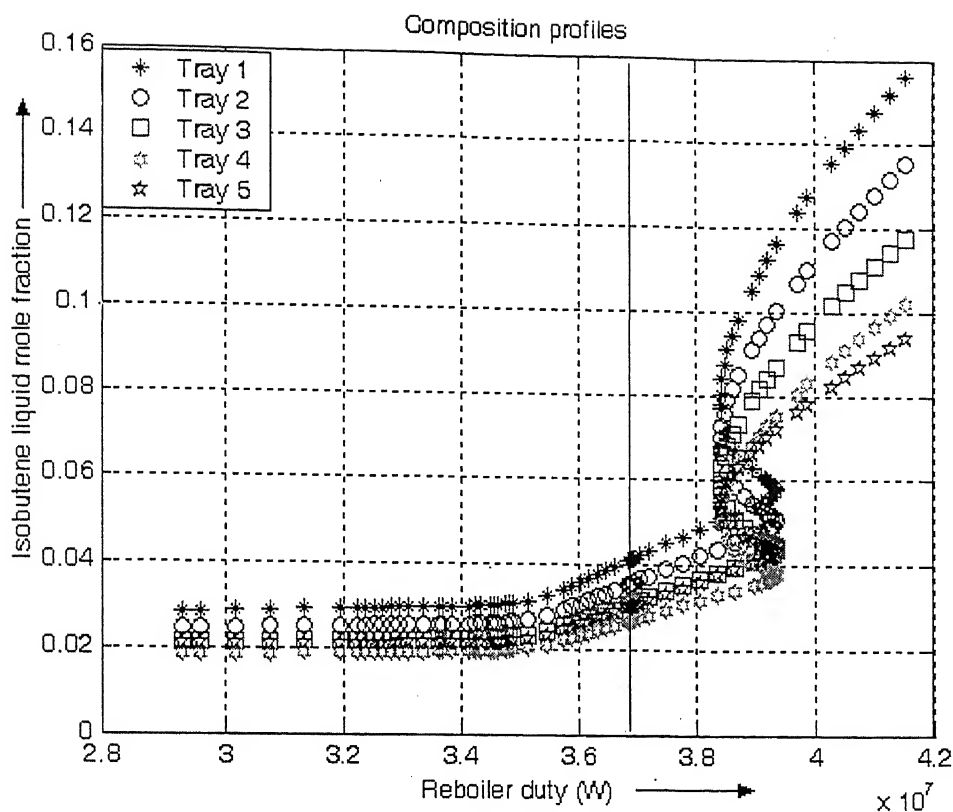


Figure 5.5: Responses of tray composition to changes in reboiler duty at fixed reflux ratio
contd...

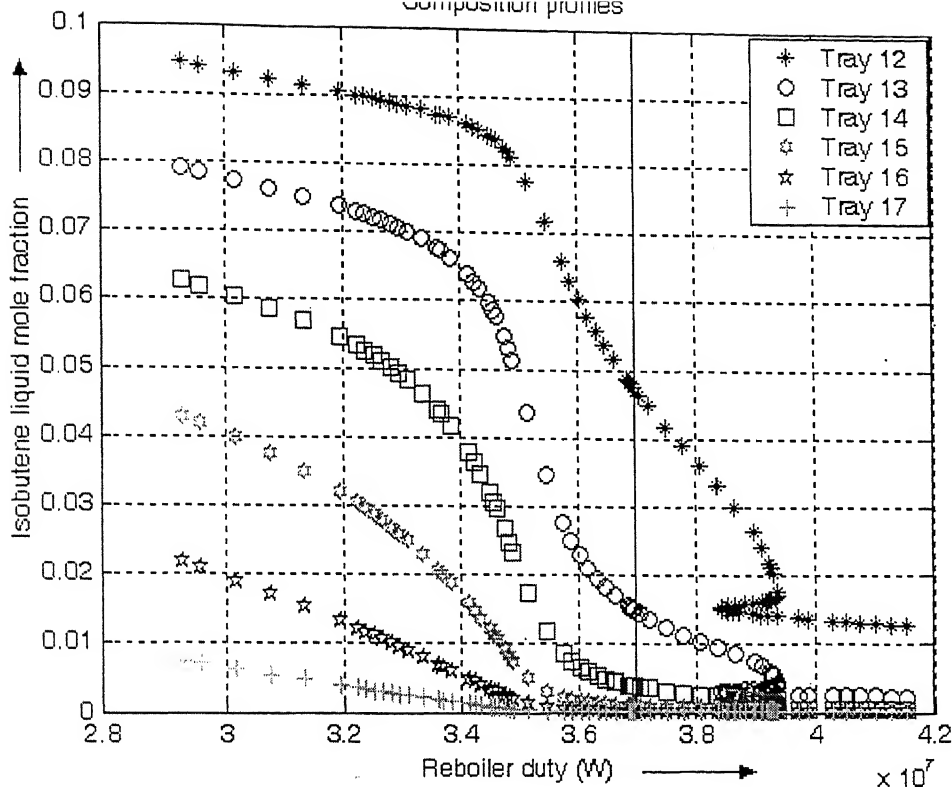


Figure 5.5: Responses of tray composition to changes in reboiler duty at fixed reflux ratio

All the tray temperatures and compositions, especially for trays 12 to 15 in the stripping section respond to changes in the reboiler duty. A small zone with output multiplicities is observed. The best tray location for a temperature sensor is the one that is most sensitive to changes in the reboiler duty. A plot of the dT/dQ also referred to as the tray temperature sensitivity with respect to reboiler duty profile in Figure 5.6, shows that tray 12 is the most sensitive to changes in the reboiler duty. The temperature or composition of a responsive tray may be controlled by manipulating the reboiler duty in order to regulate the separation, as is usually done in ordinary distillation. Temperature measurements are preferred over composition measurements due to their accuracy and quick response time.

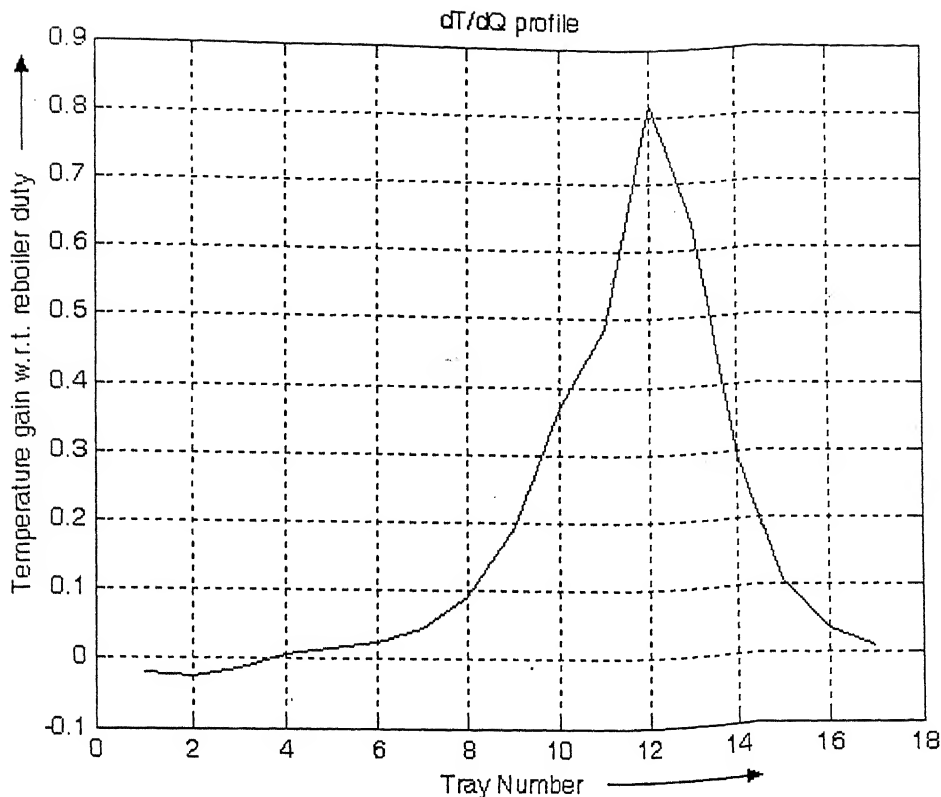


Figure 5.6: Temperature sensitivity with respect to reboiler duty

Next, the effect of varying the fresh feed flows on the column tray temperatures / compositions is evaluated. The tray temperatures / compositions for changes in the fresh methanol shown in figure 5.7 and 5.8 respectively whereas, for isobutene feeds at fixed reflux ratio and reboiler duty are plotted in Figures 5.9 and 5.10 respectively. Substantial input multiplicity in the temperature of reactive trays is evident from the plots. The reactive tray temperature should therefore not be controlled using the fresh feed as the process gain changes sign depending on the operating condition. Also the tray temperature set point can be infeasible due to sensor bias. For example a temperature set-point of 370.03 K for tray 11 does not have a feasible steady state solution as it is above the maximum temperature as seen in the Figure 5.9. The reactive tray compositions in contrast are well behaved.

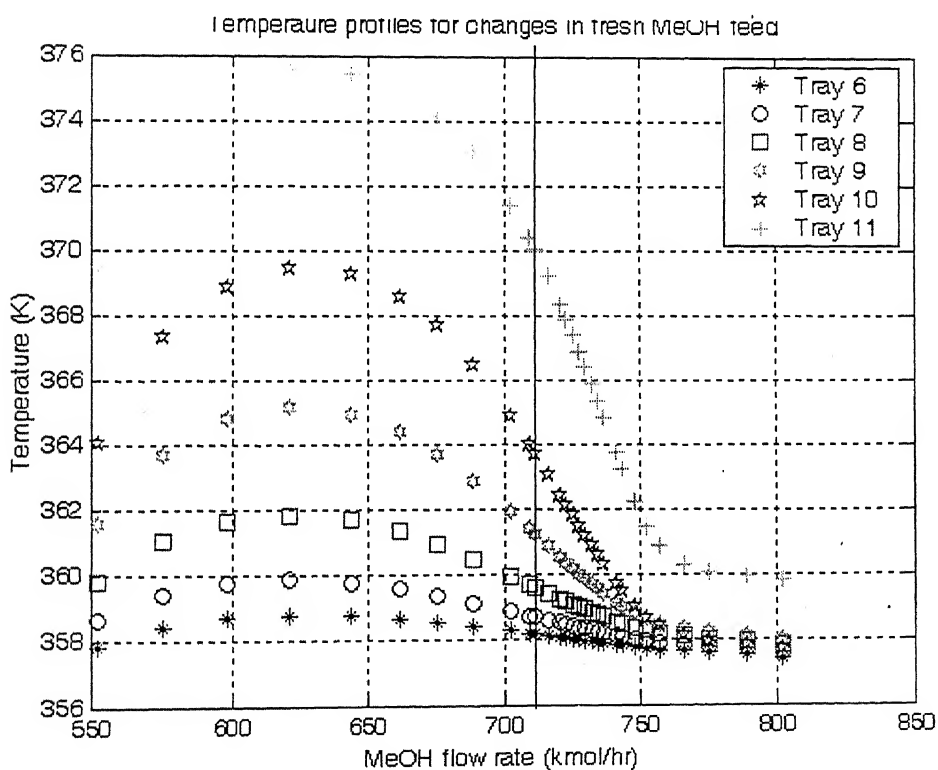
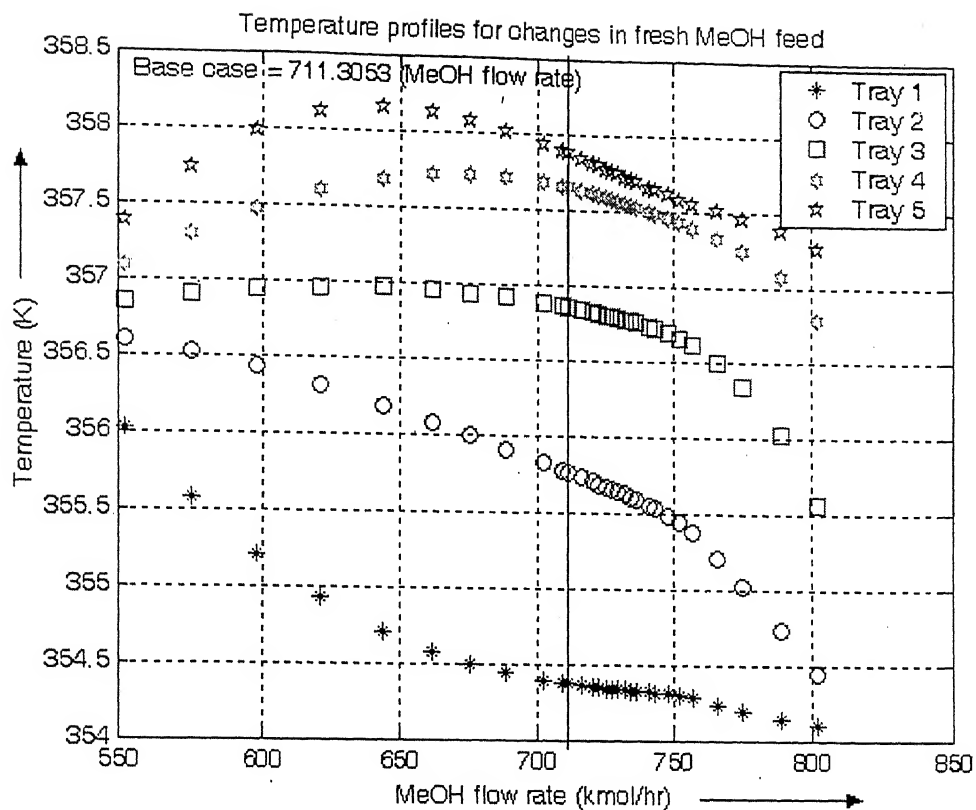


Figure 5.7: Tray temperatures for changes in MeOH feed flow

Contd...

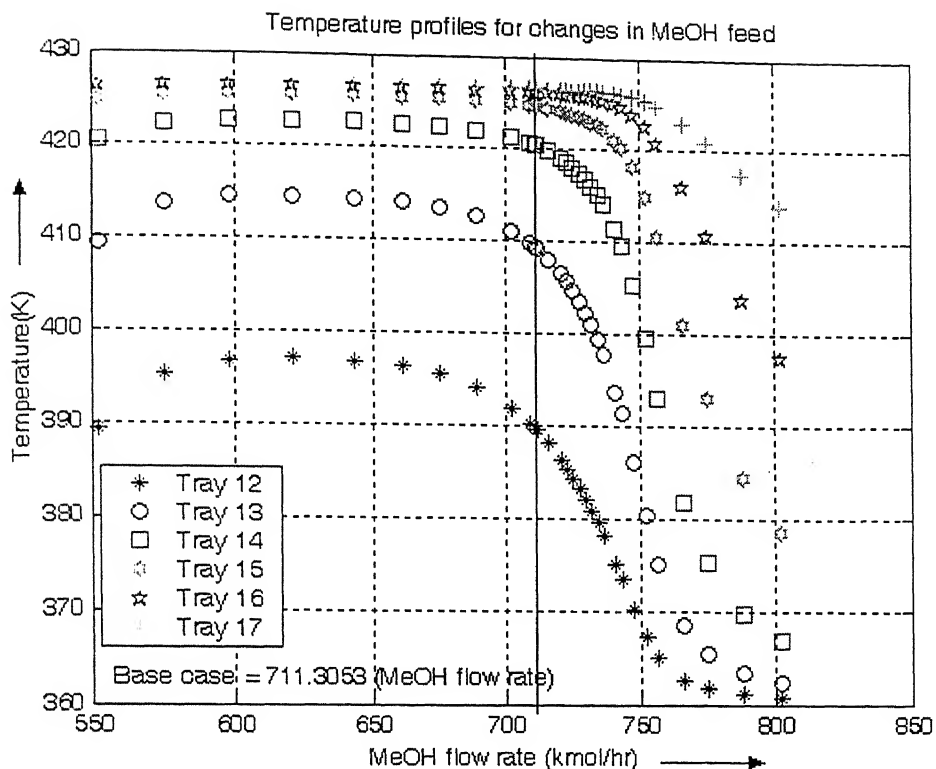


Figure 5.7: Tray temperatures for changes in MeOH feed flow

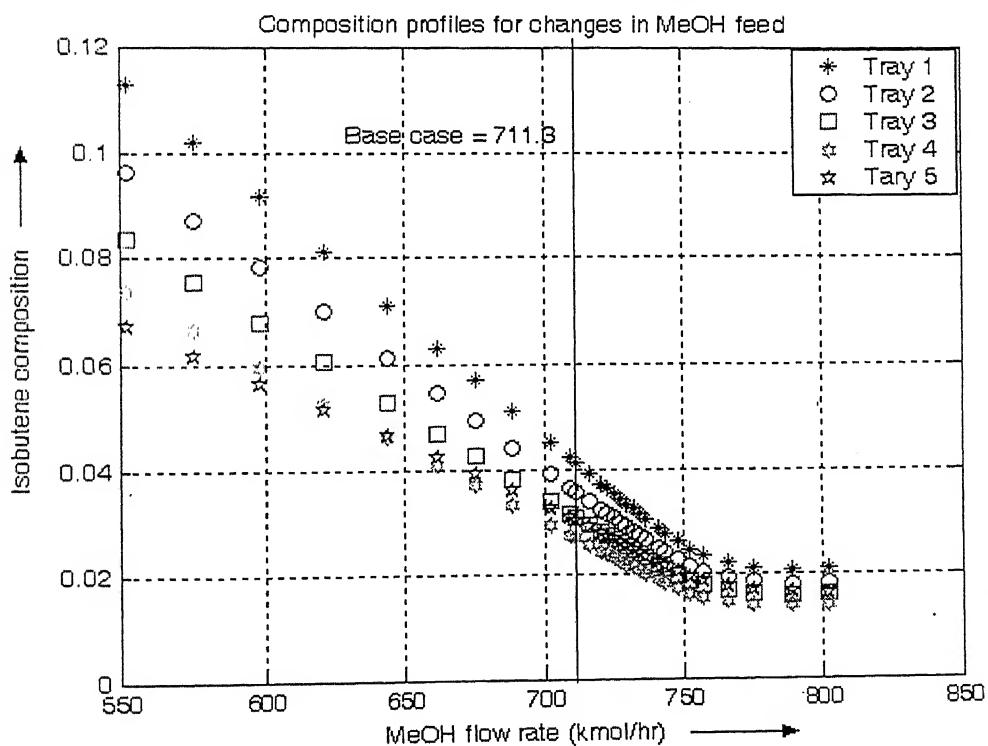


Figure 5.8: Tray compositions for changes in MeOH feed flow

Contd...

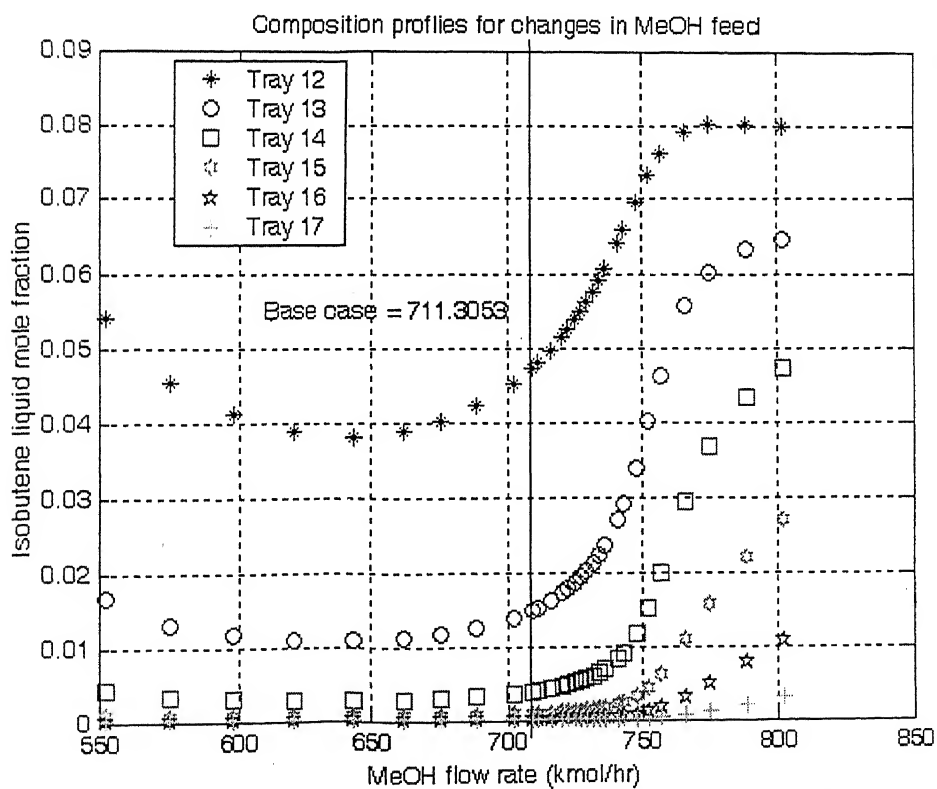
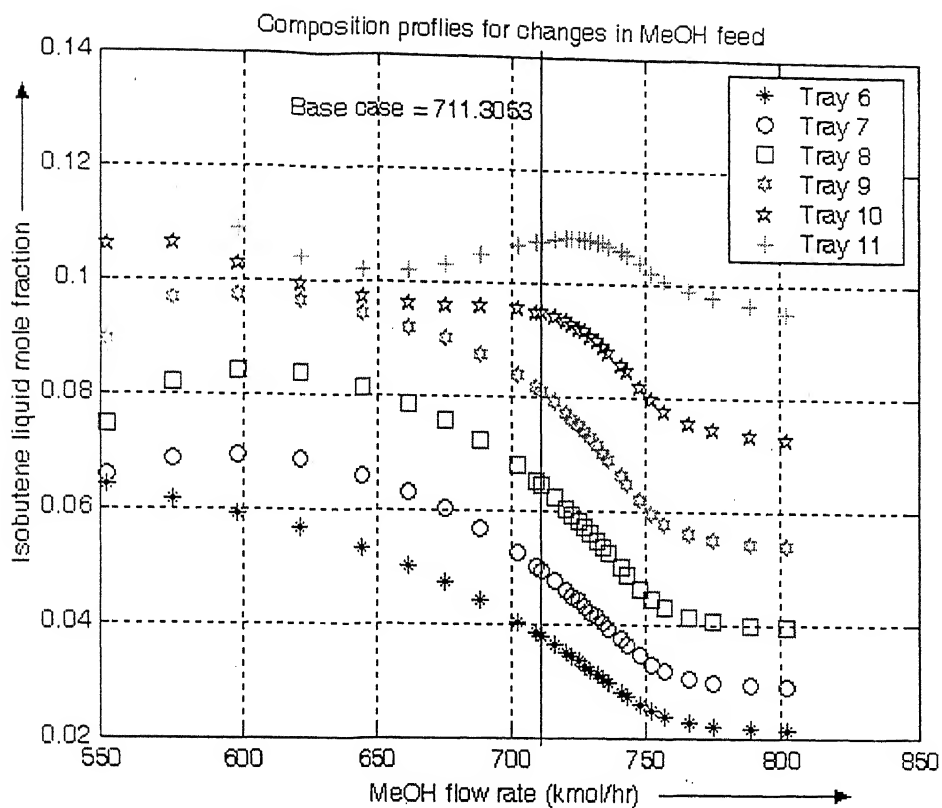


Figure 5.8: Tray compositions for changes in MeOH feed flow

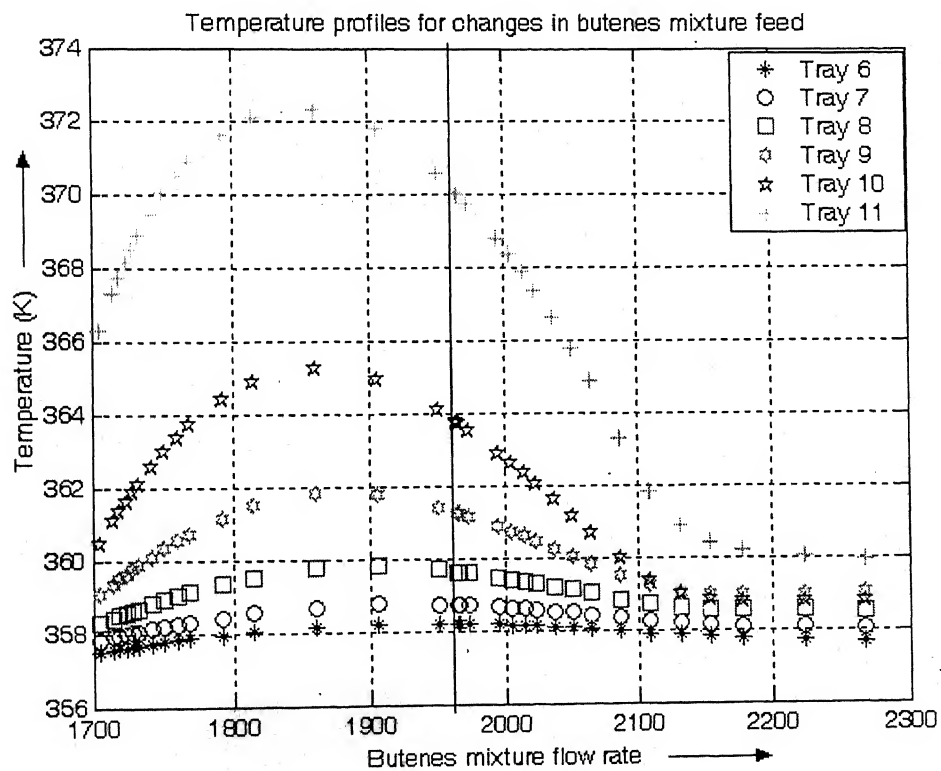
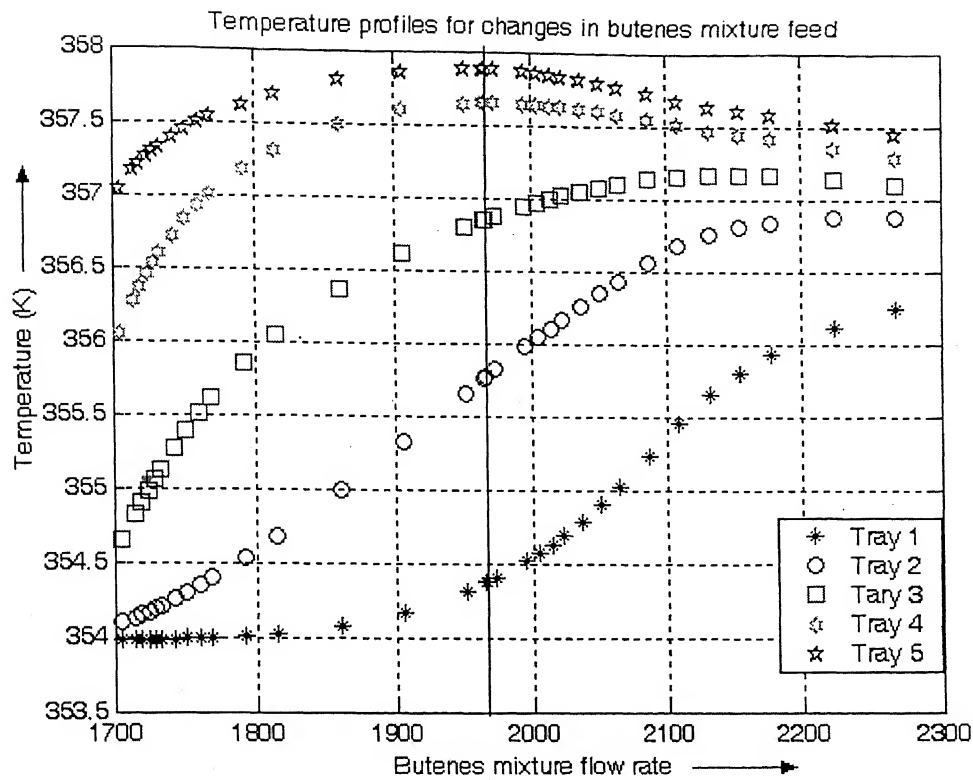


Figure 5.9: Tray temperatures for changes in Butenes feed flow

Contd...

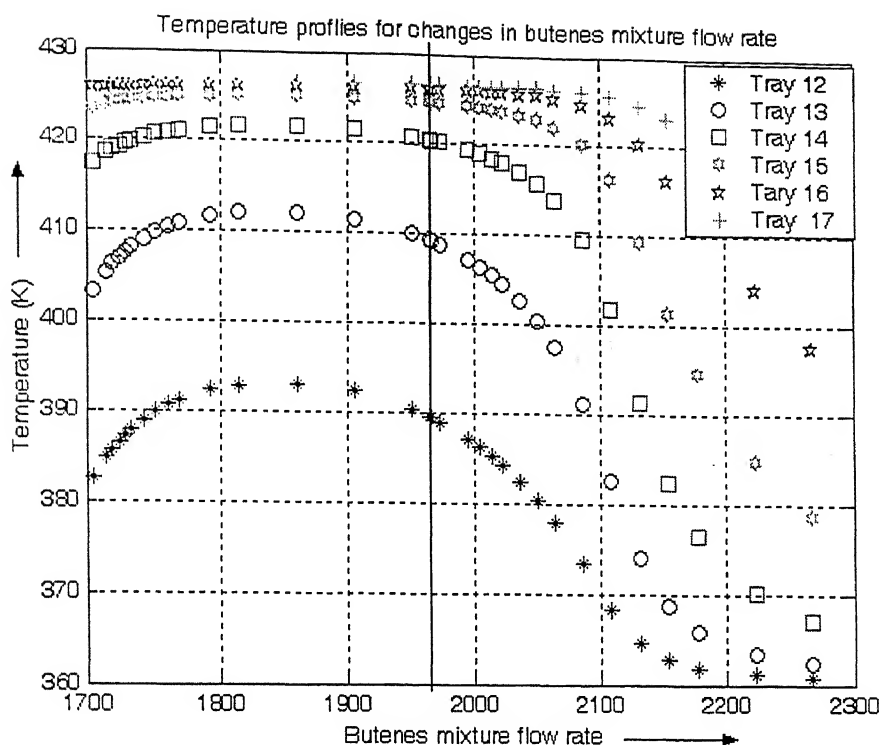


Figure 5.9: Tray temperatures for changes in Butenes feed flow

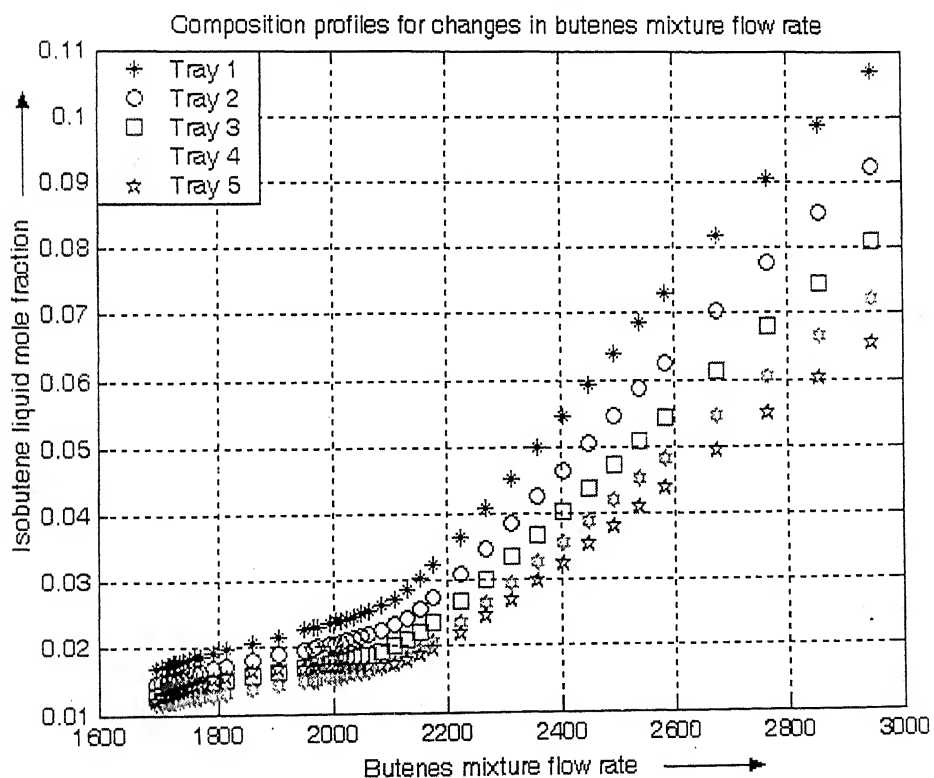


Figure 5.10: Tray compositions for changes in Butenes feed flow
Contd...

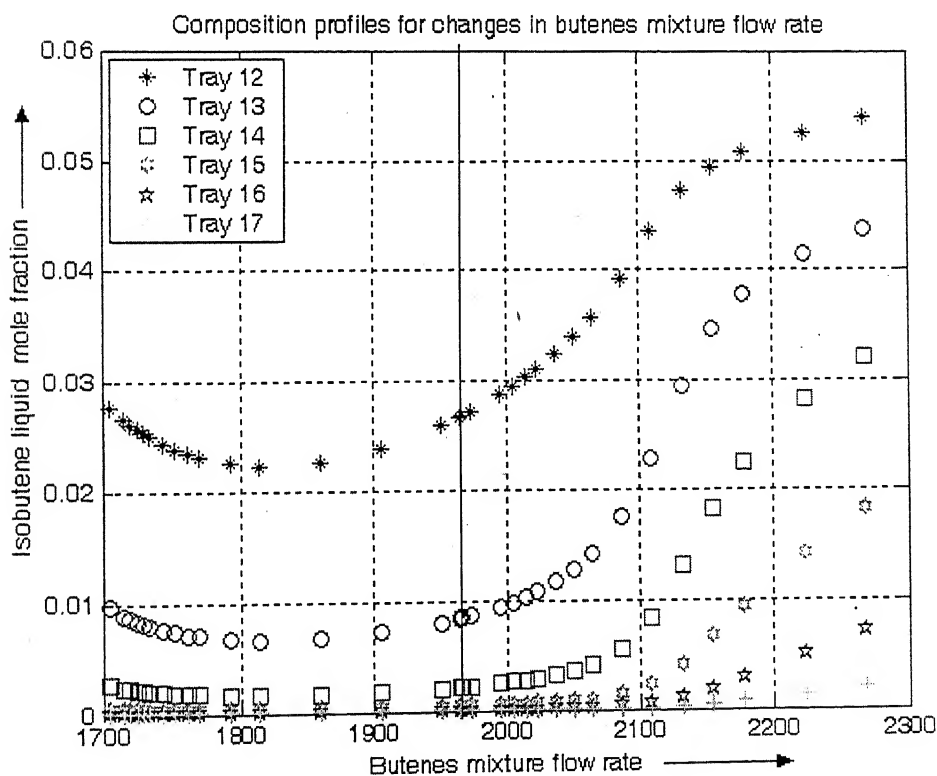
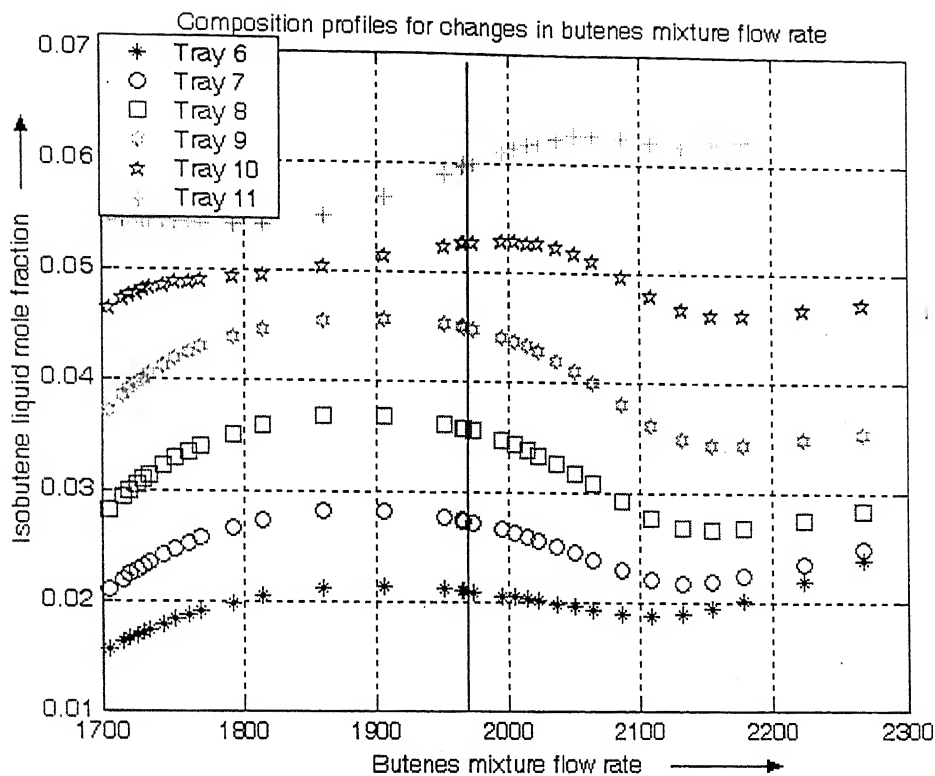


Figure 5.10: Tray compositions for changes in Butenes feed flow

A sensitive tray is needed for effective feedback control. Figure 5.11 plots the sensitivity of tray composition with respect to the fresh feed flow rates. Of the reactive trays, tray 4 is the most sensitive to changes in the fresh methanol feed while trays 7 and 8 are the most sensitive to changes in the butene feed.

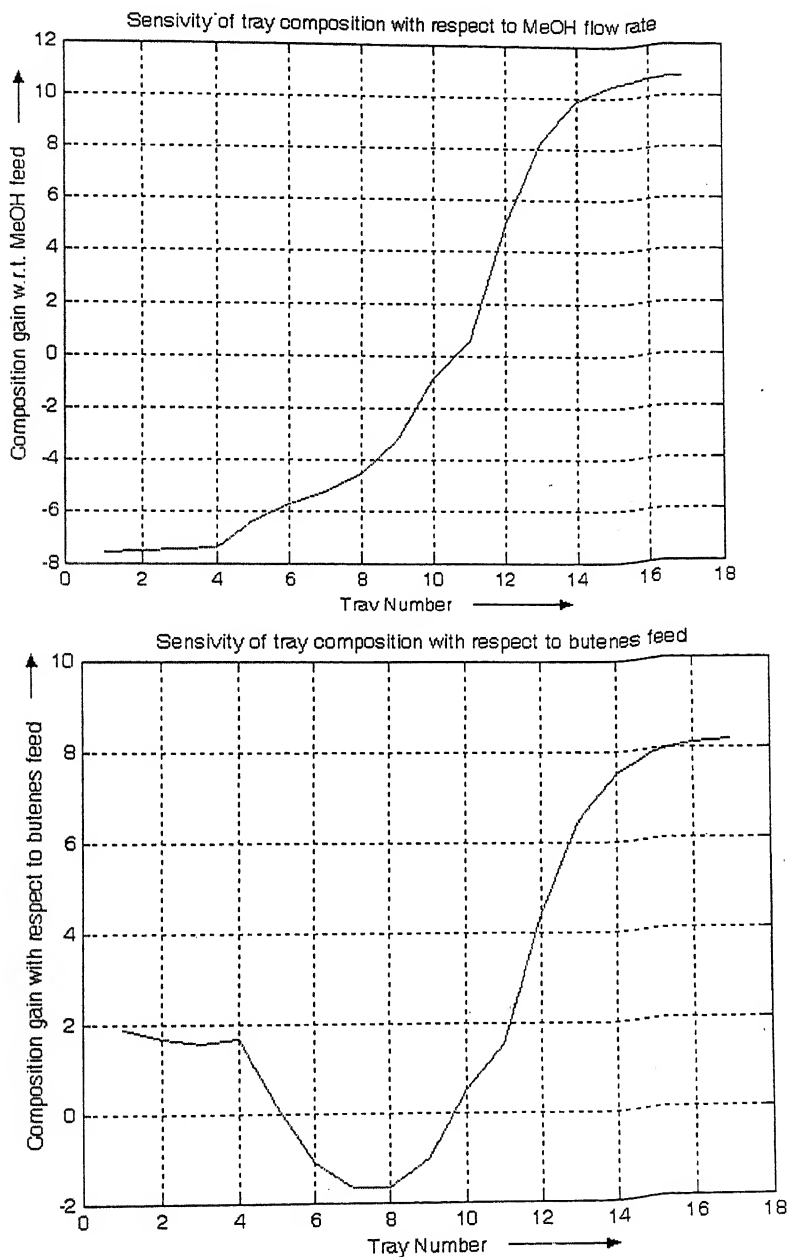


Figure 5.11: Sensitivity of the tray compositions with respect to fresh feed flow rates

5.3 Control Structure Synthesis

We start with the simplest column operation strategy of no control and then keep adding complexity in the form of control loops until the simplest control structure that achieves the desired control objective. The objective here is to maintain the product purity and reaction conversion for the principal disturbances, namely production rate variation and feedstock composition. Operating the column at fixed reflux ratio and a fixed reboiler duty is the starting point. The fresh feeds are assumed under flow control. The corresponding control structure is shown in Figure 5.1 and labeled as CS1. Figure 5.12 plots the column purity and conversion as the fresh feed rates vary about the base case values. These feed rates may be varied by an operator or may be off due to the typically high errors involved in flow measurements. Even for relatively small changes in the fresh feed rates, the product purity becomes unacceptable. This is because one of the reactants becomes excess and exits with the product stream, reducing its purity. Clearly the feeds need to be kept in stoichiometric balance in order to avoid this problem.

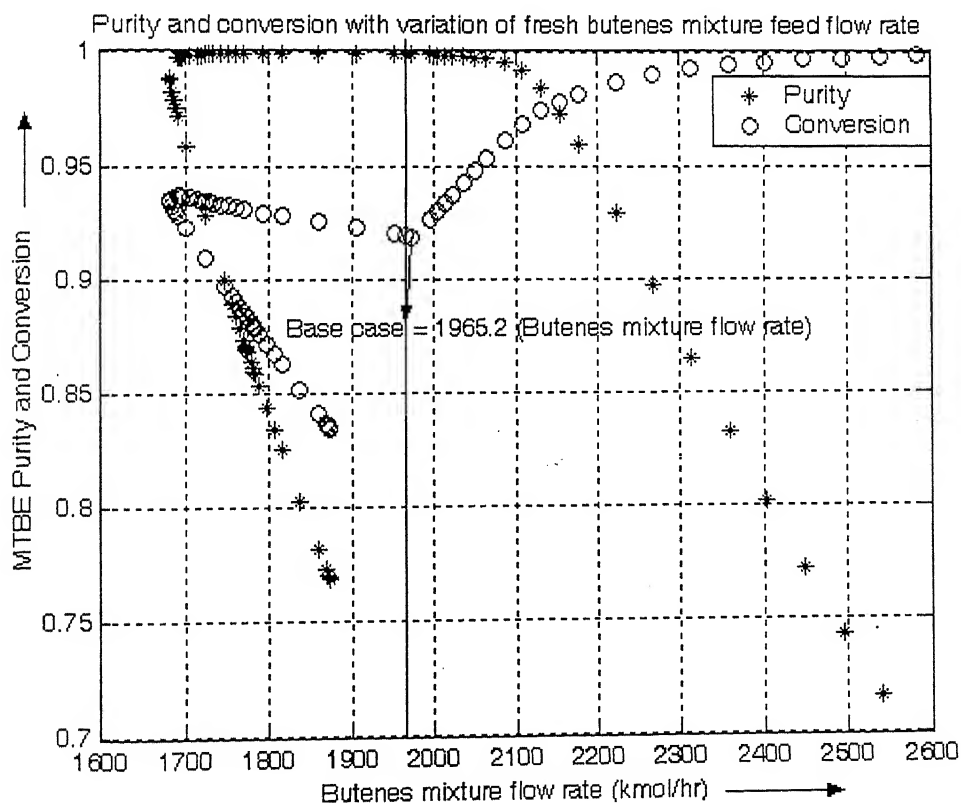
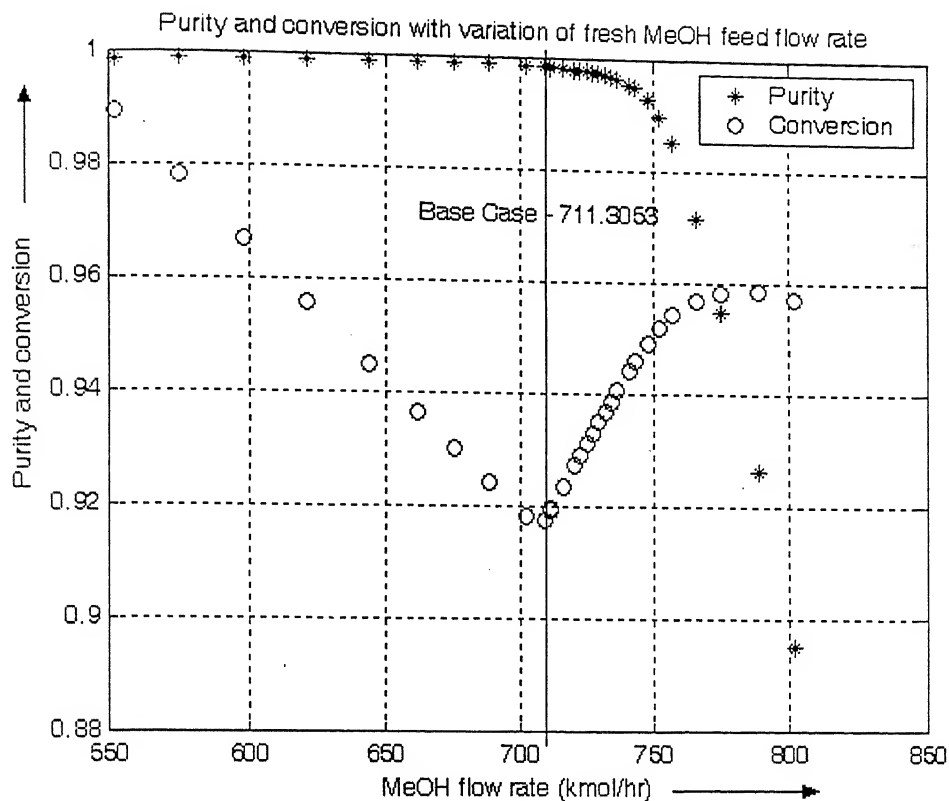


Figure 5.12: Purity and conversion with the variation of fresh feed flow rates

If the feeds are assumed to be in stoichiometric balance using some feedback arrangement, the column performance in terms of product purity and reaction conversion is still unacceptable as the production rate is changed ie more fresh feed is put into the column. This is shown in Figure 5.13. Thus operating the column at fixed reflux ratio and reboiler duty with stoichiometric feeds is not satisfactory. Appropriate control loops therefore need to be added.

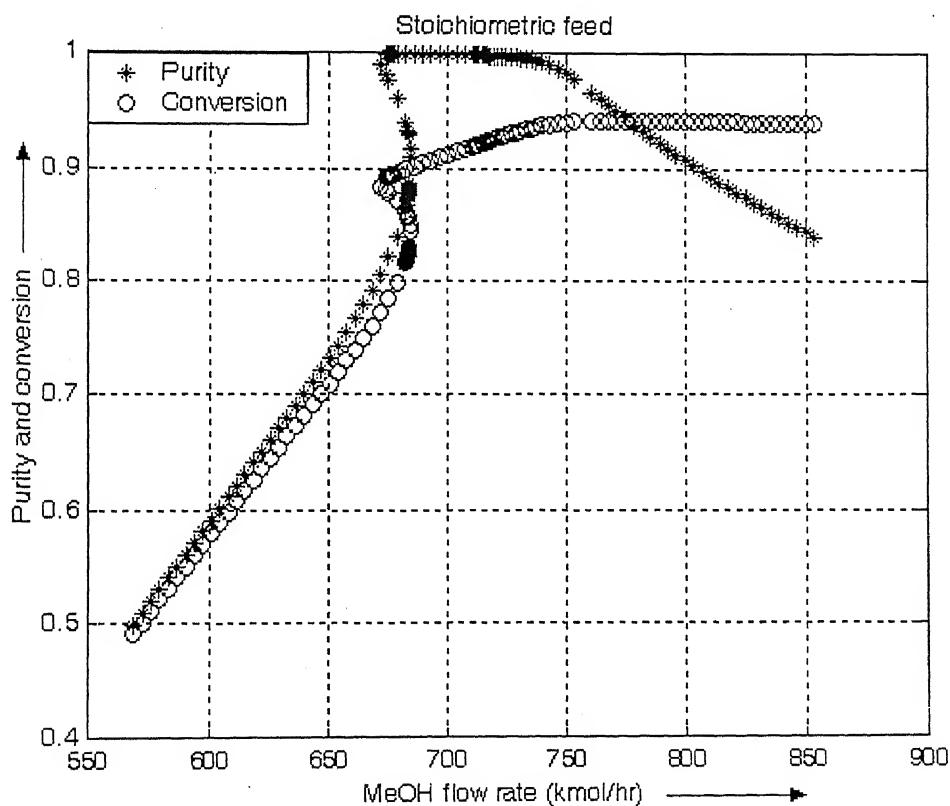


Figure 5.13: Purity and conversion vs production rate change at fixed reflux ratio and reboiler duty with stoichiometric feeds

The reboiler duty and fresh feeds need to be adjusted in a manner that is as yet not known. The previous section on input-output relationships showed that the stripping section tray temperatures are quite sensitive to changes in the reboiler duty. Accordingly, as in ordinary distillation, a tray temperature control loop that manipulates the reboiler duty to keep a tray temperature in the stripping section fixed, is added. The corresponding control structure is shown in Figure 5.1 and labeled as CS2. Since tray 12 is the most sensitive to the reboiler duty, it is chosen as the location for placing the temperature sensor. Figure 5.14 plots the conversion and MTBE purity for a fixed reflux ratio and a fixed tray 12 temperature as both the fresh feed rates are varied in ratio about the base case. Given that the fresh feed rates are nearly stoichiometric, the temperature controller ensures high conversion and purity for all feed rates, (the production rate handle).

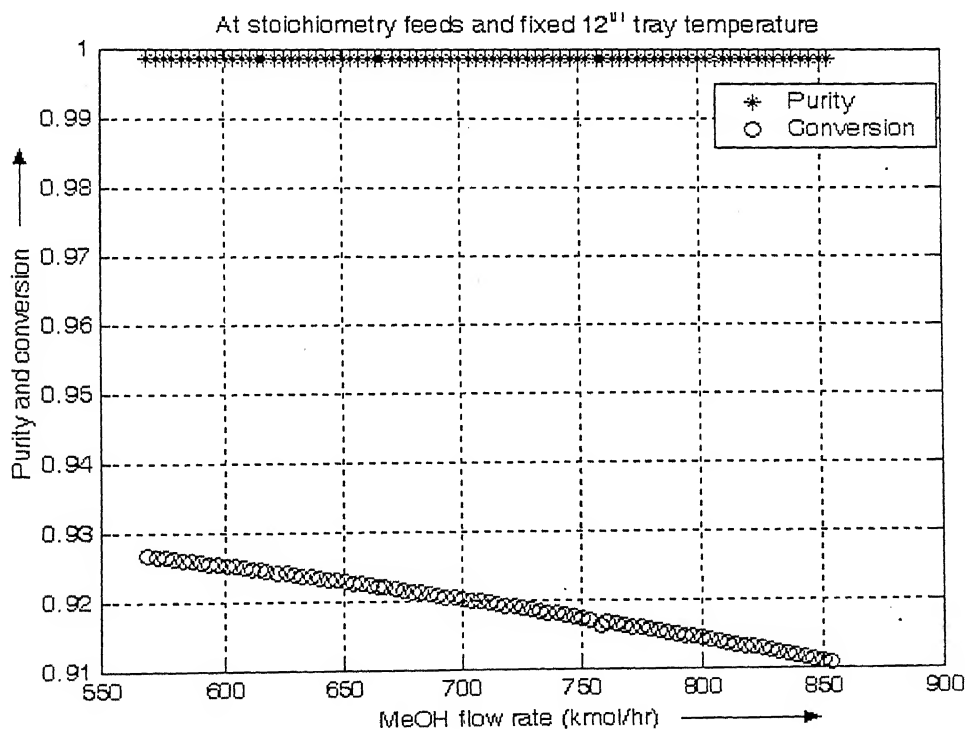


Figure 5.14: Purity and conversion with production rate change at fixed reflux ratio and tray 12 temperature with stoichiometric feeds

As before, near stoichiometric fresh feeds flows are not possible due to large error in the flow measurements. Also, even if the feed flows are equal, composition changes in the fresh feeds can upset the stoichiometric balance. This can lead to unacceptable product purity as the unreacted excess reactant must exit the column. The deterioration in steady state column performance is illustrated in Figure 5.15 for feed flow imbalances and feed composition changes.

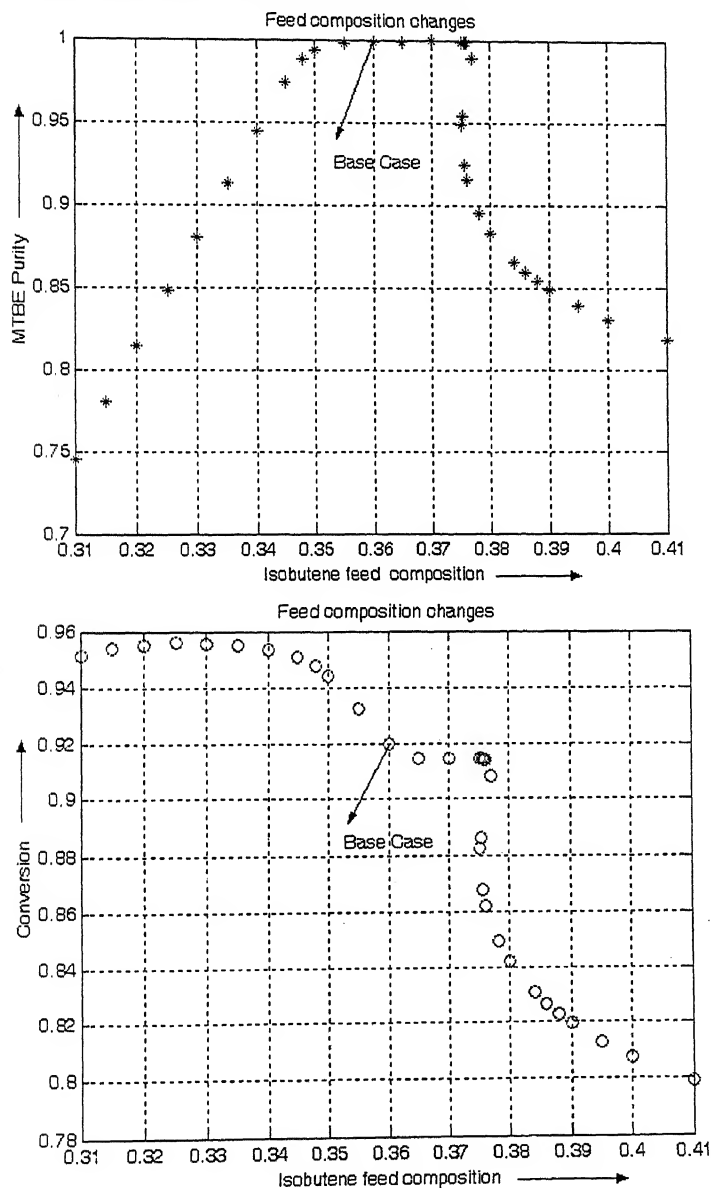


Figure 5.15: Purity and feed composition changes at fixed reflux ration and reboiler duty

It is clear that a feedback control loop arrangement is necessary in order to maintain the feeds in stoichiometric balance. The temperature or composition in a reactive tray may be controlled using one of the feed streams for this purpose. The previous section showed that due to input multiplicities, reactive tray temperatures should not be used in a control loop. The tray compositions, on the other hand, are potential controlled variables for balancing the fresh feeds. A tray composition control loop using one of the fresh feeds as the manipulation handle is therefore added. The corresponding control structures are shown in Figure 5.16 are labeled as CS3 and CS4. Note that since there are now two control loops, the reactive tray location for composition for temperature measurement and the fresh feed handle must be chosen to avoid instability due to interaction between the two control loops.

The overall decision on which fresh feed and reactive tray composition to use in the control loop is now a compromise between tray sensitivity, low interaction and quick dynamic response time. The Niederlinski Index (NI), a measure of loop interaction, is tabulated in Table 5.1 for composition measurements in different reactive trays. A negative NI indicates that the two control loops will be closed loop unstable while a NI between 0.4 to 2 is considered acceptable. For the methanol fresh feed, tray 4 shows the highest sensitivity and has an acceptable NI of 0.51. The NI for other sensitive reactive trays is near zero or negative. For the butenes fresh feed, tray 11 is sensitive and has an acceptable NI of 0.46. Note that trays 6-9, though sensitive, have a negative NI and cannot be used for control. Thus a composition controller that either manipulates the methanol feed to track the tray 4 temperature or manipulates the butenes feed to track tray 11 temperature should balance the feed flows to satisfy the reaction stoichiometry.

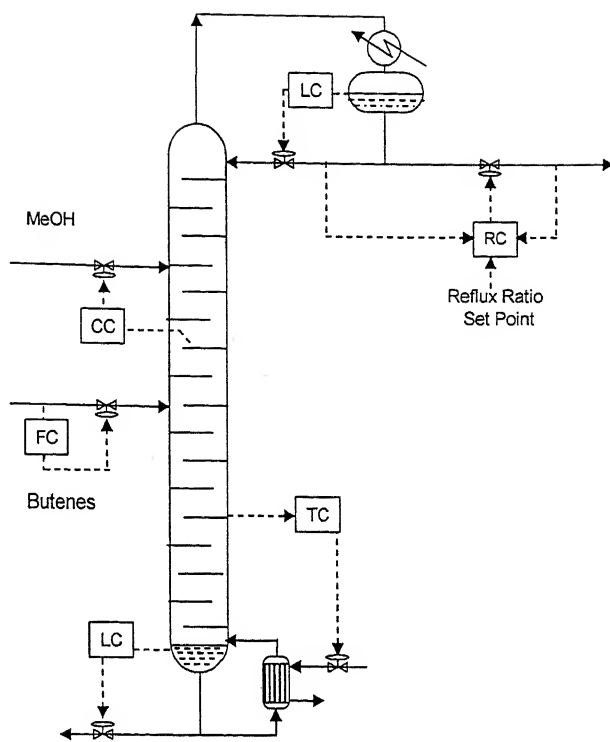
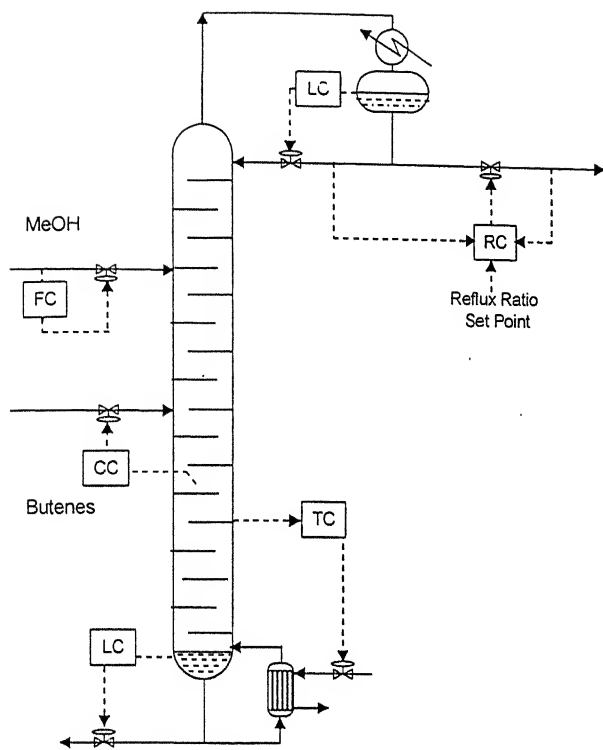


Figure 5.16: Control structures with two control loops

Table 5.1: Niederlinski Index corresponding to butenes and MeOH feed flows

Tray Number	4	5	6	7	8	9	10	11
Butenes	2.44	18.03	-1.55	-0.675	-0.513	-0.684	1.35	0.461
MeOH	0.481	0.35	0.211	0.129	0.103	0.131	0.658	-1.336

In order to assess the steady state column performance of these control structures, the product purity and reaction conversion are plotted for production rate changes and feed composition changes. Note that for CS3 the production rate handle is the fresh methanol feed while for CS4 the production rate handle is the fresh butene feed. Both the structures are able to maintain the column at high product purity and reaction conversion. Figure 5.17 and Figure 5.18 plot the column inputs (manipulated variables) with respect to the production rate for both control structures respectively. The relationships are linear for both the control structures so that simple PI controllers should provide good column regulation. Column input versus butene feed composition is plotted in Figure 5.19. Mild non-linearity in the input output relationships is observed. Simple PI controllers should again provide adequate column regulation for feed composition changes.

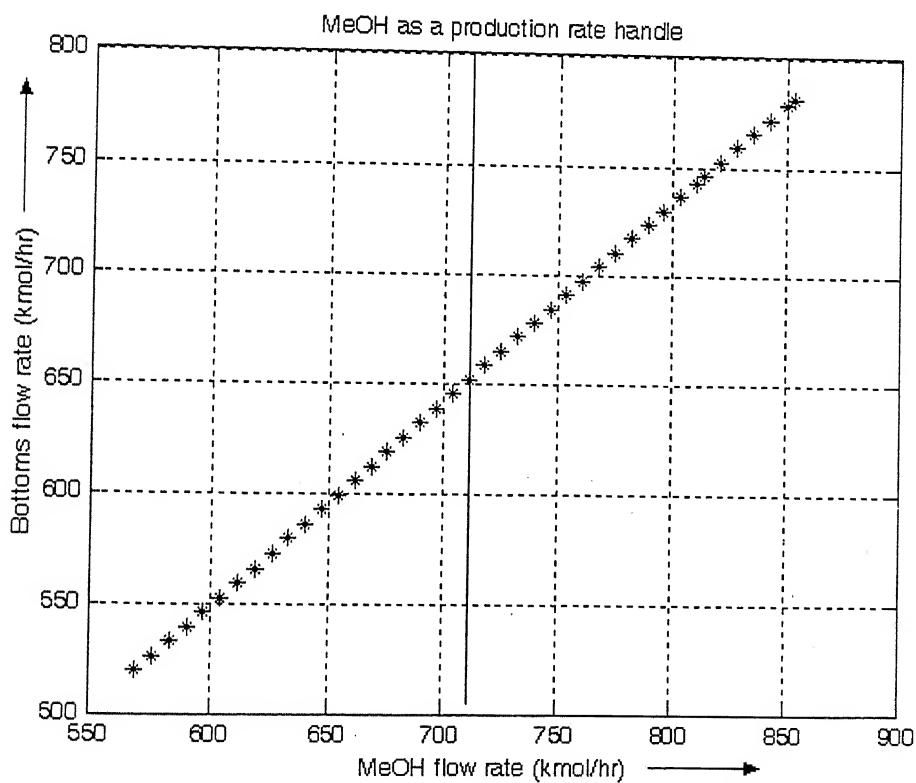
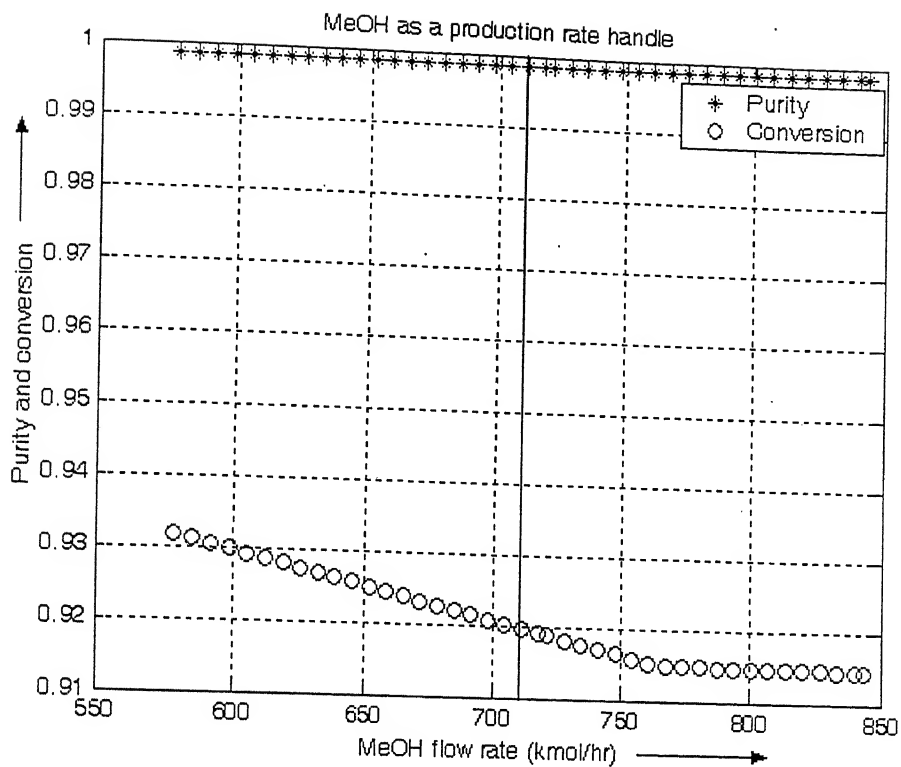


Figure 5.17: Column Performance with Production Rate Changes
Production rate Handle: MeOH

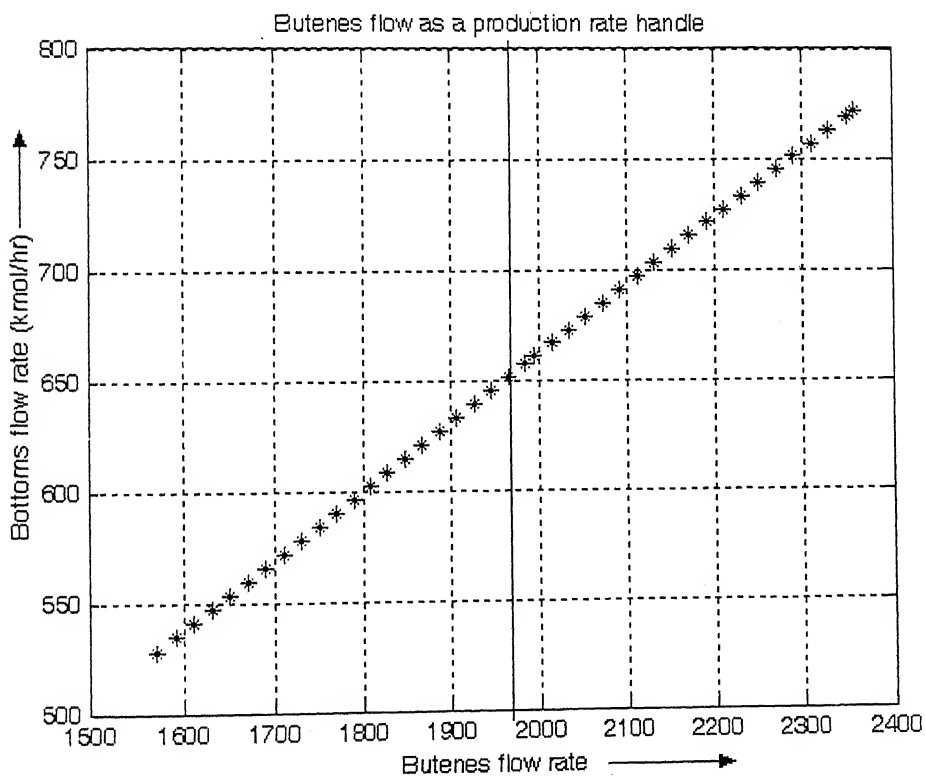
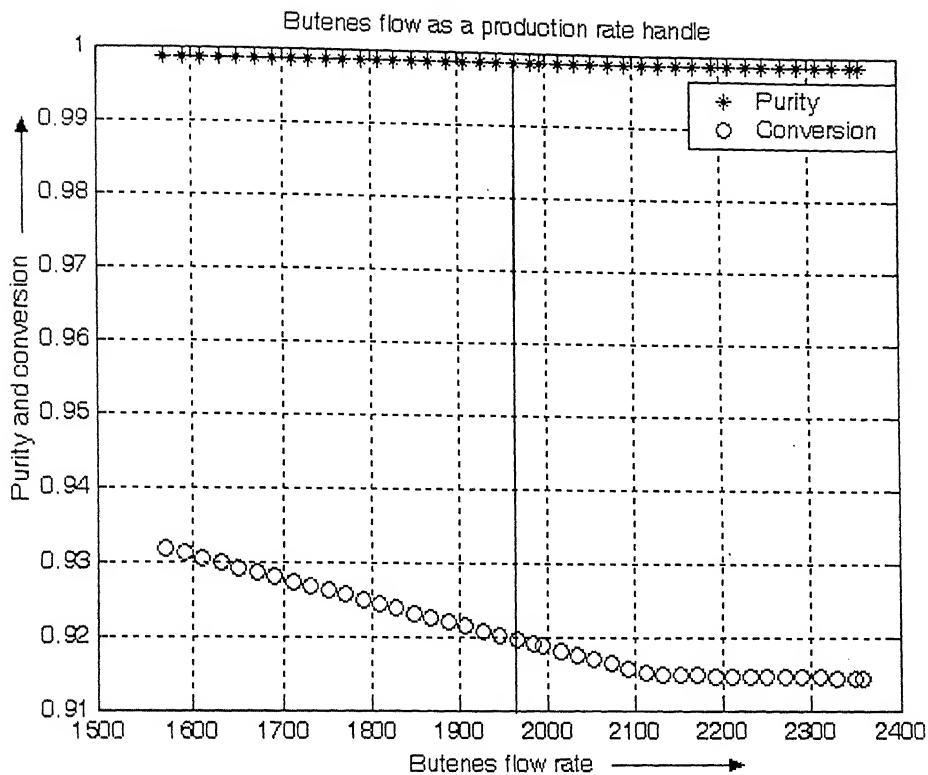


Figure 5.18: Column Performance with Production Rate Changes
Production rate Handle: Butenes

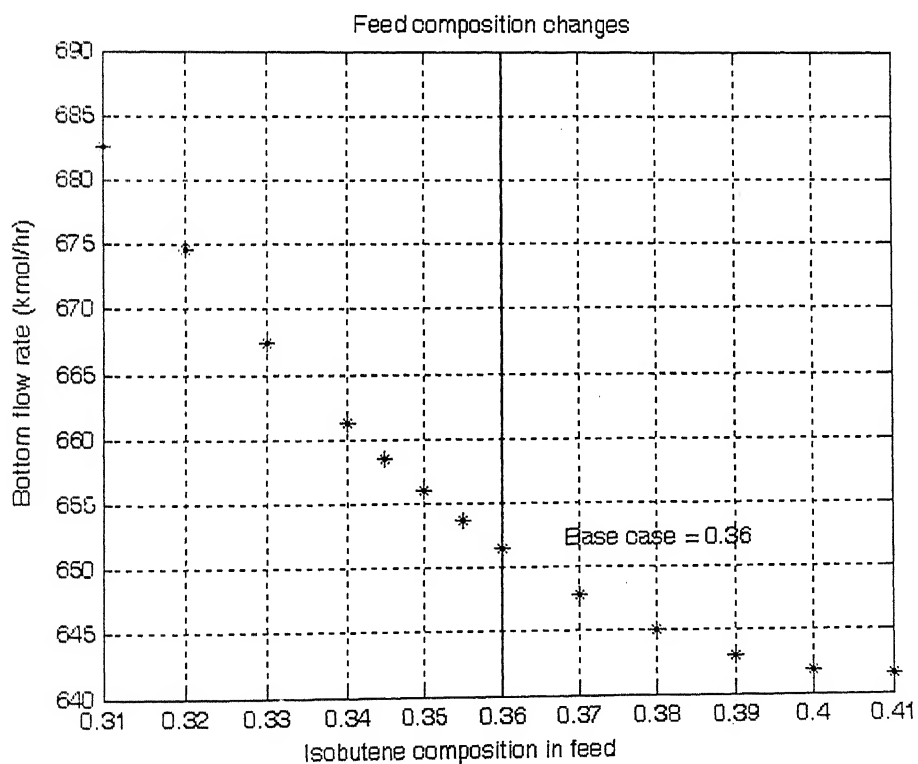
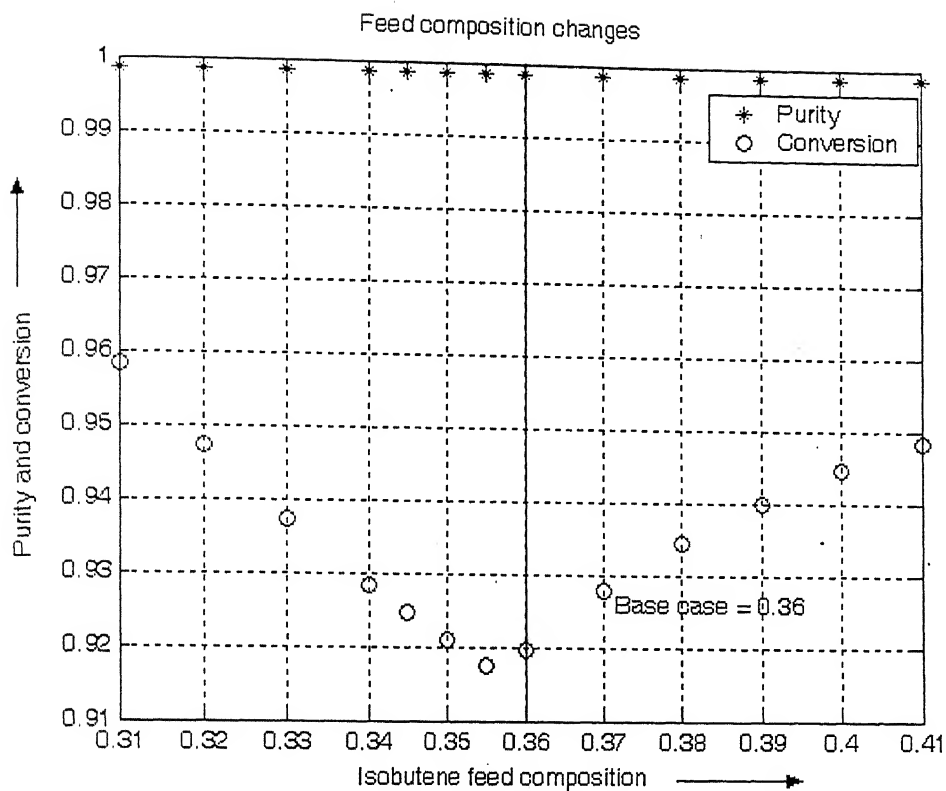


Figure 5.19: Column Performance with Production Rate Changes
Production rate Handle: MeOH

The MTBE example clearly demonstrates how systematic steady state analyses can be used for synthesizing control structures that ensure good column regulation in the presence of disturbances. These control structures need to be validated via dynamic simulations. This shall be taken up in the future work. It is highlighted that in a recent article, Wang et al (2003) show the dynamic column performance of a control structure similar to CS3. The control structure is able to handle $\pm 20\%$ changes in the production rate without any problems.

At this point, it is highlighted that several alternative control structures that are conceptually similar to CS3 are possible. These are shown in Figure 5.20 and labeled. Of the control structures shown (a) would provide the tightest column regulation. In (a), the two fresh feeds are ratioed and the reboiler duty is ratioed with the production rate handle. A reactive tray composition controller provides the ratio set-point to the former in a cascade arrangement for maintaining the stoichiometric balance. Similarly, the stripping section temperature controller provides the ratio set-point to the latter for maintaining product purity. The ratio controllers provide feed-forward compensation for production rate changes so that the master controllers in the cascade loops only have to make fine adjustments by correcting the ratio set-points. Tight control is thus possible.

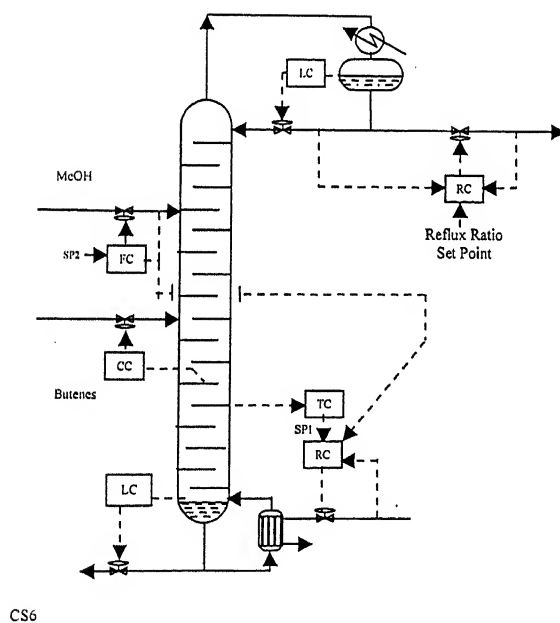
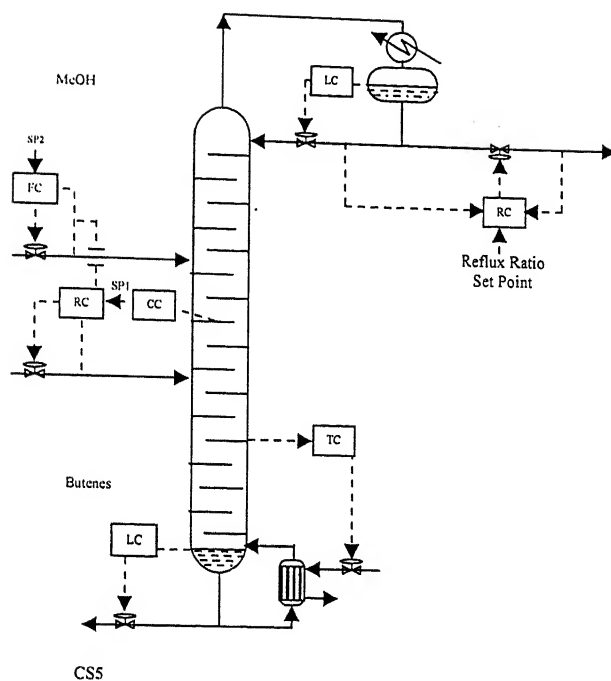


Figure 5.20: Alternative control structures

This completes a demonstration of control structure synthesis for an MTBE RD column using systematic steady state analyses. The MTBE case study shows that maintaining the stoichiometric balance of the fresh feeds is the key to successful RD column operation. The results also show the substantial effect that a control structure has on steady state multiplicities. The next chapter draws conclusions from this work and provides directions for future work.

6.1 Conclusions

Conventional methods such as Naphtali–Sandholm and Inside – Outside methods, depending on the initial guess can converge to any one of the multiple steady states, in case multiple steady states do exist. Few people obtained merely two steady states by changing initial guesses using these conventional methods. Therefore, these methods are not geared towards detecting steady state multiplicities. Homotopy continuation, a powerful tool for identifying steady state multiplicities, is applied to reactive distillation systems to assess the impact of these multiplicities on column design, operability and control. In the MTBE system, a reasonably large zone with five multiple steady states is obtained with the high conversion steady state corresponding to the design steady state. As the catalyst weight is further increased, two of these steady states disappear. Thus there were five steady states in the kinetically controlled RD regime in contrast to only three steady states in the reaction equilibrium controlled RD regime. For the methyl acetate column, three steady states in both the kinetically controlled and reaction equilibrium regimes are obtained at fixed reflux rate and reboiler duty. If the column specification is changed to fixed reflux ratio and reboiler duty, only a single steady state solution is obtained for all catalyst weights. Therefore, the number of steady states is affected by the column specification used and the catalyst weight per tray.

Homotopy continuation is used for control structure synthesis for MTBE system. The input-output relationships are systematically analyzed to synthesize robust column

operating structures that ensure high product purity and reaction conversion in the face of major disturbances. Column specifications also found very important to avoid or minimized multiple steady state in control structure synthesis. In order to decide between the fixed reflux rate vs fixed reflux ratio as a column specification, Output multiplicity was evident for both the fixed reflux rate and the fixed reflux ratio specification. It was however noted that in the latter case, the base case point was away from the zone of output multiplicity while output multiplicity occurs in the former even for the base case. Clearly, for this column the fixed reflux ratio was preferable over the fixed reflux rate. Sensitivity analysis played an important role for obtaining the sensitive tray location for the temperature / composition sensors used in the control structure. The various permutations and combinations lead to a large number of possible control structures from which a small set of "good" control structures are chosen. The preferred control structure operates at fixed reflux ratio and uses a temperature inferential control loop for maintaining the product purity by manipulating the reboiler duty. A reactive tray composition is controlled for balancing the fresh feed into the column as per the reaction stoichiometry by manipulating a fresh feed rate. The isobutene fresh feed or the methanol fresh feed can be used as the manipulated variable in the composition loop. This case study shows that maintaining the stoichiometric balance of the fresh feeds is the key to successful RD column operation. The MTBE example clearly demonstrates how systematic steady state analyses can be used for synthesizing control structures that ensure good column regulation in the presence of disturbances

6.2 Future Work

This developed homotopy continuation algorithm is working manually. In future, this homotopy continuation algorithm should be in such a way that can give whole homotopy curve automatically. A pre defined step size is needed to trace the homotopy curve. A reliable step size estimation method that predicts the step length can reduce the computation time tremendously. George (1980), den Heijer and Rheinboldt (1981), Deuffhard (1979), and Wacker (1978), have proposed different procedures to estimate step size. These proposed control structures need to be validated via dynamic simulations. This shall be taken up in the future work.

1. Agreda, V. H.; and Partin, L. R. (1984). "Reactive distillation process for the production of methyl acetate", *U.S. Patent* 4435595.
2. Agreda, V. H.; Partin, L. R.; and Heise, W. H. (1990). "High purity methyl acetate via reactive distillation", *Chemical Engineering Progress*, **86**(2), 40-46.
3. Al-Arfaj, M.A.; and Luyben, W.L. (1999). "Quantitative heuristic design of reactive distillation", Master's thesis, Lehigh University Bethlehem, P.A.
4. Al-Arfaj, M.A., and Luyben, W.L. (2000). "Comparison of alternative control structures for an ideal two-product reactive distillation column", *Industrial and Engineering Chemistry Research*, **39**, 3298-3307.
5. Al-Arfaj, M.A.; and Luyben, W.L. (2002). "Control of ethylene glycol reactive distillation column", *AIChE Journal*, **48**(4), 905-908
6. Al-Arfaj, M.A.; and Luyben, W. L. (2002). "Comparative control study of ideal and methyl acetate reactive distillation", *Chemical Engineering Science*, **57**, 5039-5050.
7. Al-Arfaj, M.A., and Luyben, W.L. (2002a). "Control study of ETBE reactive distillation", *Industrial and Engineering Chemistry Research*, **41**, 3784-3796.
8. Al-Arfaj, M.A., and Luyben, W.L. (2002a). "Design and control of olefin metathesis reactive distillation column", *Chemical Engineering Science*, **57**, 715-733.
9. Allgower, E.; and Georg, K. (1980). "Simplicial and continuation methods for approximating fixed points and solutions to systems of equations", *SIAM Review*, **22**, 28.

10. ARCO Chemical Technology, Ethers, Petrochemical Processes 95. Hydrocarbon Process. 1995, 74(3), 110
11. ASPEN PLUS steady state simulator Version 10
12. Backhaus, A. A. (1921). "Continuous processes for the manufacture of esters", *US patent* 1400849.
13. Backhaus, A. A. (1922). "Apparatus for producing high grade esters", *US patent* 1403224.
14. Backhaus, A. A. (1923a). "Process for producing high grade esters", *US patent* 1454462.
15. Backhaus, A. A. (1923b). "Process for esterification", *US patent* 1454463.
16. Barbosa, D.; and Doherty, M. F. (1988). "The simple distillation of homogeneous reactive distillation systems", *Chemical Engineering Science*, **43**, 541-550.
17. Carra, S.; Santacesaria, E.; Morbidelli, M.; and Cavalli, L. (1979b). "Synthesis of propylene oxide from propylene chlorohydrins-I. Kinetic aspects of the process", *Chemical Engineering Science*, **34**, 1123-1132.
18. Chang, Y.A.; and Seader, J.D. (1988). "Simulation of continuous reactive distillation by a homotopy continuation method", *Computers and Chemical Engineering*, **12**, 1243-1255.
19. Chen, F.; Huss, R. S.; Doherty, M.F.; and Malone, M.F. (2002). "Multiple steady states in reactive distillation: kinetic effects", *Computers and Chemical Engineering*, **26**(1), 81-93.

20. Ciric, A. R.; and Miao, P. (1994). "Steady state multiplicities in an ethylene glycol reactive distillation column", *Industrial and Engineering Chemistry Research*, **33**, 2738-2748.
21. DeGarmo, J. L.; Parulekar, V. N.; and Pinjala, V. (1992). "Consider reactive distillation", *Chemical Engineering Progress*, **3**, 43-50.
22. den Heijer, C.; and Rheinboldt, W.C. (1981). "On steplength algorithms for a class of continuation methods", *SIAM J. Numerical Analysis*, **18**, 925-947
23. Deuflhart, P. (1979). "A stepsize control for continuation methods and its special application to multiple shooting techniques", *Numer. Math.*, **33**, 115
24. Deshpande, P.B. (1985). *Distillation dynamics and control*, Instrument society of America.
25. Doherty, M. F.; and Buzad, G. (1992). "Reactive distillation by design", *Chemical Engineering Research and Design, Transaction of the Institution of Chemical Engineers, Part A*, **70**, 448-458.
26. Doherty, M. F.; and Malone, M. F. (2001). "Conceptual design of distillation systems", McGraw-Hill Higher Education, Chapter 10.
27. Guttinger, T. E.; and Morari, M. (1999a). "Predicting multiple steady states in equilibrium reactive distillation. 1. Analysis of nonhybrid systems", *Industrial and Engineering Chemistry Research*, **38**, 1633-1648.
28. Guttinger, T. E.; and Morari, M. (1999b). "Predicting multiple steady states in equilibrium reactive distillation. 2. Analysis of hybrid systems", *Industrial and Engineering Chemistry Research*, **38**, 1649-1665.

29. Hauan, S.; Hertzberg, T.; and Lien, K. M. (1995). "Why methyl-tert-butyl-ether production by reactive distillation may yield multiple solutions", *Industrial and Engineering Chemistry Research*, **34**, 987-991.
30. Higler, A. P.; Taylor, R.; and Krishna, R. (1999). "Non equilibrium modeling of reactive distillation: Multiple steady states in MTBE synthesis", *Chemical Engineering Science*, **54**, 1389-1395.
31. Izarraraz, A.; Bentzen, G. W.; Anthony, R. G.; and Holland, C. D. (1980). "Solve more distillation problems Part-9 when chemical reactions occur", *Hydrocarbon processing*, April 1980, 195-203.
32. Isla, M. A.; and Irazoqui, H. A. (1996). "Modeling, analysis and simulation of a methyl-tert-butyl ether reactive distillation column", *Industrial and Engineering Chemistry Research*, **35**, 2396-2708.
33. Jacobs, R.; and Krishna, R. (1993). "Multiple solutions in reactive distillation for methyl-tert-butyl ether synthesis", *Industrial and Engineering Chemistry Research*, **32**, 1706-1709.
34. Jalali, F.; and Seader, J. D. (1999). "Homotopy continuation method in multi-phase multi-reaction equilibrium systems", *Computers and Chemical Engineering*, **23**, 1319-1331.
35. Kaibel, G.; Mayer, H. H.; and Seid, B. (1979). "Reactions in distillation columns", *German Chemical Engineering*, **2**, 180-187.
36. Kaymak, D. B.; and Luyben, W. L. (2004). "Effect of the chemical equilibrium constant on the design of reactive distillation columns", *Industrial and Engineering Chemistry Research*, **43(14)**, 3666-3671.

37. Kaymak, D. B.; and Luyben, W. L. (2004). "Quantitative comparison of reactive distillation with conventional multi-unit reactor/column/recycle streams for different equilibrium constants", *Industrial and Engineering Chemistry Research*, **43**(10), 2493-2507.
38. Kaymak, D. B.; Luyben, W. L.; and Smith, O. J. (2004). "Effect of relative volatility on the quantitative comparison of reactive distillation and conventional multi-unit systems", *Industrial and Engineering Chemistry Research*, **43**(12), 3151-3162.
39. Keyes, D. B. (1932) "Esterification processes and equipment", *Industrial and Engineering Chemistry*, **24**, 1096-1103.
40. Kinoshita, M.; Hashimoto, I.; and Takamatsu, T. (1983). "A new simulation procedure for multicomponent distillation column processing non ideal solutions or reactive solutions", *Journal of Chemical Engineering of Japan*, **16**, 370-377.
41. Komatsu, H.; and Holland, C.D. (1977). "A new method of convergence for solving reactive distillation problems", *Journal of Chemical Engineering of Japan*, **10**(4), 292-298.
42. Kovach, J. W. III.; and Sieder, W. D. (1987). "Heterogeneous azeotropic distillation: homotopy-continuation methods", *Computers and Chemical Engineering*, **11**(6), 593.
43. Kubicck, M.; and Marek, M., (1983). *Computational Methods in Bifurcation Theory and Dissipative Structures*, Springer-Verlag, Berlin

44. Lin, W. J.; Seader, J.D.; and Wayburn, T. L (1987). "Computing multiple solutions to systems of interlinked separation columns", *A.I.Ch.E. Journal*, **33**(6), 886-896.
45. Luyben, W.L. (1992). *Practical distillation control*, Van Nostrand Reinhold New York
46. Marek, J. (1955). "Vapor liquid equilibria in mixtures containing an associating substance. II binary mixtures of acetic acid at atmospheric pressure", *Collection of Czechoslovak Chemical Communication*, **20**, 1490.
47. Mohl, K. D.; Kienle, A.; Gilles E. D.; Rapmund, P.; Sundmacher, K.; and Hoffman, U.(1999). "Steady state multiplicities in reactive distillation columns for the production of fuel ethers MTBE and TAME: Theoretical analysis and experimental verification", *Chemical Engineering Science*, **54**, 1029-1043.
48. Naphtali, L.M.; and Sandholm, D. P. (1971). "Multicomponent separation calculation by linearization", *A.I.Ch.E. Journal*, **17**, 148-153.
49. Nelson, P. A. (1971). "Countercurrent Equilibrium stage separation with reaction", *A.I.Ch.E. Journal*, **17**, 1043-1049.
50. Nijhuis, S. A.; Kerkhof, F. P. J. M.; and Mak, A.N.S. (1993). "Multiple steady states during reactive distillation of methyl-tert-butyl ether", *Industrial and Engineering Chemistry Research*, **32**, 2767-2774.
51. Pushpavanam, S. (1998). *Mathematical Methods in Chemical Engineering*, Prentice-Hall of India private limited, New Delhi.

52. Rapmund, P.; Sundmacher, K.; and Hoffman, U. (1998). "Multiple steady states in a reactive distillation column for the production of fuel ether TAME II. Experimental validation", *Chemical Engineering and Technology*, **21**, 136-139.
53. Rehfinger, A.; and Hoffman, U. (1990). "Kinetics of methyl-tert-butyl ether liquid phase synthesis catalyzed by ion exchange resin. II-macropore diffusion of MeOH as rate controlling step", *Chemical Engineering Science*, **45**, 1619-1626.
54. Rooks, E.R.; Julka, V.; Doherty, M.F.; and Malone, M.F. (1998). "Structure of distillation regions for multicomponent azeotropic mixtures", *AIChE Journal*, **44**, 1382-1391
55. Seader, J. D.; and Henley, E. J. (1998). *Separation Process Principles*. John Wiley and Sons.
56. Siirola, J. J. (1995). "An industrial perspective on process synthesis", *A.I.Ch.E. Symposium Series No*, **91 (304)**, 222-233.
57. Singh, Ram (2004). "Steady state simulation of reactive distillation columns using Naphtali-Sandholm method", M. Tech Thesis, Department of Chemical Engineering, IIT Kanpur (INDIA).
58. Sneesby, M. G.; Tade, M. O.; Datta, R.; and Smith, T.N. (1998). "Steady state transitions in the reactive distillation of MTBE", *Computers and Chemical Engineering*, **22**, 879-892.
59. Song, W.; Venimadhavan, C.; Manning, J.; Malone, M.; and Doherty, M. (1998). "Measurement of residue curve maps and heterogeneous kinetics in methyl acetate synthesis", *Industrial and Engineering Chemistry Research*, **37**, 1917-1928.

60. Sundmacher, K.; and Hoffman, U. (1994a). "A macro kinetic analysis of MTBE synthesis in chemical potentials", *Chemical Engineering Science*, **49**, 3077-3089.
61. Suzuki, I.; Yagi, H.; Komatsu, H.; and Hirata, M. (1971). "Calculation of multi component distillation accompanied by a chemical reaction", *Journal of Chemical Engineering of Japan*, **4**, 26-33.
62. Taylor, R.; and Krishna R. (2000). "Review Modelling reactive distillation", *Chemical Engineering Science*, **55**, 5183-5229.
63. Taylor, R.; and Lucia A. (1994). "Modelling and analysis of multicomponent separation processes", A.I.Ch.E. Symposium Series No. **91(304)**, 9-18.
64. Tian, Y.C.; Zhao, F; Bisowarno, B.H.; and Tade, M.O. (2003). "Pattern-based predictive control for ETBE reactive distillation", *Journal of Process Control*, **13**, 57-67.
65. Towler, G. P.; and Frey, S. J. (2000). "Reactive distillation. In S. Kulprathipanja, Reactive separation processes", Philadelphia: Taylor and Francis (Chapter 2).
66. Venkataraman, S.; Chan, W. K.; and Boston, J.F. (1990). "Reactive distillation using Aspen Plus", *Chemical Engineering Progress*, **86(8)**, 45-54.
67. Vora, N.; and Daoutidis, P. (2001). "Dynamics and control of an ethyl acetate reactive distillation coloumn", *Industrial and Engineering Chemistry Research*, **40**, 833-849.
68. Wacker, H.J. (1978). "Continuation methods", Academic Press, New York.
69. Wang, S.J; Wang, D.S.H.; and Lee, E.K.(2003). "Effect of interaction multiplicity on control system design for a MTBE reactive distillation column", *Journal of Process Control*, **13**, 503-515

70. Wayburn, T. L.; and Seader, J. D. (1987). "Homotopy Continuation methods for computer aided process design", *Computers and Chemical Engineering*, **11**, 7-25.
71. Yaws, C. L.; Yang, H. C; Hopper, J. R.; and Cawley W. A. (1991). "Property data Equation for liquid density", *Hydrocarbon processing*, **January 1991**, 103-106.